In vitro Biorelevant and *in silico* Sunscreen Performance Evaluation on the Basis of Film Thickness Frequency Distribution of Formulations and UV Filter Repartition

Inauguraldissertation
zur
Erlangung der Würde eines Doktors der Philosophie
vorgelegt der
Philosophisch-Naturwissenschaftlichen Fakultät
der Universität Basel

von

MYRIAM SOHN

aus Rosenau, Frankreich

Basel, 2016

Genehmigt von der Philosophisch-Naturwissenschaftlichen Fakultät

auf Antrag von

Prof. Dr. Georgios Imanidis, Fakultätsverantwortlicher
Prof. Dr. Jörg Huwyler, Korreferent
PD Dr. Bernd Herzog, Korreferent

Basel, den 21. April 2015

Prof. Dr. Jörg Schibler
Dekan

Acknowledgements

First and foremost, I would like to express my gratitude to Prof. Dr. Georgios Imanidis for having welcomed me in the Institute of Pharma Technology at the School of Life Sciences FHNW for my Ph.D. studies. I would like to thank him for his great supervision, the valuable and productive discussions, the deep explanations, his patience, his advices in writing the papers; he learned my never give up, especially with the convolution approach and helped in the reflection of addressing a new topic.

I would like to thank Gebert Rüf Stiftung for the funding of this research work.

Furthermore, I would like to deeply thank Dr. Bernd Herzog from BASF for his precious support during my entire Ph.D. work, his expertise and our fruitful discussions on simulations, and for his availability.

I would like to thank Prof. Dr. Jörg Huwyler of the University of Basel, department of Pharmaceutical Sciences for being co-referee for this thesis.

Special thanks to Uli Osterwalder from BASF for his helpful contribution to this work, his ideas, and positive thinking.

I would like to profoundly thank Theodor Bühler for his huge support on confocal Raman microspectroscopy measurements, his helpfulness, his time, and our dynamic discussions.

To Fabienne Thoenen a big thank for her great help in the laboratory and preparation of pig ear skin, her kindness, and helpfulness.

I thank the master students Verena Korn from the FHNW and Adeline Hêche from the University of Basel for their great help in the advancement of the laboratory work regarding the development of the methods for SPF *in vitro* on pig ear skin and film thickness distribution measurements. Thanks to Verena for her dynamism and daily good mood.

I would like to thank Patrice Belin and Denis Georges from Altimet for their support in the development of the film thickness assessment method.

My gratitude also goes to Marcel Schnyder from BASF for having supported me and believed in me when I decided to pursue doctoral studies, Andrea Zamponi and Nathalie Bouillo to have made it possible within BASF.

A warm Thank You goes to Emilie Rogg for her invaluable friendship, her endless support, advices, and encouragements during my entire thesis and before.

I keep my deepest gratitude to my Dad and Mom for their unconditional love, they encouraged me throughout my entire life, endlessly supported me in my academic studies, today I am what I am thanks to you. I deeply thank Mamama, without her I never could have pursued academic studies. A tender thought for Joël, for the 15 years spent together, with the hope that what we lived together was true. A warm thank to Staszek for his attentiveness, tenderness, and his support since one year, “bardzo cie lubie”. To my children, moje aniołky, Aymeric and Maël, all my love for you.

Abstract

Exposure to ultraviolet (UV) radiation is known to cause various damages to human health. Topically applied sunscreens are widely used by the population to prevent sun damages and are an efficient, simple, and convenient means of photoprotection. The active ingredients of sunscreens are the UV filters that are able to absorb selectively a wavelength range in the UV spectrum. The level of UV protection afforded by a sunscreen primarily depends on the UV filters contained in the product according to their concentration, absorbance profile, and photostability properties, along with the composition of the UV filter system. However, sunscreens containing the same UV filter mixture were reported to produce different level of photoprotection. Hence, expected UV performance of a sunscreen can not be solely predicted based on the UV filter system contained in the product. Therefore, the present work aims at understanding the mechanisms of UV performance by evaluating the behavior of a sunscreen after application on the skin in terms of film formation and UV filter repartition. The impact of sunscreen film thickness and UV filter repartition on the photoprotection was investigated in dependence of the sunscreen vehicle. To evaluate the performance of a sunscreen, a methodology was developed for the determination of the *in vitro* UV protection that is a further part of the present work.

The present thesis consists of four studies, which aimed at improving the understanding of the mechanisms of sun protection for effective product development. To this end, *in vitro* tests along with *in silico* approach were employed for evaluating sunscreen efficacy. The findings may improve the predictability of the performance of sunscreens during the development stage to optimize their efficacy.

In the first study, we examined the use of pig ear skin as a biological substrate for SPF *in vitro* determination with diffuse transmission spectroscopy. The polymethylmethacrylate (PMMA) plates currently employed to this purpose mostly fail in yielding a satisfactory correlation between sun protection factor (SPF) *in vitro* and *in vivo,* the SPF *in vivo* being the gold standard and, to date, the only approved method by regulatory bodies. Trypsin-separated stratum corneum and heat-separated epidermis of pig ear showed a lower roughness than full thickness skin and PMMA plates but the skin preparation substrate yielded SPF *in vitro* values that more accurately reflected the SPF *in vivo* than the PMMA plates. This study revealed that besides roughness, the improved affinity of the sunscreen to the skin substrate compared to PMMA plates may explain the better *in vivo* prediction of SPF achieved with the use of the biological substrate.

In the second study, we aimed at understanding the relationship between thickness frequency distribution of a sunscreen film formed upon application and sunscreen efficacy since sunscreen formulations with the same UV filter system were reported to produce different SPFs. We developed a method to measure the film thickness of an applied sunscreen on pig skin substrate based on topographical measurements and investigated the influence of sunscreen vehicle and of sunscreen application on the average mean film thickness (Smean) and SPF *in vitro*. Five sunscreen vehicles were investigated including an oil-in-water cream, an oil-in-water spray, a water-in-oil emulsion, a gel, and a clear alcoholic spray. This work evidenced a strong influence of vehicle and application condition on sunscreen efficacy arising from differences in the film thickness. Low vehicle viscosity resulted in smaller Smean and lower SPF *in vitro* than high vehicle viscosity; continuous oil phase formulations produced the largest Smean and SPF values. Long spreading time reduced Smean and SPF; increased pressure reduced SPF. These results are of high practical importance in the route of understanding which parameters impact sun protection and subsequently how sunscreens work.

The third study relies on the second; the purpose was to quantitatively assess the role of film thickness frequency distribution for sunscreen efficacy. We developed a computational method for calculating the SPF *in silico* using besides the spectroscopic properties of the used UV filter mixture the complete thickness distribution of a sunscreen film obtained from topographical measurements.

The investigated formulations containing the same UV filter mixture differed in their SPF *in vitro* and film thickness distribution. We found a very good agreement between SPF *in silico* and SPF *in vitro* demonstrating the high relevance of film thickness distribution for the interpretation of sunscreen efficacy. Integrating vehicle-dependent film parameters into tools for *in silico* prediction of sunscreen performance is, therefore, of high interest to improve UV efficacy predictions.

Finally, the fourth study focused on the evaluation of the repartition of an oil miscible and a water soluble UV filter in the applied sunscreen film; the UV filters should be uniformly distributed throughout the sunscreen layer for optimum efficacy. We employed confocal Raman microspectroscopy (CRM) as a highly sensitive analytical technique to precisely detect the spatial distribution of the two investigated UV filters throughout the sunscreen film applied on a pig ear substrate in three different formulations. This work revealed noticeable differences in the repartition of the two studied UV filters depending on the sunscreen vehicle, clear alcoholic spray differed from other tested oil-in-water and water-in-oil formulations. The two UV filters appeared completely disjointed in the film formed by the clear alcoholic spray formulation indicating a non-homogeneous distribution of the two UV filters in the sunscreen film. This result is of high significance as a worse repartition of UV filters in the applied film would lead to reduced photoprotection when the UV filters show a different absorbance profile which is commonly the case.

This thesis provides novel insights into the understanding of the mechanisms that influence UV efficacy. The knowledge of the behavior of sunscreens with respect to film thickness distribution and repartition of UV filters is fundamental information that allows the optimization of a sunscreen formulation during early development stage helping expedite development. This advanced understanding in combination with *in vitro* and *in silico* methodologies may improve the ability to accurately predict SPF *in vivo* performance with the objective of reducing clinical trials in humans and in the long run in the establishment of a validated *in vitro* method.

Contents

Chapter 1

Introduction

1.1. Background

Over the past decades, the behavior of people toward sun exposure has changed a lot with a marked trend for outside recreational occupations, or travelling in countries where the sunlight intensity might not be adapted for their skin. This has led to generally higher and uncontrolled exposure of people to solar radiation. Although ultraviolet (UV) sun radiation is prerequisite for life on Earth needed for photosynthesis, and shows vital biological benefits [1], it is also recognized that excessive exposure to solar radiation causes detrimental health damages [2-5]. The type of photodamage is dependent on the wavelength range; some being associated rather to the exposure to UVB or to UVA radiation.

The main means of photoprotection are avoiding sun exposure, seeking shade, wearing clothes and hats, and applying topical sunscreens. The latter is an efficient, convenient, and simple means of sun protection [6,7]. The active ingredients of sunscreens are the UV filters that are able to absorb selectively a wavelength range in the UV spectrum[8]. The protection ability of a sunscreen principally depends on the UV filter system contained in the product with respect to the absorbing, photostability and photocompatibility properties of the UV filters, along with their concentration. The performance of a sunscreen is largely described by the sun protection factor (SPF) whose determination takes into account the human sensitivity to erythema.

SPF can be determined by *in vivo* [9], *in vitro* [10], or *in silico* [11] methodologies, but only the *in vivo* based method is currently approved by regulatory bodies. *In vivo* approach being time consuming, laborious, expensive and ethically questionable, there is a considerable interest from all players in the industry in developing an *in vitro* technique able to deliver SPF *in vitro* values matching clinical SPF *in vivo* values. The determination of the SPF *in vitro* is based on the measurement of the UV light transmitted through a suitable UV transparent substrate before and after sunscreen application [12,13]. A major issue for the establishment of an *in vitro* standard remains, most certainly, the choice of the substrate for sunscreen application that would be able to simulate human skin at best with respect to roughness and surface properties. Since the beginnings of SPF *in vitro* testing, different biological and synthetic substrate types have been employed [10,12,14-17], polymethylmethacrylate (PMMA) plates being the currently favourite substrate. However, despite the availability of PMMA plates with different roughness characteristics including a type developed especially to reproduce human skin roughness [18], none of these plates succeed in yielding SPF *in vitro* values in an accurate and reproducible fashion [19] correlating with the clinical SPF. As a result, there is still missing a proper substrate to succeed in the establishment of a validated *in vitro* method.

Further, another unclear aspect in measuring sunscreen performance is the experimental variability of SPF values obtained for sunscreens containing the same UV filter mixture [20,21] despite using the same methodology for SPF determination. Beyond UV filter system, other factors must play a role for sun performance. Some studies reported that the application procedure impacted performance and cream thickness; a more rubbed application led to a smaller SPF *in vivo* [22] and a crude compared to a careful application to a smaller cream thickness [23]. The effect of careful versus crude spreading of sunscreen on the magnitude of erythema occurrence was simulated, and underlined the "importance of homogeneity of spreading on the level of delivered protection" [24]. The ideal condition for optimum performance is the achievement of an uniform sunscreen layer with constant film thickness resembling the perfectly homogeneous distribution of UV filters into a solution state [25,26]. This can, however, never be attained under normal manual *in vivo* application since skin surface is not flat and precludes the achievement of an uniform film. The importance of homogeneity of distribution of the sunscreen on SPF efficacy was reported [27]. Nevertheless, the exact effect of vehicle on film formation remains unclear.

As a result, there is still an incomplete understanding of the mechanisms that influence sun protection of sunscreens once applied on a substrate with an unclear situation on the parameters that are relevant for UV efficacy besides the mere UV filter composition and UV filter concentration.

1.2. Objectives

The general aim of this thesis is to improve the understanding of the mechanisms of sun protection by a sunscreen applied on a substrate with the identification of factors that may influence sunscreen efficacy. This work is subdivided into five chapters, which address analytical-methodological and computational aspects of the performance evaluation of a sunscreen applied on pig ear skin substrate.

The theoretical section in Chapter 2 aims at reviewing on one hand the solar radiation and its effect on human health, and on the other hand the photoprotection, from natural to artificial, the latter focusing on the use of sunscreens. It gives a review on the UV filters, UV test methods, sunscreen norms, and consumer compliances.

Chapter 3 focuses on the use of skin from porcine ear as a substrate for SPF *in vitro* measurement. The aim is to examine the relevance of using a biological preparation for SPF *in vitro* measurement with the investigation if a biorelevant substrate may produce SPF *in vitro* values correlating better with SPF *in vivo* values compared to the currently used synthetic PMMA plates.

The purpose in Chapter 4 is the determination of the film thickness frequency distribution of different sunscreen formulations. The aim is to investigate if the divergence of efficacy between sunscreen vehicles containing the same UV filter composition may arise from the difference in the film thickness of an applied sunscreen on pig skin substrate.

Chapter 5 follows the study in Chapter 4 and aims at quantitatively assessing the role of film thickness frequency distribution for sunscreen efficacy. We used a computational method for calculating the SPF *in silico* by making use besides the spectroscopic properties of the UV filter system of the complete thickness distribution of a spread sunscreen film. SPF *in silico* was compared to the SPF *in vitro* to investigate the relevance of film thickness distribution for UV efficacy.

Finally, the objective in Chapter 6 is the investigation of the repartition of an oil miscible and a water soluble UV filter in the applied sunscreen film. The purpose is to assess the influence of the sunscreen vehicle on the UV filter distribution and subsequently on the delivered photoprotection.

Chapter 2

Theoretical section

2.1. Solar radiation

2.1.1. Sunlight

The sun emits to the Earth a portion of electromagnetic energy in the form of radiation. The solar spectrum is constituted from ultraviolet (UV), visible (VIS) and infrared (IR) radiation. UV radiation encompasses wavelengths between 290-400nm and is divided into UVC (200-290nm), UVB (290-320nm) and UVA (320-400nm) part; UVA being further subdivided into UVAII band extending from 320 to 340nm and UVAI band extending from 340 to 400nm. The visible part ranges from 400 to 780nm, followed by the infrared part from 780 to 3000nm. UV, VIS, and IR differentiate themselves with their energy and penetration depth ability into the skin; the longer the wavelength, the deeper the penetration into the skin layers. The short wavelength and high energetic UVC rays are absorbed through the stratospheric ozone layer by O2 and O3 molecules present at altitudes between 10 and 50km that subsequently prevents them from passing through the stratosphere and reaching the Earth surface and the skin [28]. The energy absorbed by the ozone layer is then released in form of heat responsible for the higher temperature of the stratosphere. Also, a large part of the short-wave UVB rays are blocked.

There is a significant environmental and health issue concerning the depletion of the stratospheric ozone layer by chlorine compound contained in the emission of Cholorofluorocarbons; a depletion of the ozone layer resulting in an increased amount of carcinogenic UV radiation reaching the Earth surface and an increase in skin cancer incidences [28,29]. The residual UVB and UVA rays reach human skin, UVB radiation is largely captured by the upper skin layers, whereas UVA radiation penetrates more deeply through the epidermis and dermis, attaining the connective tissue of the dermis [30,31]. In total, the UV region represents only 5% of the solar spectrum, but was shown to produce acute and chronic harmful health damages. UV are composed from around 3.5% UVB and 96.5% UVA on a summer day [32]; both show an irradiance peak maximum between 11.30am and 1.30pm [30], although UVA irradiance remains more stable throughout the day and the year compared to UVB irradiance that varies, UVA irradiance being higher in summer than in winter, at midday than in the morning or evening, at high altitudes, and accentuated in some geographical zones [33].

In comparison to UV, VIS light and IR are regarded as less harmful, whilst the effects of IRA drew some attention recently [34,35]. Infra-red radiation represents 30% of solar rays, they were shown to engender alteration of genes expression of skin cells [36], acceleration of skin ageing [37], and contribution to the development of cancers [38].

2.1.2. Effects of sunlight exposure

With respect to its effects on human the sun shows a dual behavior since it exhibits both positive and negative effects. Positive properties of sun exposure embrace psychologically and physically effects, but excessive exposure to solar radiation leads to detrimental health issues [39].

Sun damage might be expressed by following equation proposed by Cripps [40]

$$\text{Sun damage} = \frac{\text{UV intensity x duration of exposure}}{\text{nature of defense against damage}} \qquad (2.1)$$

where, the received UV intensity varies depending on geo-orbital and environmental factors [32]; principally on the season [33], time during the day [41], latitude [33], surface reflection [42], and weather; the duration of exposure depends principally on the amount

of exposure time, occupation, and area of exposed body sites [41]; and the nature of defense refers principally to the individual natural protection factor, reinforced with artificial protection means such as sunscreens.

2.1.2.1. Benefits from sun exposure

An important vital beneficial biological effect is the synthesis of vitamin D produced in the skin after exposure to sunlight [43]. Vitamin D shows an action spectrum with a maximum (λmax) at 295nm and is, therefore, built principally under UVB exposure. Vitamin D is further metabolized to produce the biologically active vitamin D metabolite involved in the support of calcium homeostasis by interacting with specific receptors in the bones and intestine, and is, therefore, essential to develop and maintain a healthy mineralized skeleton [1]. Besides calcium fixation, active vitamin D was also involved in immunoregulation, protection against oxidative stress [44], and against infectious agents. A deficiency in vitamin D was shown to be involved in multiple types of cancers [45,46], and risk of incident hypertension [47]. Besides vitamin D formation, sunlight is also used to treat skin diseases such as psoriasis [48] and is also well known to promote feeling of well-being. Currently, more often the adverse effects of the sun are put forward as excessive exposure to sunlight was shown to induce diverse immediate and long-term photo-damages. The effect on skin and health is highly wavelength dependent; some photo-damages are induced more by UVB and others more by UVA radiation.

2.1.2.2 Adverse effects attributed mainly to UVB exposure

A single acute exposure to UVB radiation results in the immediate and familiar cutaneous response called erythema, or more commonly known as sunburn. Sunburn is characterized by a skin redness, sensation of burning, with potentially the formation of oedema and is due to the liberation of inflammatory mediators resulting in a vasodilatation. The UV dose required to induce an erythemal response is dependent on the wavelength.

The wavelength at which erythema formation is maximal (λmax) is approximately 308nm [49]. Histological and biochemical changes after induction of an erythema reaction were studied [50]. Major histological alterations were the formation of altered keratinocytes (sunburn cells) and disappearance of Langerhans cells in the epidermis, and vascular changes in the dermis. At a biochemical level, Histamine content rose inducing the early phase of sunburn through vasodilation, while Prostaglandin E2 rose progressively. At a molecular level, a major adverse effect of UVB irradiation is DNA damage [51]; UVB rays are directly absorbed by cellular DNA leading to DNA lesions such as the formation of cyclobutane pyridimine dimers (CPD) and pyrimidine photoproducts (6-4PP), the UVB signature, which maximum induction in human skin was shown to be around 300nm [52-54]. These UVB-induced DNA damages were shown to be responsible for gene mutation, e.g. inducing the dysfunction of tumor suppressor genes such as p53 protein in humans and mice [51,55-58] that was shown to contribute to skin cancer development in humans and in animals [59]. Mutations in p53 tumor suppression gene arise before the appearance of skin tumors, they were detected in sun-exposed skin from normal patients and actinic keratoses, suggesting that p53 mutations early biological indicator of skin cancer risk.

2.1.2.3. Adverse effects mainly attributed to UVA radiation

Exposure to UVA radiation leads to an immediate and weak skin pigmentation known as immediate pigment darkening (IPD) believed to be due to a photo-oxidation of existing melanin [60]; IPD is weak and difficult to measure as it is unstable and fades rapidly within minutes to about two hours depending on the UVA irradiation dose [61]. It is replaced by the persistent pigment darkening (PPD) which lasts for 24h under sufficient UVA irradiation [62]. UVA-induced skin pigmentation is not protective [63]. IPD is driven by exposure at wavelengths in the UVA to VIS region (320-700nm) [64], while PPD may result either from UVC, UVB, or UVA exposure and leads to an increase of melanin, the natural UV filter of the skin. UVA radiation is mostly responsible for chronic photo-damages such as skin pigmentation (age spots), induction of oxidative stress [65], and visible effects of premature skin ageing through the generation of reactive oxygen species (ROS) [66] and induction of Matrixmetalloproteinase (MMP) [67,68].

Photo-aged skin is characterized among others by skin dryness, wrinkles, elastosis [69-71], irregular pigmentation particularly in Asians [72], immunosuppression [2,73], and actinic keratose [74-76] since UVA rays penetrate more deeply into the dermis achieving the connective tissues compared to UVB [66,77]. A review on photoaging, its mechanisms and repair opportunities is given by Rabe *et. al* [78] .

Exposure to a very high UVA dose is also able to induce an erythema, about 1000 times higher than required for UVB [79].

At a molecular level, UVA rays are also able to induce CPDs [80-82], and to generate ROS via the absorption through endogenous photosensitizer compounds [35,83]. ROS are then able to produce diverse adverse effects such as photo-ageing [74], immunosuppression in animals and humans [84], mutation in mitochondrial DNA [66], and skin cancers [85] by damaging DNA by an indirect mechanism [86]. It was shown that UVA induced melanomas and melanoma precursors in two animal models [87].

2.1.2.4. Skin cancers

- Types of skin cancers

Exposure to UV light is the most important factor responsible for skin cancer occurrence, it is also one that can be controlled by ourselves. Both UVB and UVA radiation is classified as human carcinogen [88]. Three main types of skin cancer with respect to the involved cells exist, the two non-melanoma skin cancers including squamous cell carcinoma (SCC) and basal cell carcinoma (BCC) and malignant melanoma the most lethal form of skin cancer [89]. SCC mainly occurs in sun-exposed areas and its occurrence is associated with chronic exposure to UV radiation during lifetime [90] ; BCC and melanoma are rather associated with intermittent sun exposure e.g. sunburning. Mutation of p53 gene was shown to be involved in squamous cell carcinoma (SCC) and basal cell carcinoma (BCC). Skin cancer represents a significant and growing public health concern worldwide as incidences have steadily increased in recent decades [91]. This may be related to a change in lifestyle habits with an increase of outside recreational occupations and of vacation to countries where the sunlight may not be suited to the skin type.

- Incidences and sunscreen use

It is, thus, not surprising that Australia shows the highest incidence rate of skin cancer [92] most probably in connection with the fair skin of Australian population and the high intensity of the sun; in the opposite Japan and China show the lowest melanoma incidences most probably due to the cultural attitude difference of Japanese and Chinese people towards sun exposure. The incidences of malignant melanoma in the D-A-CH (Germany, Austria, and Switzerland) region are about quarter to half the incidences in Australia but are, however, much higher than in Japan [93]. The role of sunscreens in skin cancer prevention is still discussed controversially as some studies have shown either no association or even a positive association between sunscreen use and skin cancer [94]. However, an explanation for this paradox is the use of sunscreens with small SPF values, in an inadequate amount, and that were UVB biased at the time of most conducted studies; also the lack of considering positive and negative confounding were problematic for a correct interpretation of the study data [95]. However, an Australian study conducted in the 1990s by Green consisting of a five years long randomized trial, "the Green study" showed the protective benefits of regular application of a sunscreen with SPF 16 in prolonged prevention of SCC and reduction of incidence of new primary melanomas for up to 10 years after trial cessation [4,96]. Based on this outcome, US-FDA (Food and Drug Administration) is the first authority to officially consider sunscreens as a means to reduce the risk of skin cancer and to allow a direct claim of skin cancer risk prevention for sunscreens with a labeled SPF of at least 15 and complying with the UVA recommendation as reported in the final monograph for Sunscreen Drug Products for Over-the-Counter Human Use published in 2011 [97]. Developing efficient sunscreens with modern UV filters is essential in helping to reduce the continuous growth of new skin cancers related to sun exposure.

- Epidemiology and skin cancers

Some studies reported the positive relationship between frequency of occurrence of erythema in childhood till 15 to 20 years of age and increased risk of melanomas in adulthood [98,99]. This is supported by the fact that teenagers and young adult more often get erythema due to their poor protection behavior [100], less than 40% use sunscreens. Roughly, 25% of lifetime sun exposure occurs before 18 years of age [101].

Similarly, a positive relationship was found between incidence of skin cancers and increasing amount of ambient UV radiation, e.g. higher latitude where the sun irradiance is greater [98,102].

Further, fair skinned individuals are more disposed to develop non-melanoma skin cancers than dark skinned individuals [103,104], due to the differences in the amount of UV-induced free radicals and better prevention of DNA damage for heavily pigmented melanocytes than their lighter counterparts [105,106].

2.2. Natural photoprotection

2.2.1 Properties of human skin

When sunlight hits the skin, it can be absorbed in the different cell layers, transmitted till dissipated, or scattered back [107]. Skin being an heterogeneous material is able to scatter incident light beam as a result of abrupt changes in the refractive index (RI) of air (RI of air=1.00) and that of stratum corneum (RI of SC is of around 1.52 [108]); the RI of skin is independent of skin type and age of human subjects [109]. Approximately 4% of incident radiation is scattered back when attaining the skin surface [110]. The intensity of scattering within the dermis is inversely proportional to the wavelength; therefore, attenuation of light through scattering decreases with increased wavelength resulting in deeper penetration depth for greater wavelength. Human epidermis shows a minimal transmission in wavelengths around 275nm since it contains natural UV absorbing chromophores that absorb in this range. These include aromatic amino acids (λmax =275nm), nucleic acids (λmax =260nm), urocanic acid (λmax =277nm). Peptide bonds are responsible for the light absorption of skin of wavelengths smaller than 240nm [111].

After UV irradiation, one of the mechanisms of skin protection is the thickening of the stratum corneum with an increase of number of cell layers in stratum corneum [112]. It was reported that thickness of the stratum corneum accounts for 2/3 of the photoprotection of normal skin, whereas thickness of epidermis was not important [113]. Further, another natural protection mechanism is the synthesis and redistribution of melanin, the natural UV filter of the skin.

2.2.2 Constitutive skin color

Human skin color is considered either as constitutive or facultative [114]. Constitutive skin color refers to the base or natural skin color without any solar exposure, in the contrary of facultative skin color corresponding to a tanning induced by solar exposure [63].

Human skin possesses its own line of defense against UV light irradiation, the production of melanin, a natural UV filter [115] present in two forms, the brownish-black eumelanin and the reddish-yellow pheomelanin[116]. Difference in human skin color most probably is related to the balance between these two forms of melanin [117]. Fitzpatrick classification gives six skin phototypes with respect to skin color as given in Table 2.1 [118].

Table 2.1. Skin phototypes according to Fitzpatrick classification

Skin type	Characteristics
I	White skin, reddish hair color
	Always burns easily, never tans
II	White skin, blond hair color
	Always burns easily, tans minimally
III	Burns moderately, tans gradually
IV	Burns minimally, tans well
V	Rarely burns, tans profusely
VI	Almost never burns, deeply pigmented

There are considerable differences in melanin content and composition in the skin of the different human ethnicities [119]. The natural level of protection against UV irradiation is different among human races and is related to the amount of eumelanin versus pheomelanin: Pheomelanin being predominant in fair-skinned people is also responsible for the weak capacity of photoprotection of this people [120]. Human skin color is not random but has evolved with migration of people to adapt to sunlight intensity in the different world zones [121,122]. Natural selection of skin color allows a balance between the protection of body´s folate being destructed under UV irradiation that is necessary for DNA synthesis and cell division, and the production of vitamin D under UV exposure necessary among others for the development of the skeleton [123].

Constitutive melanin shows an absorption spectrum with a maximum around 335nm and which extends over the whole UV and VIS range [115,124-126], the absorbance spectrum of the two forms of melanin being quite similar, but differs after UVA irradiation. Differences in the amount of melanin produced in the melanocytes, in the transfer and distribution of melanosomes to the keratinocytes, are responsible for the differences in natural UV protection between humans with different skin colors [127]. This relative natural photoprotection factor or melanin protection factor against erythema varies from a factor normalized to 1 for skin type 1 to nearly 10 for skin type 6 according to Cripps [40], meaning that skin type 6 owns due to its darker skin color a natural photoprotection that is ten times greater than skin type 1. Kaidbey reported a UV transmission through epidermis five times higher for Caucasians than for black skin [128]. Further, the constitutive pigmentation was shown to afford a DNA protection factor of 2 and 4 for fair and black skinned people [129].

Absorption spectra of UV induced melanogenesis and erythema are similar suggesting that the two endpoints have a common chromophore most probably in the same epidermal site [120,130]. Also erythemal spectrum was reported to be similar to that of DNA photodamage in the form of cyclobutane pyrimidine dimers, and by spectral association for melanogenesis.

2.2.3. Facultative skin color

Facultative skin color refers to an UV-induced pigmentation. Delayed skin pigmentation i.e. tanning occurs within few days after UV exposure and lasts for months and is referred to as melanogenesis, a natural protection. The size and number of melanocytes, melanosomes and melanin increase to reinforce natural defense against UV exposure; suntan enhancing the natural protection factor by a factor between 2 and 3 for skin types II to IV [40,131], meaning that there is no correlation between the level of tan and protection against erythema. UV-induced tanning means that skin was exposed to UV radiation inducing a protection reaction.

Tanning appears to be an early reaction of the skin to signal that long-term damages are being induced [77], however, tanning is still associated by people to be a trendy, attractive, and healthy looking. A means to achieve this desirable fashion tanning is the exposure under artificial source e.g. tanning bed. Since the early 1970s sunbed industry was born and use of sunbeds is widespread today. Sunbed users mainly include young people [132]. Tanning beds predominantly emit UVA radiation, although a small amount of UVB radiation [133]. The intensity of UVA radiation of tanning lamps can be 10 to 15 times higher than that of the midday sun. These high UVA doses might be responsible of erythema occurrence reported by some sunbed users [133], their danger on human skin was addressed [77]. An association between the incidence of cutaneous melanoma and non-melanoma skin cancers with sunbed use especially when initiation occurs early in life was established [134-138]. Based on rising evidence about the carcinogenicity of artificial tanning lamps, regulation on sunbed industry was strengthen over past decade, especially for young people; sunbed use is banned for people under 18 in UK and several other European countries, Australia, parts of Canada and USA, and is completely banned in Brazil [139].

2.3. Artificial photoprotection

2.3.1. History of sunscreens

Besides sun avoidance, shade seeking, clothes and hat wearing, topically applied sunscreens are a simple, suitable, and efficient means to protect against harmful photo-damages [95]. Sunscreens contain special active ingredients, UV absorbing compounds also referred to as UV filters, to provide protection against UV irradiation. In the 1950s -1960s at the beginnings of sun protection with topical sunscreens, the prime objective was to protect against erythema, the immediate and visible sun damage. Since erythema mainly originates from UVB radiation, the first developed UV filters were absorbing in the UVB range. In 1956, the concept of SPF for rating the protection ability of a sunscreen was invented by Schulze, and allowed a direct comparison of performance between sunscreen products [140]. Firstly, sunscreens showed very low SPFs attained values up to 4.

Tremendous changes in lifestyle habits due to higher incomes and paid holiday led to an increase of outside recreational occupations and of vacation to countries where the sunlight may not be suited to the skin type. This led to the increase of the sunscreen market with the development of products with growing SPFs attaining values as high as 20 in the 1980s. In the beginnings of the 1990s, it was recognized that UVA irradiation was not as harmless as thought, and rather results in long-term health damage, especially with respect to premature ageing of photo-exposed skin.

Furthermore, over exposure to sunlight owing to sun-seeking practice of white Caucasians to get tanned or to the tendency of spending leisure time outside also led to long-term damage such as skin cancer. This conducted to a slow change in consumer attitudes toward sun exposure. Over last decade, the placement on the market of new, photostable, broad-spectrum and UVA filters allowed a considerable improvement of the sun protection profile of sunscreens claiming nowadays SPF values up to 50+ [141].

2.3.2 Requirements for good photoprotection

Osterwalder & Herzog identified four key requirements for a good UV protection [142]:

- Technology
- Assessment and measurement methods
- Norms and standards
- Compliance

These requirements interlink and are influenced by different stakeholders; achieving only one of these aspects is not sufficient for delivering an adequate photoprotection, e.g. developing a sunscreen with efficient UV filters is not enough to guarantee satisfactory photo-protection. The performance of the sunscreen product has to be evaluated and characterized according to standards, and consumers must ultimately apply the product in a sufficient manner to get the expected UV protection.

2.3.2.1. Technology

UV filters are the core ingredients of sunscreen products; they are able to reduce the intensity of UV light reaching the skin. UV filters are generally classified in organic and inorganic particulate UV filters; the organic class being further subdivided into soluble and particulate compounds. The soluble organic UV filters act by absorption, whereas the mechanism of action of particulate UV filters includes absorption, scattering and reflection [143,144]. Particulate UV filters are able to increase the optical path length of UV radiation due to their inherent scattering properties, thereby increasing the likelihood of UV radiation to meet a dissolved UV filter molecule before reaching the skin surface. They are able to amplify the UV performance of the used filtering system resulting in a boosting of the UV protection [145,146].

- Organic UV filters

UV filters contain suitable chromophors, a group of atoms, able to absorb wavelengths greater than 200nm that is possible with conjugated π–electron systems. As a generality, a large chromophor enables a stronger absorption, and a greater number of conjugated double bonds in the molecule shifts the absorption maximum towards longer wavelengths [147]. UV filters may be in the form of a liquid, a powder, or a particulate dispersion. The two commercialized particulate organic UV filters, MBBT (INCI, Methylene Bis-Benzotriazolyl Tetramethylbutylphenol) and TBPT (INCI, Tris Biphenyl Triazine), are obtained from a milling process that results in a water dispersion of particles whose average size approximates 160nm and 120nm for MBBT and TBPT, respectively [148,149]. The original particle size is reduced to achieve maximum absorbance efficacy; the absorbing properties being directly dependent on the particle size [150]. This type of UV filter combines the advantages of soluble organic UV filters as well as of particulate inorganic UV filters. Forward and backward scattering contribute to about 10% of the overall effect in the region of absorption band for MBBT [150].

- Inorganic UV filters

Micronized titanium dioxide and zinc oxide are the two main representatives of the category of inorganic UV filters [143,151,152]; some authors proposed cerium oxide as a new innovative inorganic filter [153,154], which is, however, not yet allowed for use as a UV filter. Titanium dioxide used for suncare application shows a primary particle size ranging from 10 to 30nm, but forms aggregates into dispersion resulting in a size as high as 100 nm in formulations. With this particle size, titanium dioxide is quite transparent on skin, to the opposite of titanium dioxide grades used for decorative cosmetics whose size is rather close to 200nm to provide desired opacity on skin for foundation for example. The part of light attenuated through absorption versus scattering phenomenon highly depends on the size of the particle; in the grades used for sunscreens, absorption is the major mechanism of action. Titanium dioxide being highly photo-catalytic [155], the cosmetic grades of titanium dioxide are, therefore, coated to prevent the formation of free radicals under light exposure; several types of coating exist including stearic acid and alumina, silica, dimethicone, or aluminum hydroxide and stearic acid. Regarding zinc oxide, it can be used coated or non-coated.

To be fully usable in sunscreens, Osterwalder & Herzog defined four basic requisites for UV filters [142]:

- Efficacy: UV filters are characterized by and differ in their absorbance profile, E1,1, and photostability profile
- Safety
- Registration
- Patent freedom

The lack of one of these requirements highly compromises the chances of commercialization and/or market success; safety and registration being a must.

- **Efficacy**

UV filters are characterized by their absorbance properties. UVB, UVA, or broad-spectrum UV filters are available, nowadays it is, therefore, technologically possible by combining several UV filters with complementary absorbance profiles to cover the whole UV range for achieving optimum photo-protection. First UV filters mainly consisted of UVB absorbing compounds to protect against erythema.

Over last decade, several UVA and broad-spectrum filters were developed and placed on the market enabling a breakthrough in sun protection [156,157].

Figure 2.1. illustrates the absorbance profile of two sunscreens with the same nominal SPF value of 30 but different UVA protection. The typical absorbance profile of an "old" sunscreen (black line) is UVB biased whereas the absorbance of a "today" sunscreen (dashed line) shows a more balanced absorbance within the UVA protection range.

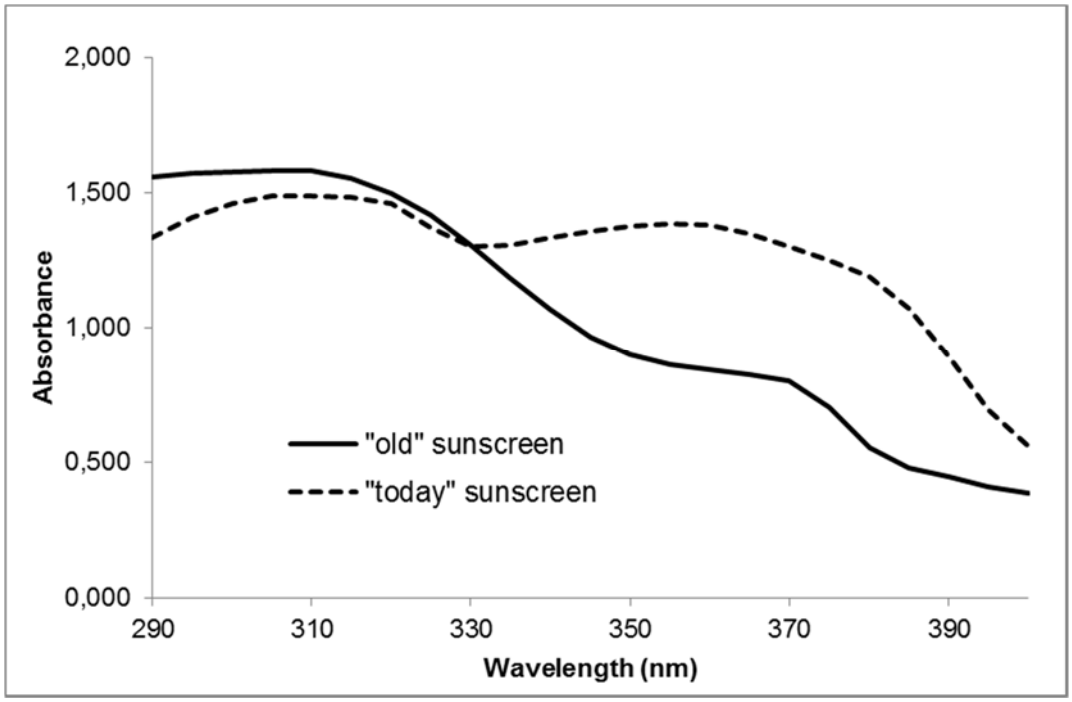

Figure 2.1. Absorbance profile of an "old" sunscreen (black line; 10% ethylhexyl methoxycinnamate, 5% titanium dioxide, 5% zinc oxide) and of a "today" sunscreen (dashed line; 1.5% ethylhexyl triazone, 2% bis-ethylhexyloxyphenol methoxyphenyl triazine, 7% methylene bis-benzotriazolyl tetramethylbutylphenol)

Generally, a smaller concentration of UV filters is necessary for UV filter mixture that shows a balanced absorbance profile in comparison to a UV filter mixture with a UVB biased UV absorbance; in figure 2.1. a concentration of 20% of UV filters is required for the "old" sunscreen type to achieve the same SPF value as for the "today" sunscreen requiring a concentration of UV filters of 10.5% only.

Besides their intrinsic absorbance properties, UV filters are characterized also by their intrinsic photo-stability and photo-compatibility with other UV filters [158]. The two worldwide accepted UVA filter BMDBM (INCI, butylmethoxy dibenzoylmethane) and UVB filter EHMC (INCI, ethylhexyl methoxycinnamate) are known to be very photo-unstable under UV exposure, thus, resulting in a loss of performance [159-161]. The photostability was shown to be impacted by the solvent used [162,163]. Moreover, their combination leads to an increased photochemical instability due to a 2+2-hetero-photocycloaddition producing non-UV absorbing cyclobutylketone photoproducts [162,164]. This photo-incompatibility finally results in a lower UV protection as expected from the mere spectroscopic characteristics of the UV filters [165]. This issue often obliged sunscreen manufacturers to use either the one or the other filter in their sunscreen development.

Molecules that absorb energy from UV radiation move from a ground state (S0) to an excited singlet state (S1) by a delocalization of an electron. This excited state being instable, several processes to dissipate the absorbed energy exist either through emissions or through radiationless pathways as depicted in the Jablonski diagram in figure 2.2. In the case of the photo-unstable UV filter BMDBM, the molecule can perform an intersystem crossing from the singlet exited state to the triplet excited state, the latter showing a longer lifetime and, therefore, promoting photo-degradation of the molecule [166]. As a consequence, the stabilization of photo-unstable UV filters such as BMDBM is possible either by quenching the excited singlet state [167,168] to avoid the formation of the triplet excited state or by quenching the formed triplet excited state [169-171]. Triplet-triplet energy transfer from the photo-unstable molecule to the quencher molecule is the most common energy transfer mechanism for photo-stabilization. To make this process working, the quenching molecule must show an equal or slightly lower energy level to that of the photo-excited state of the photo-unstable molecule in order to absorb the excitation energy [166,172].

For photostable UV filters the dissipation of absorbed energy occurs through internal conversion, the absorbed in then released into harmless heat via energy transfer by collision to surrounding molecules [173].

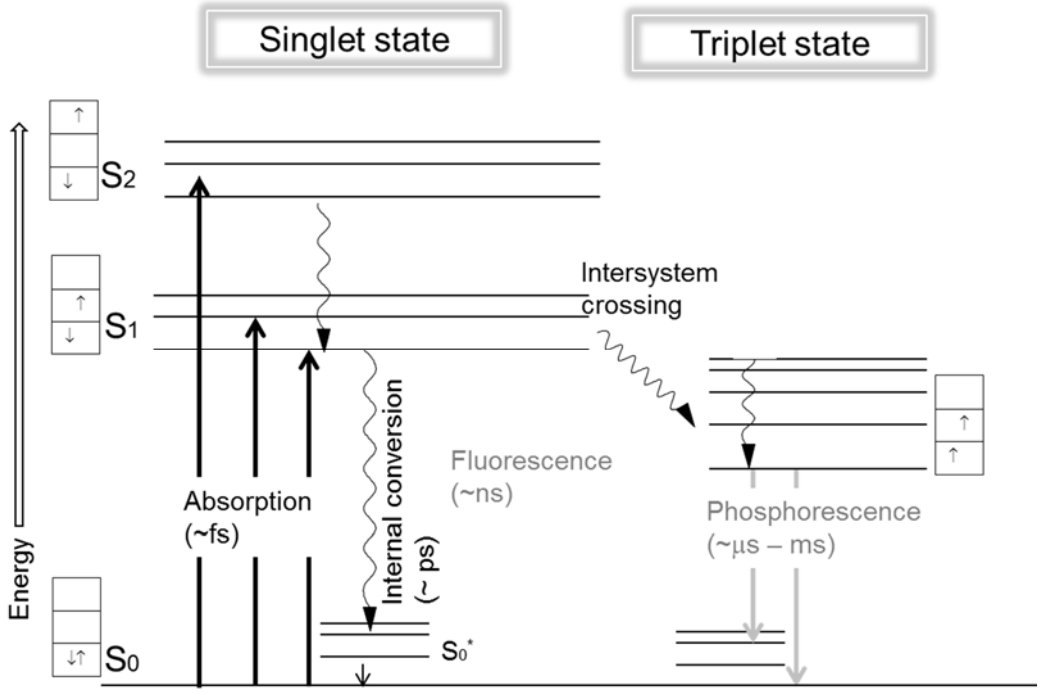

Figure 2.2. Jablonski diagram for electronic transitions and dissipation pathways after excitation of a molecule

- **Safety**

UV molecules must at first be approved to be allowed for use in sunscreens. A requisite for approval is safety, irrespectively of the regulatory environment. A dossier containing the data related to a series of toxicological tests to ensure human safety must be prepared and submitted to the relevant authority. Only UV molecules that are irreproachable with respect to their toxicological profile can be approved. As a general rule, tests including skin irritation, skin corrosion, eye irritation, skin sensitization, mutagenicity, toxicity, carcinogenicity, reproductive toxicity, and percutaneous absorption are required for the human safety and health risk assessment. In Europe, toxicological assessment is performed according to the SCCS (Scientific Committee on Consumer Safety) guidelines requirements. The safety is then evaluated by the SCCS publishing a scientific opinion that must be positive so that the European commission finally votes the official addition of the new UV molecule onto the annex VI of the European Cosmetic Regulation 1223/2009/EU listing the permitted UV filters in Europe. This is a very structured approval process.

Since 2013, there is an animal testing ban for any new cosmetic ingredient that leads to an unclear situation regarding the registration of new UV filters as no *in vitro* replacement exists for all requested human safety tests.

- **Registration status**

The regulation of sunscreens strongly differs between the main geographical regions [174]; sunscreens are regulated either as cosmetics in Europe, Over-The-Counter in US, or quasi-drugs in Japan. To be allowed for being used, UV filters must be listed on a positive list giving all permitted UV filters with their maximum allowed concentration, e.g. on annex VI of the European Cosmetic Regulation for EU or in the FDA over-the-counter sunscreen monograph for US. Other similar positive listing exists for most countries. As a general observation, the requirements for registering a new UV filter become more and more stringent, as with the example of the "nano issue" in Europe recently. TBPT, the latest approved UV filter in Europe, is an organic nano particulate UV filter that was submitted for safety evaluation to the SCCS in 2005 and placed finally on the Annex VI on the European Regulation on cosmetic products in August 2014 only. This delay of several years in the expected registration date was directly linked to consequences of the nano-related concern topic and the new requirements of registering the nano form of the UV molecule requiring new tests. New UV filters usually are developed, approved and commercialized at first in Europe followed very rapidly by other regions such as South America, Korea, Japan, and Asean. To the opposite, in the USA the registration of a new UV filter is a very long process that is very complex. The approval of the last UV filter on the sunscreen monograph in the USA dates from 1998; it was BMDBM approved in Europe already in 1978. The creation of the TEA (Time and Extent Application) procedure was aimed to ease the approval of new filters in the USA. However, this route was not yet very successful as six UV filters including EHT (INCI, ethylhexyl triazone), IMC (INCI, isoamyl p-methoxycinnamate), BEMT (INCI, bis-ethylhexyloxyphenol methoxyphenyl triazine), MBBT (INCI, methylene bis-benzotriazolyl tetramethylbutylphenol), TDSA (INCI, terephthalidene dicamphor sulfonic acid), and DTS (INCI, drometrizole trisiloxane) are in the TEA pipeline; some awaiting for approval since 2003. This missing registration of the newest UV filters in the USA locks the development of global worldwide formulations for sunscreen manufacturers and prevents the accessibility of latest technologies already available outside the USA for American consumers.

- **Patent freedom**

The UV filter molecule and its combination with other UV filters and formulation excipients should be intellectually protected as largely as possible by the UV filter manufacturer. This is necessary to ensure freedom of use of the UV filter ingredient by any sunscreen manufacturer. The risk of weak patent protection of a new compound is that the new molecule is blocked from third party patents in specific ingredient combination or application claims that hinder other sunscreen players to use the UV compound in the specific patented claims. This can be a very strong limitation of the concerned UV filter, its use, market penetration and growth, as well as finally for the end consumer who in some cases can not benefit from the newest technologies.
Besides traditional patent filling, it is nowadays possible to strategically quickly publish on the internet information related to the new ingredient e.g. combinations or claims, enabling creation of prior art in the form of technical disclosure to prevent blocking patents from third parties (e.g. www.ip.com).

A summary of the main UV filters with the wavelength of their highest absorbance (λmax), their E1,1, (absorption corresponding to a concentration of 1% (w/v) solution at an optical thickness of 1 cm), and registration status is given in Table 2.2.

Table 2.2. Main UV filters with their specific characteristics

UV filter (INCI abbr.)	**λmax (nm)***	**E1,1***	**Registration status**	**Physical form**
BEMT	310 & 343	736 & 819	World except USA, in TEA	Powder, oil soluble
MBBT	305 & 360	419 & 519	World except USA, in TEA	Particulate water dispersion
DHHB	354	900	World except USA	Powder, oil soluble
BMDBM	357	1120	World	Powder, oil soluble
TBPT	310	1170	Europe	Particulate water dispersion
EHT	314	1448	World except USA, in TEA	Powder, oil soluble
EHMC	311	803	world	Liquid, oil miscible
OCR	303	355	world	Liquid, oil miscible
PBSA	303	927	world	Water soluble, to be neutralized
EHS	305	196	world	Liquid, oil miscible
TiO2	290	500	world	Particle, powder or in dispersion

* The data of the λmax and E1,1 were provided by BASF

The values for TiO2 depend on the commercial grade; here the values correspond to Eusolex T-2000 from Merck.

2.3.2.2. Assessment and measurement methods

The efficacy of sunscreens is largely expressed by the SPF value and level of UVA protection. Methods to measure these two parameters are, therefore, necessary to characterize the level of protection of a sunscreen with respect to these two criteria. Test methods can be based on *in vivo*, *in vitro*, or *in silico* methodologies. As a general statement, i*n vivo* methods show the drawbacks of being costly, time consuming and ethically questionable. Therefore, the development of *in vitro* methods that are faster, simpler, and cheaper is of general interest.

- **Sun protection factor (SPF)**

The SPF value gives the degree of protection afforded by a topical sunscreen against erythema; it was the first criterion introduced for describing the level of protection of a sunscreen. It remains a very-well known protection-related indication for the consumer and also a purchase criterion [175]. It can be tested *in vivo*, *in vitro*, or even *in silico;* nevertheless, only the *in vivo* procedure has been validated and is approved so far by regulatory bodies [9].

Figure 2.3. illustrates the erythema effectiveness spectrum showing the wavelength range responsible for erythema formation (black line) [176]. The erythema effectiveness spectrum is the product of the erythema action spectrum [9,176] that gives human sensitivity to erythema (gray line) and the spectral irradiance of terrestrial sunlight (dashed gray line) given here for midday midsummer sunlight for Southern Europe (latitude 40°N) [15]. It is clear from figure 2.3. that erythema originates primarily from UVB radiation, but figure 2.3. also reveals that UVAII (320-340nm) radiation contributes to a certain extend to the erythema development as well [177,178].

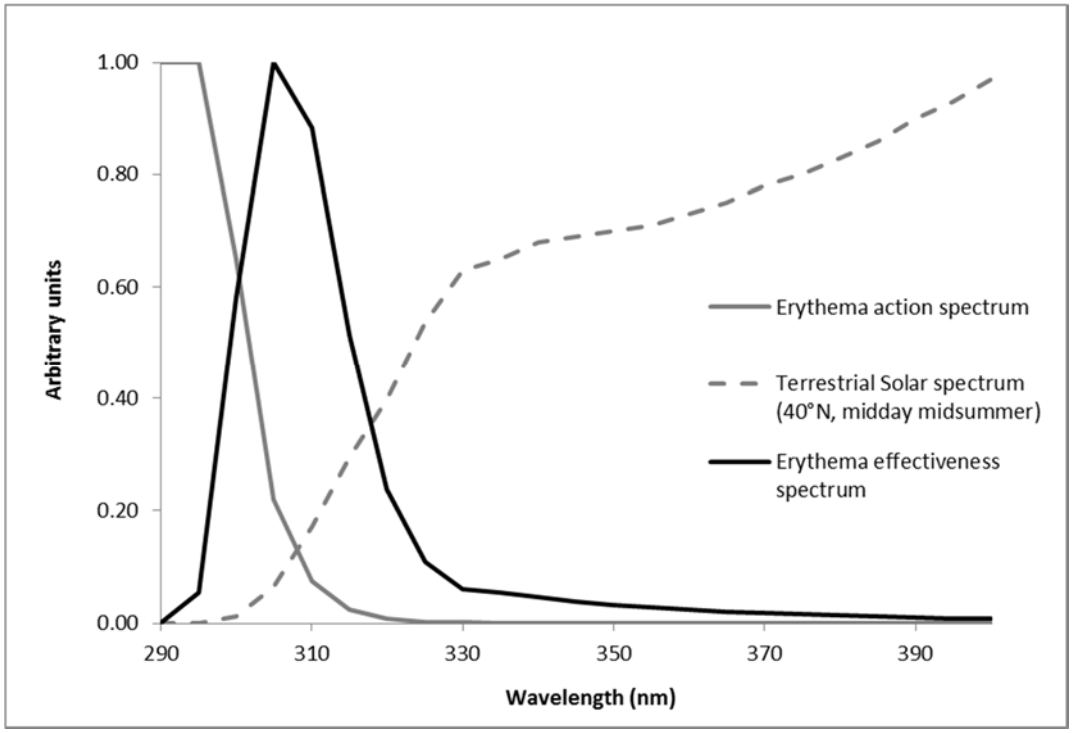

Figure 2.3. Erythema effectiveness spectrum (black line) expressing the occurrence of erythema dependent on wavelength being the product of the erythema action spectrum (gray line) [9,176] and the terrestrial solar spectrum (dashed gray line) [15]

o SPF *in vivo*

SPF *in vivo* is the gold standard for the evaluation of sunscreen efficacy; it is defined as the ratio of minimal erythemal dose (MED) on sunscreen protected skin (MEDp) and unprotected skin (MEDup) and is expressed by Equation (2.2.):

$$\text{SPF in vivo} = \frac{\text{MED}_\text{p}}{\text{MED}_\text{up}} \quad (2.2)$$

The MED describes the minimal UV energy required to initiate the first perceptible erythema, or minimal erythemal response. Erythema response is maximum 6 to 24h after irradiation depending on the applied dose [179]. It is evaluated by applying incrementally increasing UV doses from an artificial light source with a solar-simulated spectrum [9] on areas of human volunteers` back on sunscreen protected and unprotected zones. As the MEDp and MEDup are determined on the same human volunteers, skin type is not impacting the determination of the SPF *in vivo*.

The determination of this mere biological endpoint does not provide any information on the absorbance profile of the studied sunscreen, meaning that two sunscreens may exhibit the same nominal SPF value but may highly differ in their UVA protection as explained previously (section 2.3.2.1, figure 2.1.).

- SPF *in vitro*

Because of the drawbacks of *in vivo* testing, much effort has been placed into the development of an *in vitro* methodology for SPF determination. However, up to now, despite cosmetic, pharmacological and chemical laboratories, institutes, and task forces put a lot of efforts in developing an *in vitro* SPF technique correlating with the clinical *in vivo* SPF, no undertaken attempt led to reproducible, repeatable and reliable outcomes. Many challenges remain [19], a major issue most probably is the substrate used to apply the sunscreen. SPF *in vitro* determination is based on the measurement of UV transmittance through a layer of sunscreen applied on a suitable UV transparent substrate [13]. UV transmittance represents the inverse of an UV attenuation factor of a protecting sunscreen film described by the following relationship [12]:

$$\text{SPF } in\ vitro = \frac{\sum_{290}^{400} s_{er}(\lambda).S_s(\lambda)}{\sum_{290}^{400} s_{er}(\lambda).S_s(\lambda).T(\lambda)} \qquad (2.3.)$$

where, the inverse transmittance (1/T) in the UV spectral range is weighted with the erythema action spectrum [9], $s_{er}(\lambda)$, and the spectral irradiance of the UV source [9], $S_s(\lambda)$. As data for $s_{er}(\lambda)$ and $S_s(\lambda)$ are available from literature, the SPF *in vitro* is determined from UV transmittance between 290 and 400 nm before and after application of a sunscreen applied on suitable UV transparent substrate [13]. Many different kinds of substrates have been used since the beginnings of *in vitro* SPF including either biological or synthetic substrates. Biological skin substrates used for testing sunscreen performance include epidermis of human [14,180] of pig ear [181,182], and of hairless mouse [12,183].

Synthetic sources include materials such as one-side roughened quartz plates, surgical adhesive tape (transpore tape) fixed on a flat quartz plate [14,15,184], synthetic skin (vitro skin) [185], and PMMA plates [10,16,17], the latter are presently favored. PMMA plates are either sand-blasted or molded on one side to create a certain roughness varying between 5 to 17 μm depending on the plate type, supposed to simulate roughness of human skin [18,186]. However, none of these substrates succeed in achieving a reproducible method that further correlated with the clinical standard SPF [19]. Several factors were shown to impact the SPF *in vitro* measurement [187,188] , one major factor most probably being the surface properties [189]. To produce relevant data, the substrate should at best simulate human skin characteristics with respect to roughness and more particularly with respect to surface energy properties to reproduce at best the application of the *in vivo* situation. However, surface free energy of currently employed PMMA plates do not reproduce human skin surface properties; different solutions were proposed to increase the product-to-substrate affinity [189,190]. However, none of these attempts were very promising as not applicable for all formulations.

- SPF *in silico*

Some authors introduced an *in silico* approach for the calculation of the performance of sunscreens [191,192]. The evaluation of the SPF *in silico* makes use of the same algorithm as for the determination of the SPF *in vitro* (Equation (2.3.)). However, the measured UV transmittance used for the *in vitro* method is substituted by a calculated transmittance in the *in silico* approach. The calculation of the UV transmittance requires the spectroscopic performances (spectral average molar absorption coefficient and the molar concentration) of the studied UV filter mixture [193], the amount of the used UV filters [193], and the properties of the applied film meaning the nominal average film thickness along with a mathematical model to describe sunscreen film irregularity profile. Several models for expressing film thickness distribution were described starting from the “two-step film model” by O`Neil in 1984 [25], the " four-step film model" by Tunstall [194], the "calibrated two-step film model" by Herzog [193] to the “continuous height distribution model” using a Gamma function by Ferrero [191,195] and the calibrated quasi-continuous step film model by Herzog [196]. The “sunscreen simulator” calculation tool from BASF, freely available on the internet (www.basf.com/sunscreen-simulator) allows the calculation of the SPF and UVA indices.

For more precision and correlation of predicted SPF *in silico* values to the *in vivo* values, this tool further considers the photo-instabilities of the individual UV filters, the photo-incompatibilities between UV filters, the photo-stabilization effect of some UV filters on others [197] as well as the synergistic effect obtained from the distribution of UV filters in the oil and water phase of an emulsion [192]. The potential effect of the formulation base is, however, not yet taken into account.

- Meaning of SPF

A widespread misconception is that SPF 60 is not twice as effective as SPF 30 due to the small difference in percentage of filtered UV radiation between these two SPFs, 96.7% and 98.3% for SPF 30 and SPF 60, respectively. However, a much more relevant criterion for UV protection is how much UV radiation is transmitted to the skin, e.,g. 3.3% and 1.7% for SPF 30 and SPF 60, respectively meaning that only half of photons will reach the skin when using a SPF 60 compared to a SPF 30. This is a factor 2 difference confirming that SPF 60 is twice as effective as SPF 30 in the amount of light transmitted [198].

- **UVA protection**

Compared to UVB irradiation, UVA irradiation rather results in long-term sun damages, and, therefore, was considered for a long time, wrongly, as harmless regarding human health. Evidence on UVA-related health damages conducted to the development of UVA and broad-spectrum filters [173]. Several *in vitro* and *in vivo* based methods for assessing the performance of a sunscreen against UVA exposure were introduced in the different world regions. Different methods became standard for UVA testing in different regions; UK, Japan, and Australia were the pioneers in UVA protection testing.

- 1992 - UK

In 1992, Boots introduced in the UK the Boots star rating system based on the determination of the UVA:UVB ratio *in vitro*, that is the average absorbance in the UVA divided by the average absorbance in UVB range. The method was revised in 2008 and in 2011 with the introduction of an UV exposure step with a fixed dose of 17.5 J/cm^2 and represents still the standard for UVA testing in UK [199]. The protection is expressed as a number of stars, according to the value of the ratio before and after irradiation.

- 1995 - Japan

The *in vivo* determination of the UVA-PF corresponding to the measurement of the PPD was the first official standard for UVA testing established in Japan by the Japan Cosmetic Industry Association (JCIA) in 1995. UVA-PF is measured similarly to the SPF *in vivo*, but using an UVA lamp for irradiation excluding UVB radiation to produce UVA-related skin persistent pigment darkening. UVA-PF *in vivo* is the ratio of minimal persistant pigment darkening dose (MPPDD) on sunscreen protected skin (MPPDDp) and unprotected skin (MPPDDup). The MPPDD is defined as the lowest UVA dose needed to induce demarcated and easily identified persistent skin pigmentation. According to the value of the UVA-PF, different levels of UVA protection can be claimed. Since 2011, this procedure is an official ISO method and is still used in Japan as the official UVA protection testing [200].

- 1998 - Australia

In 1998 Australia established the *in vitro* Australian Standard based on UV transmittance measurement of tested sunscreen in an optical cell of 8μm thickness. Broad-spectrum claims were allowed when the transmission at any wavelength between 320 and 360nm was lower than 10%. This parameter is a pass / fail criterion that was very weak as it was achieved very easily, especially with large SPF values.

- 2006 - Europe

The effort of sun care stakeholders, task forces, suncare manufacturers, institutes for a global harmonization resulted in the validation and publication of an official ISO method in 2010 for UVA testing that is, nowadays, used as a standard in many regions including Europe, Australia, China, South America [201]. It is based on a combination of *in vitro* and *in vivo* measurements. The UVA-PF (UVA protection factor) is calculated from *in vitro* absorbance measurement from 320 to 400nm before and after irradiation according to Equation (2.4.):

$$UVA - PF_{invitro} = \frac{\sum_{320}^{400} s_{UVA}(\lambda) \cdot S_{PPD}(\lambda)}{\sum_{320}^{400} s_{UVA}(\lambda) \cdot S_{PPD}(\lambda) \cdot T(\lambda)^{C}} \quad (2.4)$$

where, S_{UVA} is the spectral irradiance for the UVA source [201], S_{PPD} is the persistence pigment darkening action spectrum [201], and C an adjustable parameter to adjust the *in vitro* spectrum in such a way that SPF *in vitro* equals SPF *in vivo* value. UVA-PF is first calculated from the transmittance curve of unexposed sample after adjustment to the *in vivo* SPF by multiplying the absorbance values with the scaling factor C. The UVA-PF value before irradiation, UVA-PF_0, is used for determining the irradiation dose corresponding to 1.2 x UVA-PF_0 in J/cm^2. The UVA-PF after irradiation is calculated as previously after mathematical adjustment of the absorbance curve using the same value for factor C. The UVA-PF must be at least one third of the SPF *in vivo* to claim an UVA protection.

- 2011 - US

In the USA, the FDA adopted in the final sunscreen monograph published in 2011 the critical wavelength (λ_c) *in vitro* method based on the approach introduced by Diffey in 1994 [202] with the addition of a fixed pre-irradiation step. It consists of determining the wavelength at which the spectral absorbance curve reaches 90% of the integral over the UV spectrum from 290 to 400nm; the larger the λ_c, the greater should be the UVA protection. Tested sunscreen must reach at least a λ_c value of 370nm to be allowed to claim broad-spectrum protection. This method, however, appears to be a weak criterion that is reached easily especially with larger SPFs and that does not allow huge differentiation between sunscreens with respect to UVA protection [203,204], moreover, the fixed irradiation dose is modest considering the highest allowed SPF claim of 50+.

- **Factors that impact performance of sunscreens**
  - Amount of applied sunscreen

Major influencing factor for delivered protection is the amount of sunscreen applied. The observed relationship between SPF and application amount is quasi-linear [19,205].

Though, for UVB biased sunscreens, this relationship shows a saturation-like effect of the SPF with increased application amount, indeed the UVB loaded sunscreen will continue to transmit the erythemally active UVAII radiation independently from the application amount. Indeed, a mere "UVB sunscreen" would reach in principle a maximum SPF of 11 only [206]. On the other hand, homeostasic sunscreens, with similar UVB and UVA protection will rather show an exponential behavior in dependence on the application amount. Yet, most sunscreens on the market show a linear relationship. Clinical SPF is measured using a defined application amount of sunscreen of $2mg/cm^2$, however, consumers generally use much less. Only 18% of respondents of an interview about suncare knowledge in New Jersey know about the right amount of sunscreen to apply [175]. Methods employed to estimate the application amount of people under real life are often based on weighing the sunscreen bottle before and after use by naïve volunteers and converting into an amount in mg/cm^2 [207-210]. Other authors used an approach based on fluorescence spectroscopy [211] or a technique using swab [212]. These studies revealed that consumers usually apply only a quarter to half of the amount used for official *in vivo* SPF determination meaning that the delivered SPF is half as high as claimed.

- Spectral source

The spectral irradiance of the light source used for *in vivo* performance evaluation differs from spectral irradiance of terrestrial sunlight as depicted in figure 2.4. The solar-simulated light source used for *in vivo* testing is UVB biased and is filtered in the UVAI and visible range [9] compared to the terrestrial sun spectrum [15]. These differences have nearly no consequences on the prediction of the real protection to natural terrestrial sunlight exposure for sunscreens showing a broad-spectrum absorbance profile as the protection provided is uniform independently from the wavelength. On the other hand, the SPF is overestimated for UVB biased sunscreens under solar-simulated light source exposure compared to the real sun protection under natural terrestrial sunlight exposure [26,213,214].

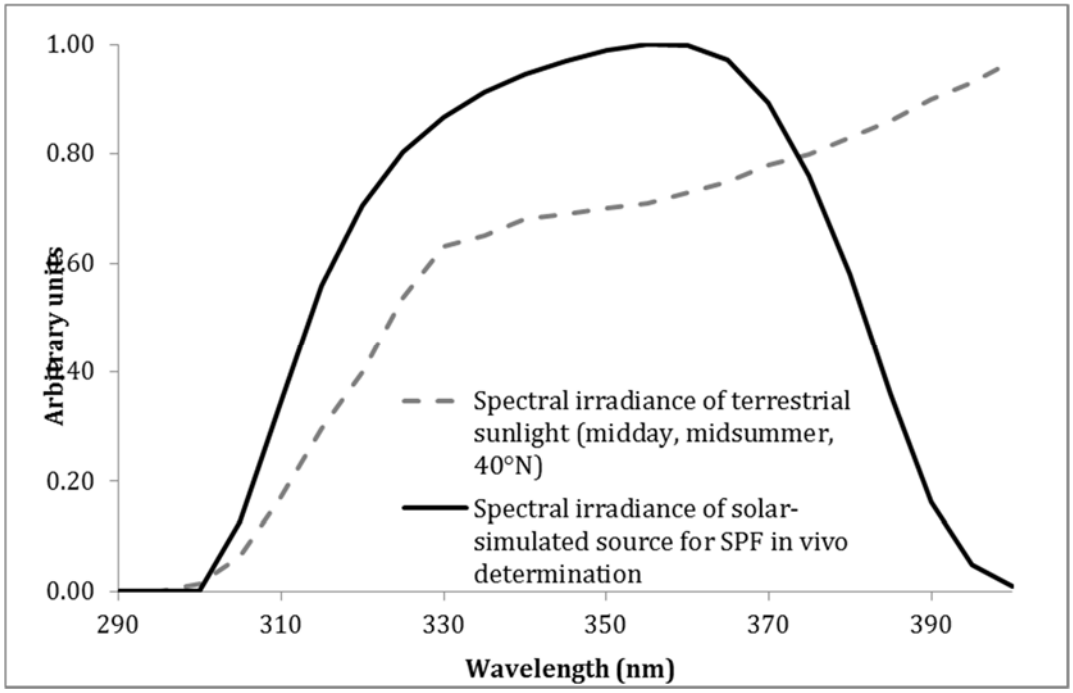

Figure 2.4. Terrestrial solar spectrum [15] versus solar-simulated [9] spectrum

o Impact of skin status on erythema sensitivity

The status of the skin e.g. dry versus wet prior UV exposure was reported to impact light transmission through skin. Pre-immersion of skin into liquid media prior UV irradiation leads to an increase in light transmission due to the reduction of reflection and scattering onto the skin surface and to the reduction of internal scattering in the cell layers and intercellular material, the skin becoming more transparent [215]. The transmission increases over all wavelengths as the refractive index (RI) of the liquid in which the skin is immersed approaches the RI of skin (RI of stratum corneum =1.52 [107]). Immersing skin into liquids with RI greater than water (RI of water=1.33) such as emollients that generally show RI>1.45 results in a greater light transmittance through skin than water does. This was shown in human volunteers after the application of an oil-in-water (OW) formulation that increased UV light transmission through the epidermis by 20% between 300 and 410 nm [216]. This effect is responsible for the increased sensitivity to erythema for wet skin e.g. during swimming or sweating, resulting in a reduced MED and a more erythematous skin for wet compared to dry skin. This was tested in humans [217] as well in hairless mice and albinos rabbits skin [218].

- Sunscreen vehicle and application

Some authors reported that sunscreens containing the same UV filter mixture produced different SPF values [20,21] and the homogeneity of the spread sunscreen film was of importance for performance [24,27].

2.3.2.3. Norms and standards

The setting of norms and standards is essential for characterizing a good UV protection. Regarding SPF measurement, there is more or less an harmonization in the SPF measurement and claim as published by the Official Journal of European Union in 2006 [219].

For UVA protection, the global picture is much more complicated than for the SPF criterion since a variety of methods and parameters are available to express UVA protection differing between the regions. Some methods are based on a pass / fail criterion, some on a rating system. Since the procedures of testing e.g. *in vivo* or *in vitro*, the irradiation step, and the claims differ between the methods, a comparison of the level of protection against UVA exposure between the methods is difficult.
Table 2.3. summaries the UVA test methods and associated allowed claims.

Table 2.3. Summary of UVA standards and associated UVA protection claims

Region	**Europe Australia Mercosur**	**UK**	**Japan**	**USA**
Method	ISO 24443	Boots star rating	ISO 24442	Final rule sunscreen monograph
UVA factor				
in vitro	UVA-PF & λc	UVA:UVB ratio	-	λc
in vivo	UVA-PF (PPD)	-	UVA-PF (PPD)	-
UVA Claim and conditions	UVA UVA-PF/SPF ≥ 1/3 and λc ≥ 370nm	UVA from three to five stars	PA+ (UVA-PF : 2-4) PA++ (UVA-PF : 4-8) PA+++ (UVA-PF:8-16) PA++++(UVA-PF≥16)	Broad-spectrum when λc ≥ 370nm

2.3.2.4. Compliance

A sunscreen exhibiting a great SPF and good UVA protection, having good photostability, and being water resistant can only be fully effective and provide the expected photoprotection if the final user applies it in the amount used in the performance testing procedure and as uniformly as possible. This is known as consumer compliance. Lack of compliance has different reasons, technological, UV knowledge-related, awareness, and varied messages through public education.

- Technological reasons

Among the mentioned technological reasons, the bad sensorial aspect of sunscreens e.g. tackiness, greasiness, difficulty of application, is a major factor [220-222]. Aesthetics appears to be a key criterion for the amount applied by volunteers [223]. A consumer study with four distinct sunscreens has shown a strong correlation between the distribution properties and the willingness to use the sunscreen [93]. It is, thus, the ultimate objective for sunscreen manufacturers to develop formulations that improve consumer compliance by proposing products that consumers are willing to apply properly to achieve the promised protection that is, the right amount in a uniform way.

- UV knowledge-related reasons

Merely 50% of the respondents know the meaning of SPF, however, only 18% know about the right amount to apply [175].

- Awareness

Quite a high percentage of individuals, 86%, 70%, and 64% of respondents of a study on sunscreen knowledge know that sunscreen can prevent sunburn, skin cancer, and signs of skin aging, respectively [175]. Despite the spread knowledge of UV-induced damages, 83% of young adults reported at least one sunburn during the summer.

- Public education

Increase awareness of sun-safety behaviors is primordial. Wang summarized the aspects of public education in photoprotection [224]. There are two main motivation factors to increase awareness of people on UV-induced photodamage aiming at increasing compliance. These are health-based and appearance-based [225-227]; health-based messages focusing on skin cancer risks and appearance-based on skin aging. Messages should come from health care providers, or media and organization; they should be simple, straightforward, and appeal to people´s intellectual and emotional receptivity.

2.3.3. The ideal sunscreen, outlook in the future of photoprotection

2.3.3.1. Homeostasic UV protection

There are two basic dimensions in UV protection, the quality and quantity of protection. The ideal sunscreen should protect against the different known photo-damages, short term as well as long-term, particularly sunburn, skin photo-aging, and skin cancer, coming rather from the one or the other wavelength range. During evolution, human skin has evolved and adapted to be in harmony with the terrestrial solar spectrum [122]. This means that in avoiding sun or seeking natural shade the quantity of sunlight reaching our skin is quantitatively reduced while only minimally qualitatively modified. as an example, fabrics are an efficient means of homeostasic UV protection as fabric absorbs light uniformly over the whole UV range [228,229]. Further, protecting skin by wearing fabric during UV exposure was shown to reduce photoaging, skin pigmentation, and skin dehydration [230].

The ultimate goal is, therefore, the development of innovative sunscreens that would protect similarly to textile. The ideal sunscreen should provide uniform protection over the entire UV range in order to attenuate the intensity of sunlight without modifying the quality of this natural solar spectrum to which human has adapted and evolved.

2.3.2.2. Benefits of daily photoprotection

There are more and more daily care products containing UV protection on the market with SPF reaching values up to 30. There is no recommendation on the UVA protection a daily care should afford; however, it is meaningful that day care products provide a broad protection over the UV range, ideally attaining homeostasis. Exposure measurement to solar UV radiation in an urban environment during typical outdoor activities e.g. shopping, walking, sitting in a café, cycling, or at an open air pool revealed that there are some risk situations and UV protection should be applied for certain activities even in a city [231]. A daily UV protection was shown to reduce significantly UV-induced histologic damage in human skin compared to the protection afforded by sunscreens with equal or higher SPF value applied in an intermittent manner [232]. A day care with a photostable and broad-spectrum protection was shown to prevent major alterations connected with photoaging [233,234], a balanced absorbance spectrum in UVA achieving better protection against fibroblast alteration and MMP-1 release , higher SPF do not compensate for low UVA protection [235], daily use of a broad-spectrum sunscreen was also shown to reduce solar keratose a precursor of SCC [236] and to provide a better protection against UV induced suppression of contact hypersensitivity [237]. It is, therefore, highly recommended to apply a daily UV protection, more particularly with a broad-spectrum absorbance profile.

Chapter 3

Porcine ear skin as a biological substrate for *in vitro* testing of sunscreen performance

3.1. Abstract

The purpose of the study was to examine the use of skin from porcine ear as a biological substrate for *in vitro* testing of sunscreens in order to overcome the shortcomings of the presently used polymethylmethacrylate (PMMA) plates that generally fail to yield a satisfactory correlation between sun protection factor (SPF) *in vitro* and *in vivo*. Trypsin-separated stratum corneum and heat-separated epidermis provided UV transparent substrates that were laid on quartz or on PMMA plates and were used to determine surface roughness by chromatic confocal imaging and measure SPF *in vitro* of two sunscreens by diffuse transmission spectroscopy.

M. Sohn et al., "Porcine ear skin as a biological substrate for in vitro testing of sunscreen performance," Skin Pharmacol. Physiol. 28(1), 31–41 (2015).

The recovered skin layers showed a lower roughness than full thickness skin but yielded SPF *in vitro* values that more accurately reflected the SPF determined by a validated procedure *in vivo* than PMMA plates, although the latter had in part roughness values identical to those of intact skin.

Combination of skin tissue with a high roughness PMMA plate also provided accurate SPF *in vitro*. Besides roughness, the improved affinity of the sunscreen to the skin substrate compared to PMMA plates may explain the better *in vitro* prediction of SPF achieved with the use of biological substrate.

3.2. Introduction

Over the past decades, lifestyle habits have undergone substantial changes with a marked trend for outside recreational occupations that have led to generally higher and uncontrolled exposure of people to solar radiation. Although ultraviolet (UV) sun radiation is vital with biological benefits such as the synthesis of vitamin D [1], it is also recognized that excessive exposure to solar radiation causes detrimental health issues. UVA and partly UVB rays reach human epidermis and dermis at an intensity that enables them to produce diverse immediate or long-term photo-damages, as thoroughly compiled by Seité and Matsumura [238].

Besides the appearance of the known erythema mainly as an immediate response to UVB exposure, a major adverse effect is DNA damages [51] that can, on the long run, lead to skin cancer. UVA radiation is mostly responsible for chronic photo-damages such as skin pigmentation (age spots), induction of oxidative stress [65], photoimmunosuppression [2], visible effects of premature skin ageing [76] and contribution to skin cancer by generation of radical oxygen species [35].

Topically applied sunscreens constitute a suitable and commonly employed measure to protect skin from sun damages. To date, the SPF is still the predominant criterion used to describe the degree of photo-protection afforded by a topical sunscreen.

The only validated procedure for SPF determination is an *in vivo* measurement on human volunteers [9] based on erythemal response, a biological endpoint mainly attributed to UVB radiation. *In vivo* methods have the drawbacks of being costly, time consuming and ethically questionable. Therefore, there is considerable interest from the industry in developing an *in vitro* approach to SPF testing.

Although industry players have put a lot of effort in developing an SPF *in vitro* technique that correlates with the clinical SPF *in vivo*, no undertaken attempt has been validated, many issues still remaining [19].

One major influence factor for successful establishment of a standard method for SPF *in vitro* testing is the choice of a substrate for sunscreen application that best mimics human skin. The current use of roughened polymethylmethacrylate (PMMA) plates for this purpose failed to yield satisfactory results [19]. The reason of the persisting discrepancies between *in vivo* and *in vitro* data might be that PMMA plates do not properly imitate human skin.

Attempts to use alternative substrates to better imitate skin surface have been reported. Very early studies with hairless mouse epidermis for SPF *in vitro* measurements with a scanning spectrophotometer provided encouraging results [12,183]. Other workers used human epidermis as substrate and demonstrated a good correlation between *in vitro* and *in vivo* protection factor that was measured, however, only at one wavelength [180].

The aim of the present work was to investigate the use of skin from porcine ear as a biological substrate for *in vitro* testing of sunscreen performance. The pig ear skin was compared to PMMA plates that are currently the industry standard for SPF *in vitro* measurement. Porcine skin is already extensively employed in pharmacological and toxicological research as an *in vitro* model of human skin because of the high degree of similarity between the two tissues [239,240]. A number of studies employing pig as *in vitro* model of human tissue have been summarized by Simon [241]. These studies report of the overall anatomical and physiological resemblance between pig and man. The likeness of stratum corneum (SC) between skin of porcine ear and human skin encompasses several aspects. Corneocytes of pig skin have a polygonal shape [242,243] and size [243,244] which are close to the morphological examinations reported for human corneocytes [243,245]. Moreover, thickness [239,240,242,243], barrier function [239], and penetration properties [246] of the SC have been found to be analogous in pig and in human.

A UV transparent substrate, which is a prerequisite for transmittance measurement, was obtained by isolating only the upper skin layers of pig ears using two different preparation methods. In a first step, we characterized the recovered upper skin layers with respect to thickness and roughness and compared the results to data available for human skin. In a second step, we measured the SPF *in vitro* of two distinctive sunscreens using the different porcine skin substrates and a standardized solar irradiance profile. The results were compared to SPF *in vitro* obtained with PMMA plates and to the SPF *in vivo* of the individual sunscreens and evaluated with respect to substrate properties that are relevant for proper prediction of SPF.

3.3. Materials and methods

3.3.1. Chemicals and equipment

The following reagents were used: Trypsin 2.5% (10X) liquid (Gibco, Zug, Switzerland); sodium chloride, sodium hydroxide 1 M, sodium phosphate monobasic and trypsin inhibitor from glycine max (Soybean) 10000 U/mg (Sigma-Aldrich, St Gallen, Switzerland); Tinosorb S, Tinosorb M, Uvinul T150, Uvinul A Plus, Uvinul MC80 abbreviated as BEMT, MBBT, EHT, DHHB, EHMC, respectively (BASF AG, Ludwigshafen, Germany); Eusolex 232 abbreviated as PBSA (Merck, Darmstadt, Germany).

Quartz plates were obtained from Helma Analytics (Zumikon, Switzerland), polymethylmethacrylate (PMMA) plates from HelioScreen Labs (Marseille, France), Schönberg Kunststoffe (Hamburg, Germany) and Shiseido Irica technology (Kyoto, Japan), and petri dishes from Nunc (Roskild, Denmark).

The following equipment was used: Electric shaver (Favorita II GT104, Aesculap, Germany), epilator (Silk-épil7 Xpressive Pro, Braun, Germany), dermatome (Air Dermatome, Zimmer Inc., United Kingdom), water purification equipment (Arium 61215, Sartorius, Goettingen, Germany), Raman confocal laser scanning microspectrometer (Alpha 500R, WITec, Ulm, Germany), surface texture analysis instrument (Altisurf 500, Altimet SAS, Thonon-les-Bains, France), UV transmittance analyzer (Labsphere UV-2000S, Labsphere Inc., North Sutton, NH, USA).

3.3.2. Preparation of biological substrate

Ears of freshly slaughtered pigs were obtained from the local slaughterhouse (Basel, Switzerland) no more than a few hours postmortem. The study did not require the approval of the ethics committee of animal research as the ears were taken from pigs not specifically slaughtered for the purpose of this study. The ears were washed under running tap water, shaved, and epilated.

The full thickness skin of the dorsal side was removed from the underlying cartilage using a scalpel and served as the starting material for further preparation. Two different methods were used for tissue preparation. The methods and the used support materials are summarized in Table 3.1.

Table 3.1. Skin sample types used in the study

Skin preparation	Material for deposition	Analysis
Trypsin-separated SC	Quartz	UV Transmittance measurement
	PMMA SPF Master PA-01	UV Transmittance measurement
	Petri dish	Thickness measurement
Heat-separated epidermal membrane	Quartz	UV Transmittance measurement
	Petri dish	Thickness measurement

3.3.2.1. Method 1 - Isolation of stratum corneum (SC) by trypsin treatment (modified method after Kligman [247])

Sheets of full thickness skin were dermatomed to a thickness of around 500 µm. This tissue was immediately used or stored at -20°C until further use. After washing with water purified by reverse osmosis, the dermatomed skin was laid flat with the stratum corneum facing upward on filter papers saturated with trypsin solution (0.5% in phosphate buffer at pH 7.4) in a glass petri dish and stored for 4 h at 37°C in a saturated vapor atmosphere. The digestion occurred from the dermis end of the tissue, ensuring that SC remained undamaged. The top layer representing stratum corneum was carefully removed using forceps and washed with purified water. Compared to Kligman [247], the recovered SC slice was additionally immersed in trypsin inhibitor solution (0.01% in phosphate buffer at pH 7.4) for 2 h at 37°C to stop the enzymatic reaction. The tissue was washed again with purified water and kept in phosphate buffer. Finally, pieces of SC were placed flat either on quartz plates or on PMMA SPF Master PA-01 plates for SPF *in vitro* measurement, or on polystyrene petri dishes for thickness analysis. When SC was laid on PMMA plates, vacuum was applied to prevent air enclosure between the SC and the plate. The plates with the SC were stored at 4°C in a desiccator over saturated sodium chloride solution (relative humidity of 80%) until use.

3.3.2.2. Method 2 - Isolation of epidermal membrane by heat treatment

The sheet of full thickness skin was immediately used or stored at -20°C until further use. The skin was thawed if necessary at room temperature and immersed in a water bath at 60°C for 60 s. Subsequently, the epidermal membrane was separated from the dermis by gentle peeling off [248]. The isolated epidermal membrane was then laid on quartz plates for SPF *in vitro* measurement or on polystyrene petri dishes for thickness analysis. The prepared samples were stored at 4°C in a desiccator over saturated sodium chloride solution until use.

3.3.3. Skin tissue thickness measurement

Raman confocal laser scanning microspectroscopy (Alpha 500R, WITec, Ulm, Germany) was employed for tissue thickness measurement. Raman spectra were recorded from 0 to 4000 cm^{-1} (spectral grating of 600 g/mm, spectral resolution of 3 cm^{-1} per pixel) using a 532 nm excitation laser source, a Nikon EPI plan 100x 0.95 numerical aperture (NA) objective and an integration time of 1s. The equipment permitted an x-y resolution of 340 nm and a z resolution of 500 nm. This technique combines Raman spectroscopy with confocal microscopy allowing a depth analysis of the sample.

The thickness of the isolated tissue was assessed by scanning the samples over a line of 40 µm in the x direction (with 120 points per line) and over a depth of 40 µm in z direction (with 240 lines per image). The measurements were conducted in cluster analysis modus with the WITec control software. The raw data were evaluated with WITec Project Plus 2.04 software.

3.3.4. Polymethylmethacrylate plates

Three types of PMMA plates served as synthetic UV transparent substrate. The plates are roughened on one side to mimic skin surface and differ in their manufacturing process and topographical property (Table 3.2).

Table 3.2. Characteristics of PMMA plates

	Helioplate HD6	**Schönberg**	**SPF Master PA-01**
Manufacturer	HelioScreen Labs	Schönberg	Shiseido Irica technology
Manufacturing process	Mold injected	Sand-blasted	Mold injected
Surface size as supplied	4.7 cm x 4.7 cm	5.0 cm x 5.0 cm	5.0 cm x 5.0 cm
Surface size adjusted for the study	2.0 cm x 2.0 cm	2.0 cm x 2.0 cm	2.0 cm x 2.0 cm
Roughness Ra or Sa given by the supplier	Ra=4.5 µm	Ra=5.9 µm	Sa=17.8 µm
Applied amount of sunscreen for SPF *in vitro* testing	1.3 mg/cm^2	1.3 mg/cm^2	2.0 mg/cm^2

3.3.5. Surface topographical assessment

We carried out surface topographical measurements of skin specimens laid on quartz or PMMA plates and of the PMMA plates by chromatic confocal imaging based on white light chromatic aberrations principle using the Altisurf® 500 instrument. This allowed non-contact surface topography measurement and analysis. The employed optical sensor allowed an axial resolution (z) of 5 nm and a lateral resolution (x-y) of 1.1 µm. The motorized x-y table permitted scanning of samples in the mm range based on which the three-dimensional microtopographical surface structure of the samples was reconstructed.

In this study, an area of 5 mm × 5 mm was scanned in 10 µm increment steps and the arithmetical mean height over an area, Sa (Equation 3.1., ISO 25178 guideline [249]), was selected as a representative measure of skin surface topography [250]. This measure was also used for the PMMA plates.

$$Sa = \frac{1}{LxLy}\int_{0}^{Lx}\int_{0}^{Ly}|Z(x,y)|dxdy \qquad (3.1.)$$

where, Lx and Ly is the length in the x and y direction, respectively. Z(x,y) is the altitude of the sampling point measured from the sampling surface. Use of an areal parameter such as Sa for describing surface texture better serves the needs of the present study compared to, for example, the roughness over a profile (e.g. Ra in ISO 4287 guideline [251]) which has also been used to describe skin surface.

3.3.6. Sunscreen formulations

We tested the *in vitro* and *in vivo* performance of two Oil-in-Water (OW) sunscreens. The filter system and the SPF *in vivo* of the sunscreens measured in accordance with ISO24444:2010 guidelines [9], are given in Table 3.3.

Table 3.3. Tested sunscreens

Sunscreen	***In vivo* SPF**	**UV filter (%) as active ingredient [b]**					
designation	**mean ± SD[a]**	EHMC	BEMT	MBBT	DHHB	EHT	PBSA
OW Nr.1	27.5 ± 7.6	5	2	4	-	-	-
OW Nr.2	19.9 ± 5.8	-	2	-	4.5	3	2

[a] SPF *in vivo* evaluated in accordance with ISO24444:2010 guidelines, with n=5

[b] abbreviation: EHMC, Ethylhexyl Methoxycinnamate; BEMT, Bis-Ethylhexyloxyphenol Methoxyphenyl Triazine; MBBT, Methylene Bis-Benzotriazolyl Tetramethylbutylphenol, DHHB, Diethylamino Hydroxy Hexyl Benzoate; EHT, Ethylhexyl Triazone; PBSA, Phenylbenzimidazole Sulfonic Acid

3.3.7. Measurement of the sun protection factor *in vitro* using spectral transmission of ultraviolet radiation

SPF *in vitro* is derived from diffuse transmission spectroscopy measurements based on the model proposed by Sayre [12].

$$\text{SPF } in\ vitro = \frac{\sum_{290}^{400} s_{er}(\lambda).\, S_s(\lambda)}{\sum_{290}^{400} s_{er}(\lambda).\, S_s(\lambda).\, T(\lambda)} \qquad (3.2.)$$

where, $s_{er}(\lambda)$ is the erythema action spectrum as a function of wavelength λ [9], $S_s(\lambda)$ is the spectral irradiance received from the UV source at wavelength λ [9], and $T(\lambda)$ is the measured transmittance of the light through a sunscreen film applied on a suitable UV transparent substrate [13].

The spectral UV transmittance was recorded from 290 to 400 nm in 1 nm increment steps through a substrate before and after application of a sunscreen using the Labsphere UV-2000S. The linear range of the device was checked by measuring the absorbance of increasing concentrations of the UVB filter ethylhexyl methoxycinnamate in ethanol solutions and plotting the measured absorbance data against the expected absorbance.

The blank transmittance spectrum before application of the sunscreen was recorded for the PMMA plates using the plates covered with glycerin and for the skin substrates using the bare skin specimens on quartz or PMMA SPF Master PA-01 plates without further treatment [248]. For the PMMA plates, a single blank transmittance spectrum was measured in the center of a plate and used for the evaluation of the SPF values of all plates of the same type. For the skin samples, a blank transmittance spectrum was recorded in each single measurement position. We applied 1.8 mg/cm^2 of sunscreen on the skin samples; the amount of sunscreen applied on the PMMA plates is given in Table 3.2. The application of the sunscreen and the equilibration step were conducted as previously reported [223].

A surface area of substrate of 2 cm × 2 cm was used in the SPF measurements. This area was chosen because skin specimens of this dimension could be easily prepared. The impact of the surface area of the substrate on SPF *in vitro* was assessed by comparing PMMA plates with a size of about 5.0 cm × 5.0 cm which are routinely used, with plates cut to 2.0 cm × 2.0 cm.

3.3.8. Statistical analysis

Statistical analysis was performed using Statgraphics centurion XVI (Statpoint Technologies, Inc., Warrenton, VA, USA) software. The statistical significance at 5% confidence level of the difference between two groups was evaluated using Mann-Whitney test.

3.4. Results and discussion

3.4.1. Skin thickness

Thickness of human and porcine ear skin is commonly measured by light microscopy of histological sections of stained skin biopsies using formalin-paraffin or freezing preparation [240,252]. Thickness of SC was measured by tape stripping requiring determination of the amount of removed corneocytes [253]. Such procedures are generally time consuming and may introduce artifacts due to preparation or data evaluation. A non-invasive method based on confocal Raman spectroscopy that required no tissue preparation was introduced for measuring SC thickness *in vivo* on human volunteers [254]. This was based on the fact that water content remains constant in the viable epidermis [255].

In the present investigation, we employed a procedure for assessing the thickness of trypsin-separated and of heat-separated skin using also confocal Raman microspectroscopy. The Raman spectra acquired for the skin samples and polystyrene petri dish are shown in figure 3.1.

The Raman spectrum of the skin was identical for the trypsin separation and the heat separation procedure. Raman profiles of skin and the polystyrene of the petri dish differed noticeably (figure 3.1.). As an example, a peak that is characteristic to the skin is detectable at 1650 - 1690 cm^{-1} corresponding to the amide I band [256]. This amide I band is absent in the polystyrene of the petri dish.

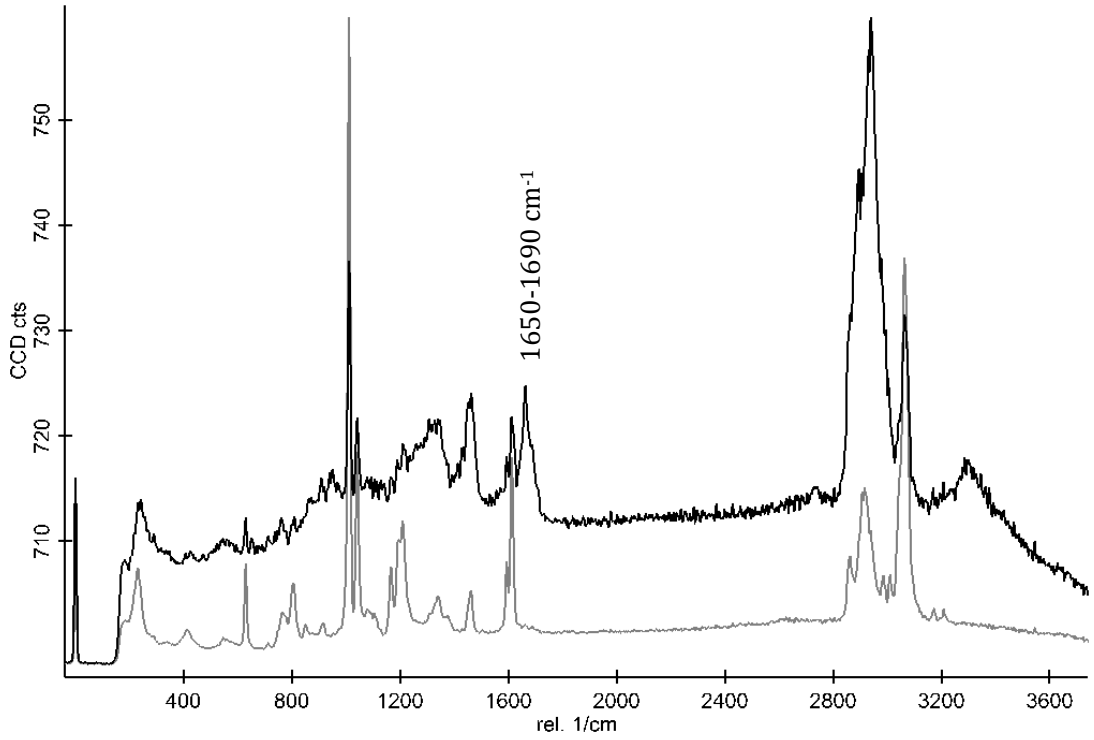

Figure 3.1. Raman spectra of skin specimen (black) and polystyrene petri dish (grey)

A cluster analysis was performed by the software in which the number of clusters was set equal to three. This analysis detected spectral differences between the materials as a function of depth. Figure 3.2. shows the result of this analysis. A clear differentiation between air, skin tissue and polystyrene is evident. From this representation, estimation of thickness of the skin specimens was possible after correction by multiplying the extent of the optical skin layer with the ratio of refractive index of stratum corneum to air, being equal to 1.55 [215,257].

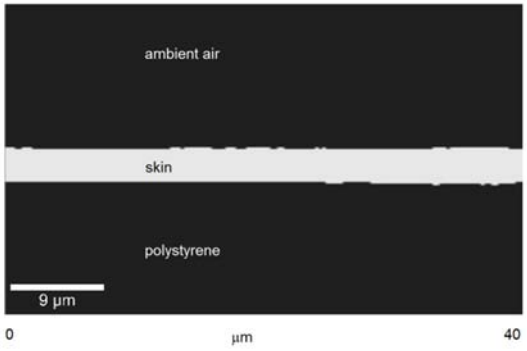

Figure 3.2.a.

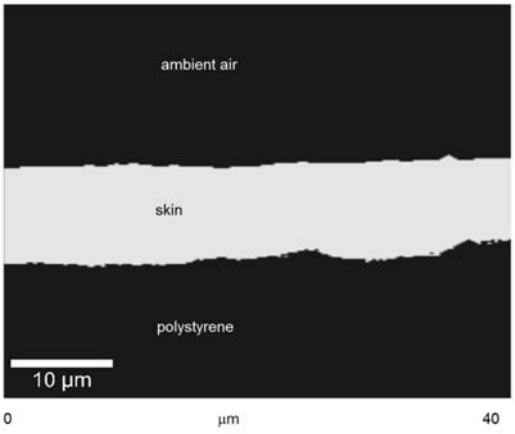

Figure 3.2.b.

Figure 3.2. Visualization of cluster evaluation obtained from Raman spectra differences corresponding to air (top black zone), skin tissue (white zone) and polystyrene (bottom black zone). Vertical coordinate corresponds to depth in Z direction (40 µm).
Figure 3.2.a. trypsin-separated skin, Figure 3.2.b heat-separated skin.

The trypsin separation and the heat separation procedure gave skin layer thicknesses of about 5.9 µm (n=2) and 14 µm (n=2), respectively. Both procedures allowed the separation of an upper skin layer from the full thickness skin, the heat separation, however, led to the recovery of a thicker tissue layer than the trypsin separation, which was consistent with results of other authors [247]. This is because the trypsin procedure enables recovering the SC exclusively, whereas the heat procedure leads to the recovery of almost the entire epidermis.

The thickness obtained via trypsin separation was smaller than previously published data on SC thickness of porcine ears using two photon microscopy [242], quantitative tape stripping procedure [253], cryo-scanning electron microscopy [258], or common histological examination [240]. This difference may be explained by the water evaporation occurring during the storage and equilibration of the skin specimens over salt solution in our experiment. This step was required for the subsequent SPF measurements. These results demonstrate that the developed method makes possible to measure the thickness of isolated skin layers at multiple locations in a fast, exact and convenient manner requiring no special preparation.

3.4.2. Surface topographical assessment

Different methods have been used for roughness measurement of human skin such as topographical analysis using digital stripe projection technique [250], a stylus profilometry on skin replica [259], 3D optical in vivo topography analysis [260] and confocal scanning laser microscopy [261]. A non-exhaustive list of the invasive, semi-invasive and non-invasive methods is given in [262]. The ideal system to assess the real topography of skin should allow a non-contact measurement, a spatial resolution in the micrometer range, a range of measurement covering the amplitude of the skin relief, a three-dimensional reconstruction and the collection of the data in a reasonable time. Most of these recommendations were fulfilled by the white light aberrations principle of measurement used in the present study.

Sa roughness parameter values of the different substrates are reported in Table 3.4.

Table 3.4. Sa arithmetical mean over a surface of selected substrates

Selected substrates	**Sa (µm) measured**
Full thickness pig skin [a]	21.7
Human skin [b]	22 on back forearm [261] 17.4 on back [18]
Heat-separated pig skin fixed on quartz plate [c]	2.56 ± 0.74
Trypsin-separated pig skin fixed on quartz plate [d]	1.26 ± 0.20
Trypsin-separated pig skin fixed on SPF Master PA-01 PMMA plate [a]	19.2
PMMA Helioplate HD6 [e]	6.07 ± 0.03
PMMA Schönberg plate [e]	6.05 ± 0.51
PMMA SPF Master PA-01 [e]	22.23 ± 1.90

[a] n=1 ear, [b] according to paper, [c] n=13 ears (61 single measurements),[d] n=3 ears, [e] n= 3 plates

Sa of full thickness skin of porcine ear had a value of about 22 µm. This result is in accordance with the data available for human skin roughness [261]. An illustration of the surface of full thickness pig ear skin is given in figure 3.3.

Figure 3.3. illustrates the differences in altitude (µm range on scale) and the highly organized architecture of the skin surface including the v-shaped furrows. This pattern is characteristic also for human skin as shown using optical laser profilometry [262] or scanning electron microscopy [255]. These results hence confirm that full thickness skin of porcine ear presents the same surface architecture as human skin.

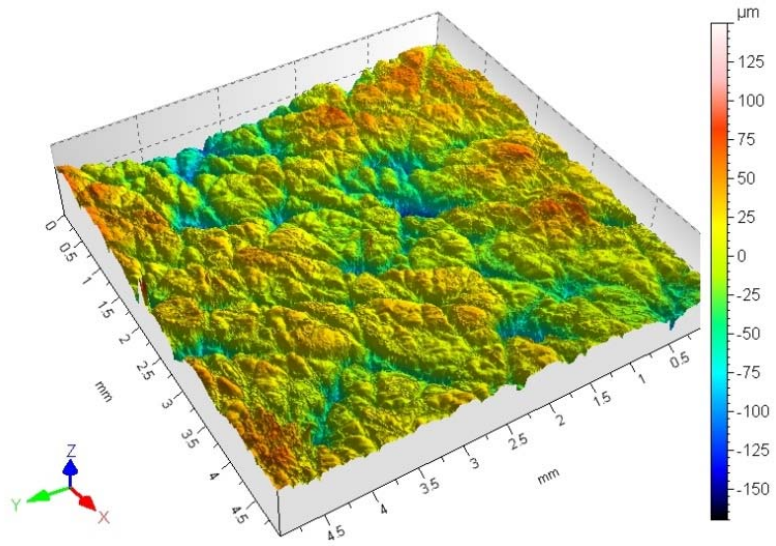

Figure 3.3. Three dimensional view of full thickness skin from porcine ear

The roughness parameter Sa of the isolated tissue layers decreased compared to full thickness tissue to 1.26 µm and 2.56 µm for trypsin-separated and heat-separated porcine skin, respectively. A three-dimensional representation of the surface of a heat-separated sample is shown in figure 3.4. This Figure illustrates that the typical topographical relief of full thickness skin was lost as a result of the preparation procedure. The topographical relief of the full thickness skin is principally characterized by clusters separated by invaginations resembling valleys also referred to as furrows which are extensions of the SC into the epidermis and can reach down into the basal layer [242].

By removing the connective tissue (dermis) these valleys disappear resulting in a more flat skin surface and a loss of skin roughness. Additionally, the trypsin-separated SC which is thinner than the heat-separated epidermal membrane (about 6 µm compared to 14 µm) showed a considerably smaller Sa value than the heat-separated skin layer. These results indicate that the thickness of the skin sample affects its roughness.

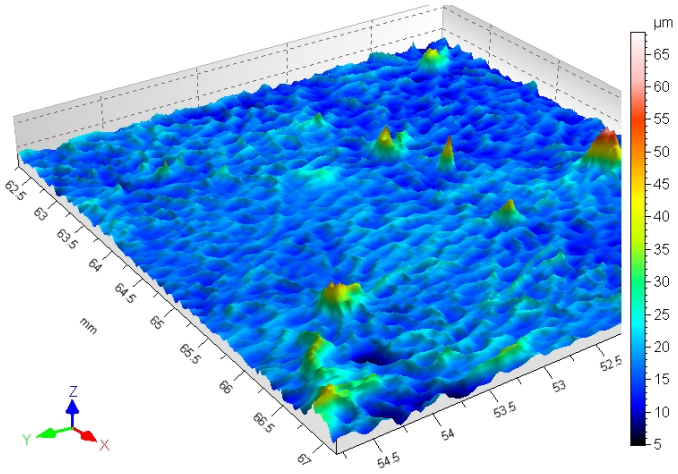

Figure 3.4. Three dimensional view of heat-separated epidermal membrane from porcine ear

Two of the PMMA plates (Helioplate HD6 and Schönberg) exhibited a Sa value of approximately 6 µm. This value is smaller than the one of full thickness skin but larger than those of the two skin preparations. By comparison, the SPF Master PA-01 PMMA plates, which were developed to mimic the topography of human skin [18], had a Sa value of roughly 22 µm, which was comparable to that of full thickness skin.

The Sa measures of all PMMA plates were in line with the data provided by the suppliers for the used batches.

Finally, to obtain a UV transparent skin-surfaced substrate having the Sa of full thickness skin, trypsin-separated SC was laid on the SPF Master PA-01 PMMA plates. The measured Sa of this combined substrate was approximately 19 µm (Table 3.4).

The effect of the different substrates and their Sa values on SPF *in vitro* is discussed below.

3.4.3. Measurement of sun protection factor

Three types of skin preparations were used for SPF measurements, i.e., heat-separated epidermal membrane on quartz plates, trypsin-separated SC on quartz plates and trypsin-separated SC on PMMA plates (SPF Master PA-01). Directly after the preparation procedure, the skin samples looked translucent and became transparent during storage under controlled temperature and humidity conditions. The time required to reach sufficient transparency for UV transmittance measurements with trypsin-separated SC and heat-separated epidermal membrane samples was 24 hours and four days, respectively, after preparation. This is related to thickness of the obtained tissue layer.

The impact of the size of the plate on SPF *in vitro* was firstly determined with the three types of PMMA plates using sunscreen OW Nr.1. The measurements were carried out by two operators. The SPF *in vitro* values of 5.0 cm × 5.0 cm (n=3) plates were not found to be significantly different from SPF *in vitro* values of 2.0 cm × 2.0 cm (n=3) plates independently of plate type and operator (Mann-Whitney, $p>0.05$; results not shown). As a result, a sample area of 2.0 cm × 2.0 cm was used for further studies.

SPF *in vitro* data measured on PMMA plates and on skin preparations were compared to the SPF *in vivo*. The results for each substrate with sunscreen OW Nr.1 and OW Nr.2 are shown in Figure 3.5. and Figure 3.6., respectively. Relative standard deviation for OW Nr.1 and operator 1 was 32-38% for PMMA plates and 38% for skin substrate; for operator 2, 21-43% for PMMA plates and 32-57% for skin substrate. Relative standard deviation for OW Nr.2 and operator 1 was similar to OW Nr.1. A statistical analysis of the difference between SPF *in vivo* and SPF *in vitro* for each substrate is summarized in Table 3.5.

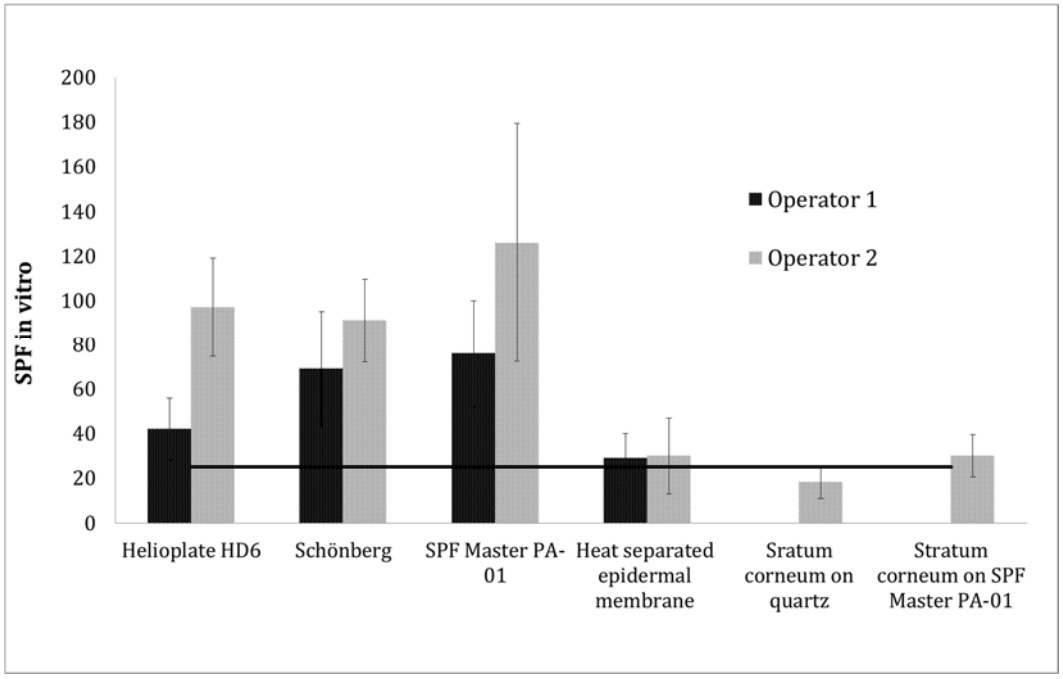

Figure 3.5. Average SPF *in vitro* (columns) and standard deviation (bars) of sunscreen OW Nr.1 measured on three types of PMMA plates (Helioplate HD6, Schönberg, and SPF Master PA-01 each n=9) and three types of skin preparation (heat-separated epidermal membrane on quartz, trypsin-separated SC on quartz, and trypsin-separated SC on SPF Master PA-01 plate, each n=63). The SPF *in vivo* (drawn horizontal line) is equal to 27.5 (standard deviation 7.6).

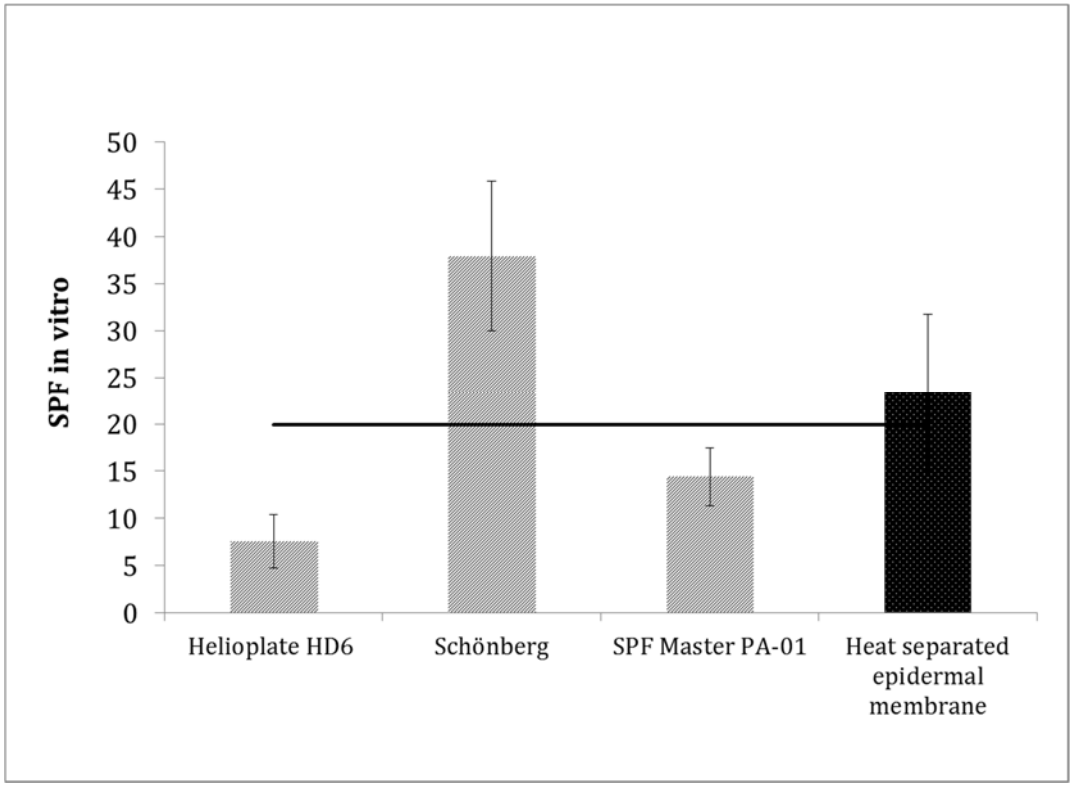

Figure 3.6. Average SPF *in vitro* (columns) and standard deviation (bars) of sunscreen OW Nr.2 measured on three types of PMMA plates (Helioplate HD6, Schönberg and SPF Master PA-01 each n=12) and on heat-separated epidermal membrane on quartz, n=33. The SPF *in vivo* (drawn horizontal line) is equal to 19.9 (standard deviation 5.8).

Table 3.5. Difference between SPF *in vitro* and SPF *in vivo* for evaluated substrates

Sunscreen	Substrate	Statistical significance at 5% confidence level of the difference between SPF *in vitro* and SPF *in vivo* (Mann-Whitney)
OW Nr.1	Trypsin-separated SC on quartz	Yes ($p<0.05$)
	Trypsin-separated SC on SPF Master PA-01	No ($p>0.05$)
	Heat-separated epidermal membrane on quartz	No ($p>0.05$)
	Helioplate HD6	Yes ($p<0.05$)
	Schönberg	Yes ($p<0.05$)
	SPF Master PA-01	Yes ($p<0.05$)
OW Nr.2	Heat-separated epidermal membrane on quartz	No ($p>0.05$)
	Helioplate HD6	Yes ($p<0.05$)
	Schönberg	Yes ($p<0.05$)
	SPF Master PA-01	No ($p>0.05$)

The reproducibility was assessed using sunscreen OW Nr.1. It is worth pointing out that SPF *in vitro* obtained with PMMA plates may depend among other factors on the operator [19]. In the present study, there was a statistically significant difference between SPF *in vitro* values measured by the two operators for all types of PMMA plates (Mann-Whitney, $p<0.05$) but not for the heat-separated epidermal membrane (Mann-Whitney, $p>0.05$). This result might suggest that the biological substrate possibly provides more reproducible data than the habitually used synthetic plates even though standard deviation of the results by the two operators may vary.

For sunscreen OW Nr.1, trypsin-separated SC on PMMA SPF Master PA-01 plate and heat-separated epidermal membrane on quartz plate yielded SPF *in vitro* results that were not statistically significantly different from the SPF *in vivo* value. Of the skin-based substrates, only the result of trypsin-separated SC on quartz plate was significantly different from the SPF *in vivo*, although this significance was barely reached ($p=0.036$).

In the contrary, SPF *in vitro* values obtained with the PMMA plates were about four to five times larger than and significantly different from the SPF *in vivo* (Figure 3.5. and Table 3.5.)

These results demonstrate that synthetic plates were not adequate for testing the SPF of this sunscreen since none of the PMMA plates approached the SPF in vivo. With two out of the three skin preparations on the other hand, the SPF *in vivo* value was also obtained *in vitro*.

The SPF *in vitro* of sunscreen OW Nr.2 was evaluated by one operator using the three PMMA plate types and the heat-separated epidermal membrane on quartz. Also with this sunscreen, the skin preparation produced no significantly significant difference from the *in vivo* reference. Of the PMMA plates, the ones manufactured by mold injection (Helioplate HD6 & and SPF Master PA-01) gave lower and the one manufactured by sand blasting (Schönberg) higher SPF *in vitro* values than the *in vivo* reference. This was different from the result obtained with sunscreen OW Nr.1. Nevertheless, the result of PMMA SPF Master PA-01 showed no statistically significant difference to the SPF *in vivo* while the other two PMMA plates did. Interestingly, the PMMA SPF Master PA-01 plate has the greater roughness (Sa = 22.23 µm) of the two mold injected plates. Generally, an impact of substrate roughness on efficacy, reproducibility and repeatability of *in vitro* sunscreens measurements has also been reported by Fageon et al. and Ferrero et al. [10,16].

The outcome of the SPF *in vitro* assessment with two different OW sunscreens showed that the used biological substrate yielded results reaching in most cases the SPF *in vivo* value while the PMMA plates generally did not. Roughness differed considerably between the skin-based preparations (Sa 2.56 versus 19.2), this, however, did not seem to affect the determined SPF *in vitro*. Only trypsin-separated SC on quartz having the smallest roughness (Sa 1.26) did not reach the reference SPF value. This preparation may therefore not be suitable for SPF *in vitro* testing suggesting that a minimal roughness of the substrate may be required. Conversely, none of the synthetic substrates having different roughness characteristics achieved a satisfactory SPF *in vitro* with the two OW sunscreens. Even the SPF Master PA-01 plate which has a Sa value and a surface pattern similar to that of human skin did not always yield accurate results. This implies that roughness may not be the sole critical surface characteristic of the substrate to be considered for achieving accurate SPF *in vitro* measurements.

Besides surface topography, the affinity of the sunscreen for the substrate seems to be equally important. Affinity refers to the propensity of the sunscreen to be distributed and adhere to the substrate upon spreading. *In vitro* measurements carried out on skin-based substrates are assumed to better simulate the product-to-substrate affinity that applies to the *in vivo* situation. This may explain why these substrates, including the heat-separated epidermal membrane on quartz and the trypsin-separated SC on PMMA SPF Master PA-01 plates, resulted in more accurate SPF *in vitro* values compared to the PMMA plates.

It should be pointed out that the present data were collected with OW formulations. An a priori transfer of the results to other types of formulations can not be made at this point. For example, WO or single phase formulations might exhibit a different affinity and/or spreading behavior. Therefore, additional investigations are required for generalizing these observations.

The affinity aspect was further invoked in connection with the poor SPF *in vitro* value obtained with highly hydrophobic mold injected plates that caused a lack of adherence of the product and consequently a non-uniform protection film for some sunscreen formulations [190]. To increase the adherence of the sunscreen on molded PMMA plates the authors proposed the use of a chemical pretreatment of the plate prior the application of the sunscreen. Chemical pretreatment, however, might alter the structure of the applied emulsion and seems, therefore, not to be an ideal solution. Alternatively, modification of interfacial properties of the molded PMMA plates by plasma treatment to improve the product-to-substrate affinity was proposed [263]. However, in this evaluation the required plasma treatment producing different levels of surface energy was product dependent and no single treatment was suitable for the entire set of products.

In addition to roughness and affinity, the influence of other experimental factors on SPF *in vitro* has already been examined such as the application process [10], the spectrum of the lamp source [214] or the amount of product applied [18,180,248]. Other possible influence factors such as the impact of pressure or the formation of the film during product application have not been fully explored yet constituting a still open area of research in the field.

The approach introduced in this study provided interesting insights in the in vitro methodology for predicting SPF in vivo. It could be useful in the final stage of product development for determining absolute SPF value prior to carrying out clinical studies. Also, use of the method may be recommended for sunscreen performance verification, for example, in case of change of raw material, vehicle composition or manufacturing process. Since, however, the method is rather laborious, it may not be appropriate for screening or large scale product comparison tests.

3.5. Conclusion

Substrates for SPF *in vitro* measurement that involve the use of skin tissue layers appear to provide a better prediction of SPF for the tested OW formulations than conventionally used PMMA plates. A minimal surface roughness of the skin-based substrate seems to be required. However, reproducing the natural roughness of skin in a PMMA plate alone was not sufficient to achieve accurate SPF *in vitro* values. Instead, improved affinity of sunscreen for the substrate imparted by the use of skin tissue is concluded to be critically important. Significantly, despite the loss of the original relief of full thickness skin during preparation, the use of tissue as a substrate was adequate for *in vitro* testing of the performance of the sunscreens.

Chapter 4

Film thickness frequency distribution of different vehicles determines sunscreen efficacy

4.1. Abstract

Sunscreen efficacy depends primarily on the absorbance properties of the contained UV filters. However, sun protection factor (SPF) frequently differs between sunscreens with the same filter composition. We tested here the hypothesis that thickness frequency distribution of the sunscreen film is also responsible for and can explain the divergence in SPF values. For this, we developed a method to measure film thickness from the difference of topography before and after application of 2mg/cm^2 of sunscreen on pig ear epidermal membrane.

M. Sohn et al., "Film thickness frequency distribution of different vehicles determines sunscreen efficacy," J. Biomed. Opt. 19(11), 115005 (2014).

.

The influence of five vehicle formulations and of application pressure and spreading time on film thickness frequency distribution, mean thickness (Smean) and SPF *in vitro* was investigated. The vehicle had a significant impact, low vehicle viscosity resulting in smaller Smean and lower SPF *in vitro* than high viscosity; continuous oil phase produced the largest Smean and SPF values. Long spreading time reduced Smean and SPF and increased pressure reduced SPF. There was a positive correlation between Smean and SPF *in vitro*, underlining the relevance of film thickness for interpreting UV protection differences of formulations with the same filter composition. This work demonstrated a strong influence of vehicle and application condition on sunscreen efficacy arising from differences in film thickness distribution.

4.2. Introduction

Topically applied sunscreens constitute a suitable and commonly employed measure to protect skin from sun damages [6,7]. Efficacy of sunscreens in terms of sun protection factor (SPF), UVA protection, photostability, and balanced absorbance depends primarily on the intrinsic absorbance and photostability properties of UV filters contained in the product in conjunction with the used concentration [20,264]. The ideal sunscreen achieves balanced protection by attenuating equally UVB and UVA radiations, similarly to the protection afforded by clothing and shade [228,229]. Therefore, an appropriate UV filter system should combine UVB and UVA filters to achieve optimized UV shield [141]. Reasonably, the amount of product applied also affects protection [180,265-268]. However, the SPF frequently differs between sunscreens with different vehicle formulations containing the same filter composition [20,21] yet the cause of this difference has not been investigated. Also, *in vitro* inter-laboratory trials with the same sunscreen have produced variable results [19] and the application procedure was further found to influence the measured SPF [22,269]. In addition to the absorbing property of the UV filters and the amount of applied product, homogeneity of distribution of the sunscreen was found to play an important role with respect to SPF *in vivo* [27]. The ideal situation for optimal performance is to achieve a film with uniform thickness, resembling the perfectly homogeneous distribution of a solution of UV filters in an optical cell.

Understandably, this condition can never be reached under *in vivo* condition of application due to the skin surface topography. Skin relief shows ridges and furrows that preclude the formation of an even sunscreen film [270]. In addition, manual application makes it practically impossible to achieve a uniform film. This irregularity of the film thickness is probably a cause of the reported experimental variability of SPF and was suggested to be responsible for the divergence of orders of magnitude between predictions based on UV transmission of dilute transparent filter solutions and clinical study results [25].

The aim of the present work was to understand the relationship between film thickness frequency distribution and efficacy of sunscreens. To this end, we developed a method for determining the precise thickness distribution of the applied sunscreen film based on topographical measurements with high spatial resolution. We used epidermal membrane of pig ear skin as a biological substrate for *in vitro* sunscreen application as we recently showed that using this substrate for SPF *in vitro* testing provided better prediction of SPF *in vivo* than conventionally used synthetic substrates. Substrate-to-product affinity rather than topography was discussed to be responsible for this better prediction of SPF *in vivo* (section 3.4.3.). Skin of pig ear has also been used for *in vitro* assessment of UV-induced damages on DNA [271], UV filter penetration [181,272], and sunscreen photostability tests. [182] Using the developed film assessment method we investigated the sunscreen film residue in terms of thickness and homogeneity of distribution for five sunscreen vehicles and different application conditions. In parallel, we measured SPF *in vitro* on the same preparations to determine UV protection efficacy. The impact of vehicles with the same UV filter combination and of the application conditions on film parameters and SPF *in vitro* as well as the correlation between film parameters and SPF *in vitro* was then assessed. Identification of formulation and application related factors that may impact film characteristics and UV protection was a further goal of the present work. This is put forth as fundamental aspect for understanding the mechanism of sunscreen efficacy.

4.3. Materials and methods

4.3.1. Chemicals and equipment

The following reagents were used: Potassium Carbonate from Sigma-Aldrich, St Gallen, Switzerland; Tinosorb S abbreviated BEMT (INCI, Bis-ethylhexyloxyphenol Methoxyphenyl Triazine), Uvinul N539T abbreviated OCR (INCI, Octocrylene), Salcare SC 91, Cetiol AB, Lanette O, Dehymuls LE, Edeta BD, all from BASF SE, Ludwigshafen, Germany; Eusolex 232 abbreviated PBSA (INCI, Phenylbenzimidazol Sulfonic Acid) from Merck, Darmstadt, Germany; Parsol 1789 abbreviated BMDBM (INCI, Butyl Methoxydibenzoylmethane), Amphisol K from DSM, Kaiseraugst, Switzerland; Neo Heliopan OS abbreviated EHS (INCI, Ethylhexyl Salicylate) from Symrise, Holzminden, Germany; Arlacel 165 from Croda, East Yorkshire, England; Keltrol RD from CP Kelco. Atlanta, GA, USA; Carbopol Ultrez 10, Carbopol Ultrez 21 from Lubrizol, Brussels, Belgium; Tegin OV from Evonik Industries, Essen, Germany; Paracera M from Paramelt, Heerhugowaard, The Netherlands; Beeswax white from Koster Keunen, Bladel, The Netherlands; Glycerin from Sigma-Aldrich, St Gallen, Switzerland; Tris Amino Ultra-Pure from Angus, Buffalo Grove, IL, USA; Phenonip from Clariant, Muttenz, Switzerland.

Quartz plates with a size of 4.2 cm × 4.2 cm were obtained from Hellma Analytics, Zumikon, Switzerland.

The following equipment was used: Electric shaver (Favorita II GT104, Aesculap, Germany), epilator (Silk-épil7 Xpressive Pro, Braun, Germany); water purification device (Arium 61215, Sartorius, Goettingen, Germany); precision balances (XS105 Dual range and XA3001S, Mettler-Toledo, Columbus, OH, USA); surface metrology instrument (Altisurf 500, Altimet, Thonon-les-Bains, France); UV transmittance analyzer (Labsphere UV-2000S, Labsphere Inc., North Sutton, NH, USA).

The following software packages were used: BalanceLink (Mettler Toledo, Columbus, OH, USA) with balance XA3001S for the recording of pressure during spreading of sunscreen; Phenix and Altimap (Altimet, France) for topographical measurement and evaluation, respectively; UV-2000 (Labsphere Inc., USA) for UV transmittance measurement; Statgraphics centurion XVI software (Statpoint Technologies, Inc., Warrenton, VA, USA) for statistical evaluation.

4.3.2. Preparation of skin substrate

We used epidermal membrane of pig ears as a biological substrate for sunscreen application as described in section 3.3.2., method 2 (3.3.2.2.). Ears of freshly slaughtered pigs were obtained from the local slaughterhouse (Basel, Switzerland) no more than few hours postmortem. The study did not require the approval of the ethics committee of animal research as the ears were taken from pigs not specifically slaughtered for the purpose of this study. The epidermal membrane was isolated using a heat separation procedure. The full skin was immersed in a water-bath at 60°C for 90 s. The epidermal membrane was separated from the dermis by gentle peeling off, cut to a dimension of 2 cm × 2 cm, laid flat on quartz carrier plates, and stored at 4°C in a desiccator over saturated potassium carbonate solution until use.

4.3.3. Characterization of sunscreen formulations

We assessed SPF *in vitro* and film thickness distribution of five different sunscreens. The formulations included an oil-in-water cream (OW-C), an oil-in-water spray (OW-S), a water-in-oil emulsion (WO), a gel (GEL) and a clear lipo-alcoholic spray (CAS). They contained the same UV filter combination and emollient. The filter system was composed of 8 w-% OCR, 5 w-% EHS, 2 w-% BMDBM, 1 w-% BEMT, and 1 w-% PBSA. Based on this UV filter composition a SPF *in silico* of 25 was calculated with the BASF sunscreen simulator [273]. The detailed composition of the sunscreens and their respective SPF *in vivo* values are given in Table 4.1. SPF *in vivo* values were measured in accordance with ISO24444:2010 guidelines [9].

The sunscreens showed different rheological characteristics (figure 4.1.). GEL had the highest shear viscosity followed by OW-C and WO, whereas OW-S and CAS were much less viscous. Viscosity of all sunscreens decreased with increasing shear rate whereas hysteresis depended on the formulation.

Table 4.1. Composition (w-%) and SPF *in vivo* of investigated sunscreens

Sunscreen designation		**OW-C**	**OW-S**	**GEL**	**WO**	**CAS**
SPF in vivo ± SD [a]		38.8 ± 8	24 ± 5	19.4 ± 5	19.5 ± 3.1	17.8 ± 2.2
Ingredient type	**Trade name**	**Composition (w-%)**				
Emulsifier system	Arlacel 165	1.5	-	-	-	-
	Amphisol K	1.5	2.5	-	-	-
	Dehymuls LE	-	-	-	1.0	-
	Tegin OV	-	-	-	2.0	-
Thickener system	Lanette O	0.5	-	-	0.5	-
	Keltrol RD	0.15	-	0.15	-	-
	Salcare SC 91	1.8	-	1.8	-	-
	Carbopol Ultrez 10	-	-	0.2	-	-
	Carbopol Ultrez 21	-	-	0.15	-	-
	Paracera M	-	-	-	0.5	-
	Beeswax	-	-	-	1.0	-
Emollient	Cetiol AB	5.0	5.0	5.0	5.0	5.0
Filter system	Mixture of UV filters	17.0	17.0	17.0	17.0	17.0
Neutralizing agent	Tris Amino Ultra Pure	qs	qs	qs	qs	-
	Neutrol TE	-	-	-	-	qs
Additional ingredients	Glycerin	3.0	3.0	3.0	3.0	-
	Edeta BD	0.2	0.2	0.2	0.2	-
	Phenonip	1.0	1.0	1.0	1.0	-
	Water	qs	qs	qs	qs	-
	Ethanol	100% -	100% -	100% -	100% -	qs 100%

[a] SPF *in vivo* and standard deviation evaluated in accordance with ISO24444:2010 guidelines with n=5

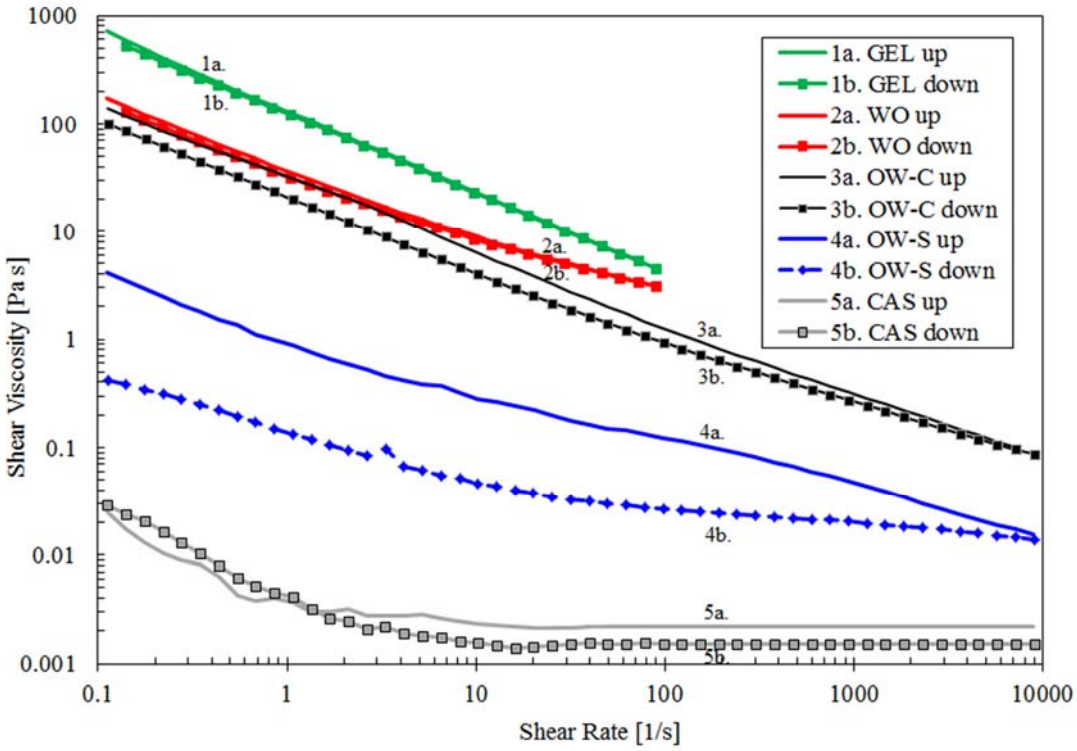

Figure 4.1. Rheological behavior of sunscreens measured with AR-G2 rheometer (TA instrument), CP 4° / 40mm, Gap 100 µm, T = 23 °C

4.3.4. Application of sunscreen

We applied 2.0 mg/cm^2 of sunscreen nominally corresponding to a film thickness of 20 µm. The sunscreen was applied in form of 20 to 30 small drops evenly distributed over the skin surface and spread manually with the fingertip using a pre-saturated finger coat. Two spreading procedures were employed. In the first, the sunscreen was spread on the specimen with light circular movements followed by left-to-right linear strokes from top to bottom starting at each side of the specimen (designated spreading 1); in the second, the complete linear stroke step was repeated four times (designated spreading 2). The spreading procedure 2 resulted in a longer application time. Furthermore, the pressure used to distribute the product was varied for spreading 1 between low and high, corresponding to a force of 100 ± 14 g and 281 ± 35 g, respectively. These values represent extremes used in the authors' laboratory with this substrate preparation.

The two pressure and spreading conditions were used solely with the gel formulation (GEL). All other sunscreen formulations were applied with high pressure and spreading procedure 1.

4.3.5. Measurement of the sun protection factor *in vitro* using spectral transmission of ultraviolet radiation

Measurement of SPF *in vitro* is based on diffuse UV transmission spectroscopy according to the approach proposed by Sayre [12],

$$\text{SPF } in\ vitro = \frac{\sum_{290}^{400} s_{er}(\lambda).S_s(\lambda)}{\sum_{290}^{400} s_{er}(\lambda).S_s(\lambda).T(\lambda)} \quad (4.1.)$$

where, $s_{er}(\lambda)$ is the erythema action spectrum as a function of wavelength λ [9], $S_s(\lambda)$ is the spectral irradiance of the UV source at wavelength λ[9] ,and $T(\lambda)$ is the measured transmittance of the light through a sunscreen film applied on a suitable UV transparent substrate at wavelength λ [13].

For SPF determination, the spectral UV transmittance was registered from 290 to 400 nm in 1 nm increment steps through skin substrate preparations before and after application of a sunscreen using Labsphere UV-2000S. The UV transmittance of four positions per 2 cm × 2 cm skin substrate was measured to cover virtually the complete surface area of the preparation.

The blank transmittance spectrum was recorded at first for each single position before sunscreen application followed by topographical measurement of the bare skin (see section 4.3.6.). Subsequently, sunscreen was applied and topographical measurement was performed again. After completion of topographical measurement which lasted approximately 4 h, UV transmission through the sunscreen-covered skin substrate was measured. Stability of SPF *in vitro* values over 4 h was checked and confirmed for all sunscreens.

4.3.6. Assessment of the sunscreen film

The layer of sunscreen applied on pig skin substrate was investigated using topographical measurements with an optical probe based on white light chromatic aberration principle (Altisurf 500 instrumentation). The instrumentation allowed non-contact surface topography measurement and analysis. The employed optical sensor yielded an axial resolution (z) of 5 nm and a lateral resolution (x-y) of 1.1 μm. The motorized x-y stage permitted scanning of samples in the mm range. Skin preparations on quartz plates were fixed on the stage using a custom made holder.

Surface topography of bare skin and skin covered with sunscreen was measured in order to assess the sunscreen film. Skin preparations were removed from the desiccator and allowed to equilibrate for 12 h next to the device at room conditions before starting topographical measurements. Repeated measurements on bare skin using the "loop" option of the operating software revealed that this equilibration was necessary to allow stabilization of the surface position along the z axis (data not shown). After measuring the surface topography of bare skin sunscreen was applied, equilibrated for 15 min, and the same area was scanned again.

Figure 4.2. illustrates the area of topographical and UV transmittance measurements.

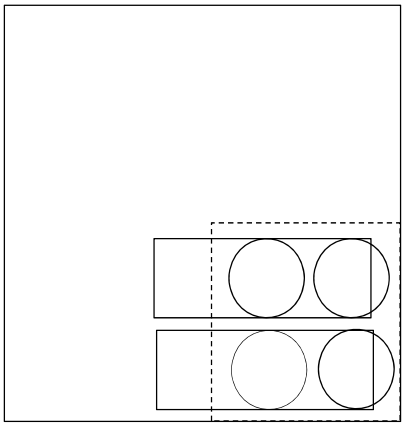

Figure 4.2. Illustration of areas for topographical and UV transmittance measurements; the big square corresponds to the carrier quartz plate, the dotted small square to the skin surface area with a dimension of 2 cm x 2 cm, the four circles correspond to the areas of UV transmittance measurements (SPF) with a diameter of 1 cm and the two rectangles to the two areas of topographical measurements.

Topographical measurements were performed on two rectangular areas (approximately 23 mm × 8 mm) per specimen (figure 4.2.). A part of the rectangular area (about 5 mm × 8 mm on left hand side) corresponded to quartz without skin and served as reference. The skin area (right hand side of the rectangle) measured about 18 mm × 8 mm. Topography was recorded in lines each extending over the quartz and the skin part of the rectangle with an increment step of 10 µm. The rectangular areas were scanned with lines in 10 µm intervals resulting in 1 840 000 single measurement points per rectangle.

The raw data of the topographical measurements were redressed by a line-by-line leveling correction of each rectangular surface to the same x-y plane using the quartz part of each measured line (left side of rectangle, figure 4.2.) This redressing procedure was carried out with the data of bare skin and skin covered with sunscreen and was essential in order to correct for variation due to positioning and due to environmental factors changing in the course of the experiment. Each rectangular surface area was divided into two zones of 8 mm × 8 mm coinciding with the four positions (circles) of UV transmittance measurements figure 4.2.).

The film thickness of applied sunscreen was obtained as the difference of the redressed skin topography data with and without sunscreen computed for each single measurement point. The result was expressed as a distribution of frequencies of film thickness over the measured surface area normalized to 100 % and is referred to as thickness distribution curve. A threshold of 0.5% of area und the curve was applied to remove extreme values at both ends of the film thickness distribution.

To validate this measurement and calculation method, a surface area of bare skin was measured twice and film thickness was computed. The result was found to be centered around 0 µm (n=8), confirming the validity of the method for measurement of the sunscreen film thickness distribution on skin.

Data extracted from the distribution curve and serving to characterize the applied sunscreen film are given in Table 4.2.

Table 4.2. Data extracted from the thickness distribution curve of applied product

Parameter	Meaning
Smean (μm)	Average of film thickness over the measured area
Smean to median ratio	Indicator of film homogeneity
Abbott-Firestone curve	Cumulative frequency of occurrence of film thickness

Smean is the frequency weighted average thickness. The Smean to median ratio of the thickness distribution is a measure of skewness of distribution and is used as an expression of film homogeneity; the smaller this ratio the greater the homogeneity of the film. The Abbott-Firestone curve is commonly used in surface metrology [274] and is employed here to depict the experimentally determined thickness distribution, indicating thickness and uniformity of applied product layer.

4.3.7. Statistical analysis

Statistical analysis was performed using Statgraphics centurion XVI software (Statpoint Technologies, Inc., Warrenton, VA, USA). The impact of formulation vehicle on SPF *in vitro* and on film parameters was assessed with Kruskal-Wallis non-parametric test, and the impact of application conditions was assessed with Mann-Whitney U test, both with a statistical significance at 5% confidence level. In case Kruskal-Wallis test revealed a statistically significant difference among sunscreens for an investigated parameter, a multiple pairwise comparison test using Bonferroni approach was performed to identify which sunscreens differed significantly from which other. Correlations between film parameters and SPF *in vitro* values within each formulation were assessed using Spearman`s rank correlation coefficient test.

4.4. Results

4.4.1. Film assessment

The film thickness distribution of sunscreen, extracted from the topographical measurements, is visualized three-dimensionally for qualitative assessment in figure 4.3., and is displayed quantitatively as a distribution curve of thickness frequency. From the distribution curve, the Abbott-Firestone curve (cumulative frequency) was deduced (figure 4.4.).

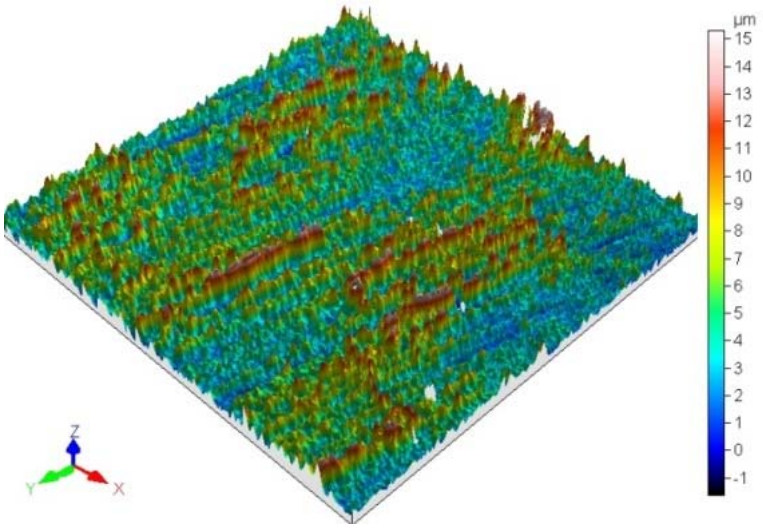

Figure 4.3. Example of three-dimensional visualization of film thickness distribution of OW-C sunscreen

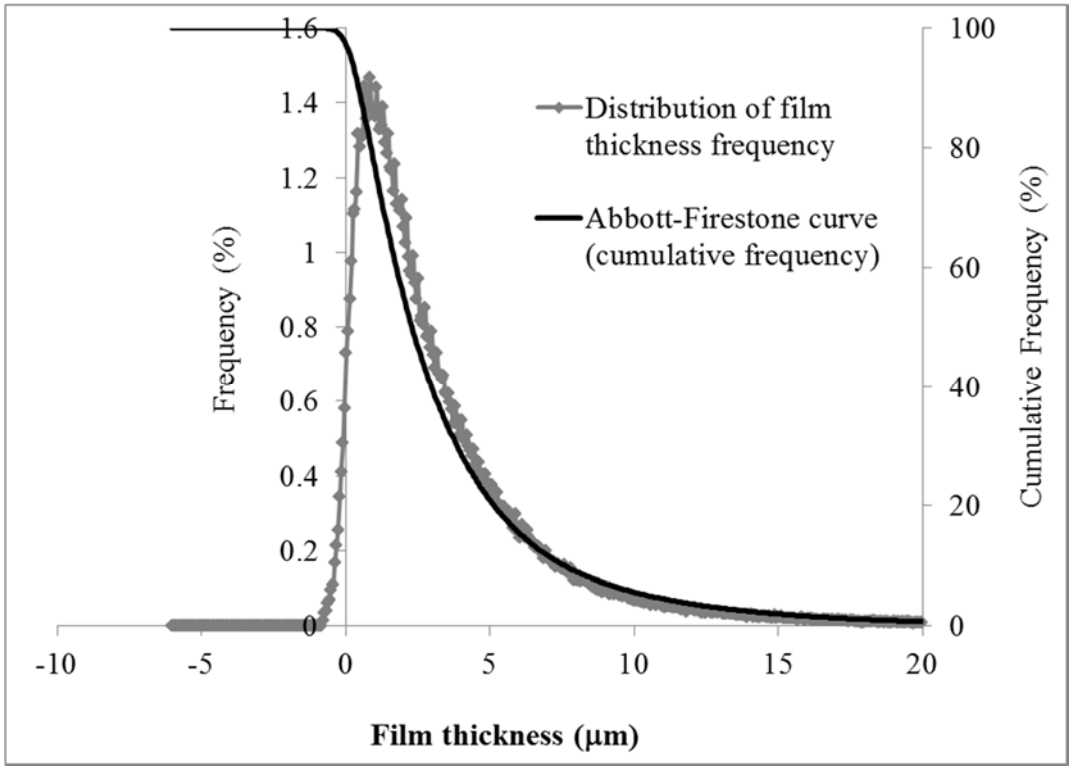

Figure 4.4. Example of distribution of film thickness frequency and Abbott-Firestone curve of OW-C sunscreen

Thickness distribution was always positively skewed, the degree of skewness varying between the different sunscreens. In the example of figure 4.4., the most frequently occurring film thickness was in the range of 2 to 4 µm while a thickness as large as 10 to 13 µm was recorded. A small percentage of area under the thickness distribution curve lay below a film thickness of 0 µm, which was likely due to experimental error. This was included in the calculation of the Smean value.

4.4.2. Impact of vehicle on film parameter values and SPF *in vitro*

Figure 4.5. gives the average of Abbott-Firestone curves of all measurements with each investigated sunscreen using high pressure and spreading 1 conditions of application.

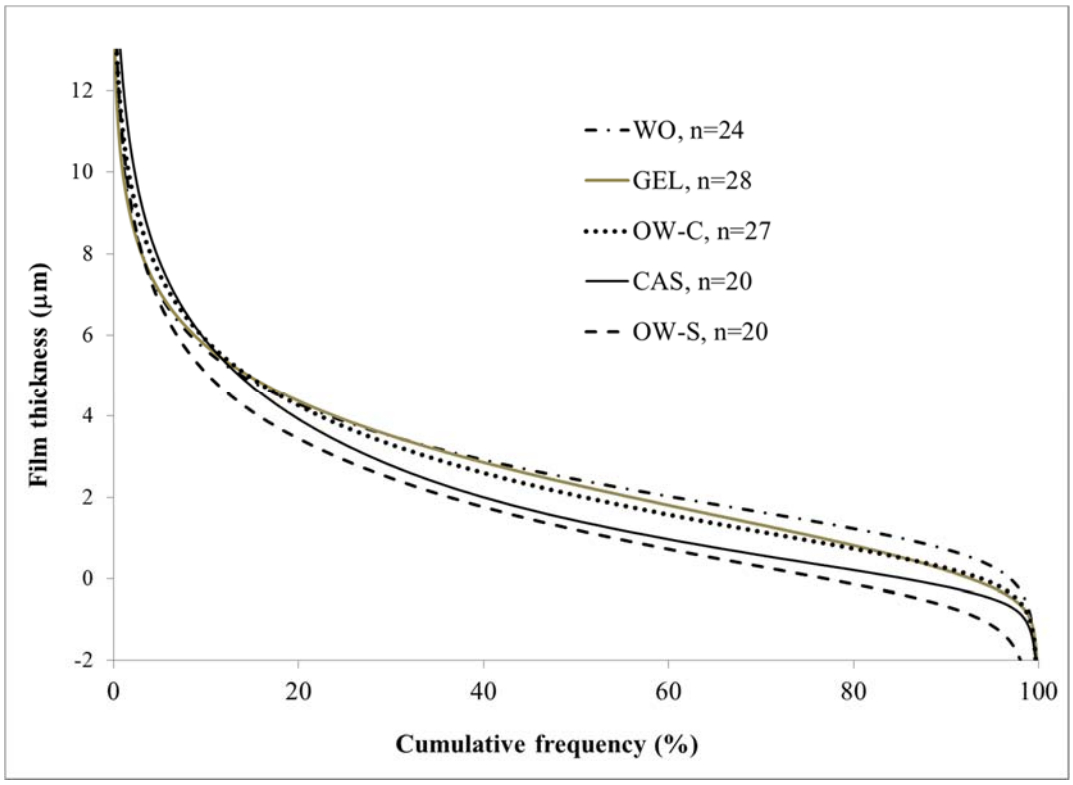

Figure 4.5. Abbott-Firestone profiles of investigated sunscreens applied with high pressure and spreading 1

The Abbott-Firestone profiles differed considerably between the sunscreens (figure 4.5.). Film thickness was different for the different vehicles and decreased roughly in the order WO>GEL>OW-C>CAS>OW-S. For WO for example, a film thickness of 2.41 µm corresponds to 50% of cumulative thickness frequency meaning that 50% of the measured surface area of the sample exhibited a film thickness greater than 2.41 µm. As a comparison, 50% of the measured area of OW-S exhibited a thickness greater than merely 1.20 µm. Moreover, the shape of the curve differed between the used vehicles, the WO, for example, showed a more flat-shaped profile compared to CAS (figure 4.5.).

These differences between the vehicles are reflected by the calculated film thickness parameters Smean and Smean to median ratio of distribution.

Table 4.3. gives the values of the median and interquartile range for the film parameters of all individual measurements of each investigated sunscreen. Also, SPF *in vitro* values of these sunscreens are given in Table 4.3.

Table 4.3. Medians of SPF *in vitro,* Smean, and Smean to median ratio of thickness distribution with interquartile range Q1 – Q3 (in brackets) for investigated sunscreens with high pressure and spreading 1.

Sunscreen	**SPF *in vitro***	**Smean (μm)**	**Smean to median ratio**
OW-C (n=27)	33 (30 – 48)	2.3 (2.0 – 2.7)	1.30 (1.25 – 1.44)
OW-S (n=20)	16 (13 – 26)	1.6 (1.2 – 2.0)	1.41 (1.30 – 1.96)
GEL (n=28)	28 (20 – 34)	2.6 (2.4 – 3.1)	1.19 (1.16 – 1.23)
WO (n=24)	72 (55 – 85)	2.9 (2.6 – 3.2)	1.19 (1.17 – 1.21)
CAS (n=20)	14 (7 – 20)	2.2 (1.7 – 2.6)	1.71 (1.44 – 1.99)

SPF *in vitro* varied markedly between the investigated sunscreen formulations attaining values from 14 for CAS to 72 for WO. SPF *in vitro* values are compared to the SPF *in vivo* in figure 4.6. SPF *in vitro* values generally approached SPF *in vivo* and, considering the declared variation range, a satisfactory agreement between SPF *in vitro* and *in vivo* for spreading 1 and high pressure condition is found. WO sunscreen was an exception, with surprisingly low and high SPF *in vivo* and SPF *in vitro,* respectively. *In silico* estimation of SPF gave a value of 25 (figure 4.6.). This computational approach takes into account the absorbance spectrum of each UV filter, their photostability and mutual stabilization or de-stabilization, and their distribution in the phases of the vehicle and uses the Gamma distribution function to describe film irregularity. [275] The estimated value lay within the range of the experimental values of all vehicles, yet the *in silico* calculation can not predict the effect of formulation on SPF. In figure 4.6. the Smean of the formulations is also visualized.

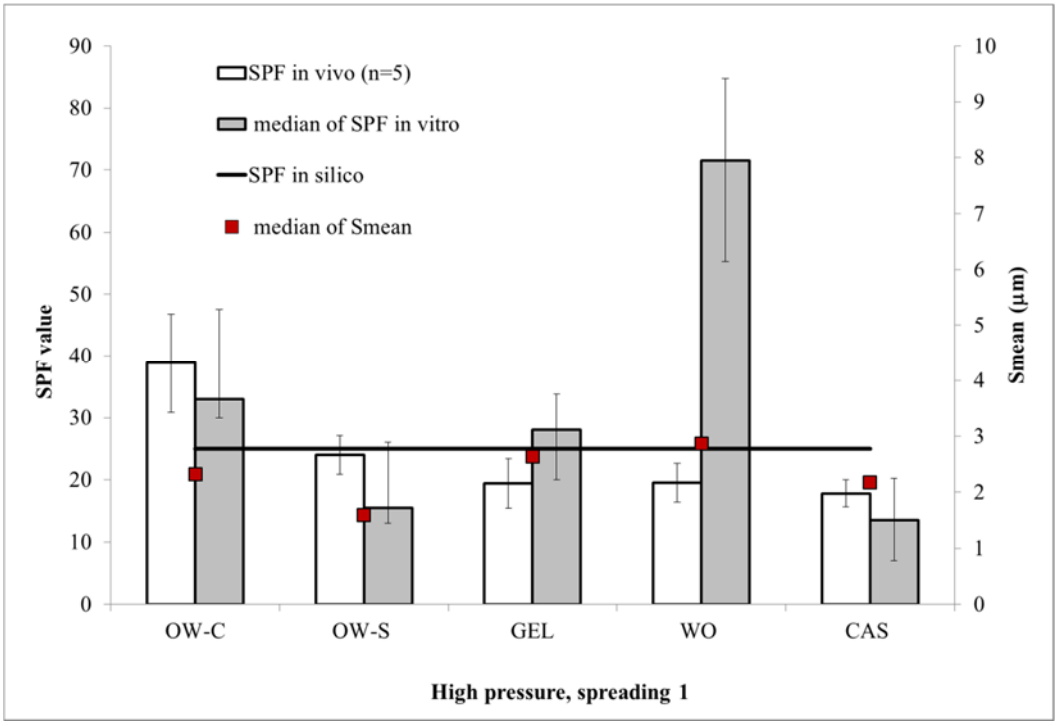

Figure 4.6. SPF *in vivo* (white columns) with standard deviation (bars), medians of SPF *in vitro* (gray columns) with interquartile values (bars) with OW-C n=27, OW-S n=20, GEL n=28, WO n=24, CAS n=20, SPF *in silico* (black line), and medians of Smean values (square) of sunscreens applied with high pressure and spreading 1

The impact of vehicle on SPF *in vitro* and film parameters was evaluated with Kruskal-Wallis test (Table 4.4.).

Table 4.4. Impact of vehicle on SPF *in vitro*, Smean, and Smean to median ratio of thickness distribution

Parameter	**Statistically significant difference** [a]
SPF *in vitro*	Yes ($p<0.05$)
Smean	Yes ($p<0.05$)
Smean to median ratio	Yes ($p<0.05$)

[a] between the different formulations on SPF *in vitro*, Smean, and Smean to median ratio of thickness distribution at 5% confidence level (Kruskal-Wallis)

This statistical test revealed a significant effect of vehicle on all tested parameters. To identify which sunscreens differed significantly from each other with respect to the studied parameters, a multiple pairwise comparison test based on Bonferroni approach was employed. The results are given in Table 4.5.,4.6., and 4.7.

Table 4.5. Multiple pairwise comparison test using Bonferroni approach for SPF *in vitro*

Group classification [a]	**WO**	**OW-C**	**GEL**	**CAS**	**OW-S**
Group 1	X	-	-	-	-
Group 2	-	X	X	-	-
Group 3	-	-	X	X	X

[a] sunscreens that were non-significantly different from each other with respect to SPF *in vitro* were assigned to the same group

Table 4.6. Multiple pairwise comparison test using Bonferroni approach for Smean

Group classification [a]	**WO**	**GEL**	**OW-C**	**CAS**	**OW-S**
Group 1	X	X	-	-	-
Group 2	-	X	X	-	-
Group 3	-	-	X	X	X
Groupe 4	-	-	-	X	X

[a] sunscreens that were non-significantly different from each other with respect to Smean were assigned to the same group

Table 4.7. Multiple pairwise comparison test using Bonferroni approach for Smean to median ratio

Group classification [a]	**WO**	**GEL**	**OW-C**	**CAS**	**OW-S**
Group 1	X	X	X	-	-
Group 2	-	-	-	X	X

[a] sunscreens that were non-significantly different from each other with respect to Smean to median ratio were assigned to the same group

This multiple comparison test resulted in a group classification of the investigated sunscreens. Formulations of one group differ statistically from those of another group while formulations that belong to the same group do not differ significantly from each other with respect to the considered parameter. When the same formulation is contained in two different groups it does not differ significantly from the formulations of either group. The number of groups was different for the tested parameters; two, three, and four groups were found for Smean to median ratio, SPF *in vitro*, and Smean, respectively. A small number of groups means less difference between the sunscreens.
WO yielded a significantly higher SPF *in vitro* than all other sunscreens, a greater Smean than OW-C, CAS and OW-S and a smaller Smean to median ratio than CAS and OW-S. OW-C gave a higher SPF *in vitro* and a smaller Smean to median ratio than CAS and OW-S. The GEL and OW-C formulations did not differ significantly from each other with respect to any of the criteria. Also, CAS and OW-S did not differ from each other. OW-C yielded greater SPF *in vitro*, a greater Smean and a smaller Smean to median ratio than OW-S, which was interesting being that these two sunscreens varied only in their content of thickeners, hence their viscosity characteristic.

Finally, the correlation of the SPF *in vitro* with both film parameters for the individual measurements within each sunscreen was evaluated using Spearman rank correlation test. A significant positive correlation between SPF *in vitro* and Smean was found for every sunscreen formulation ($p<0.05$). A negative correlation was found between SPF *in vitro* and Smean to median ratio for WO; OW-S, and CAS ($p<0.05$), whereas no correlation was found for OW-C and GEL.

4.4.3. Impact of pressure and spreading procedure on film parameter values and SPF *in vitro*

In addition to the vehicle, the impact of the application conditions, i.e., spreading procedure and pressure on film parameters and SPF *in vitro* was studied using the GEL sunscreen. In total, three conditions of application were investigated, spreading 1 with high pressure, spreading 1 with low pressure, and spreading 2 with high pressure.

Figure 4.7. shows the average of Abbott-Firestone curves of the GEL sunscreen for each application condition and Table 4.8. gives the median and interquartile range values of SPF *in vitro* and the film parameters for the investigated conditions.

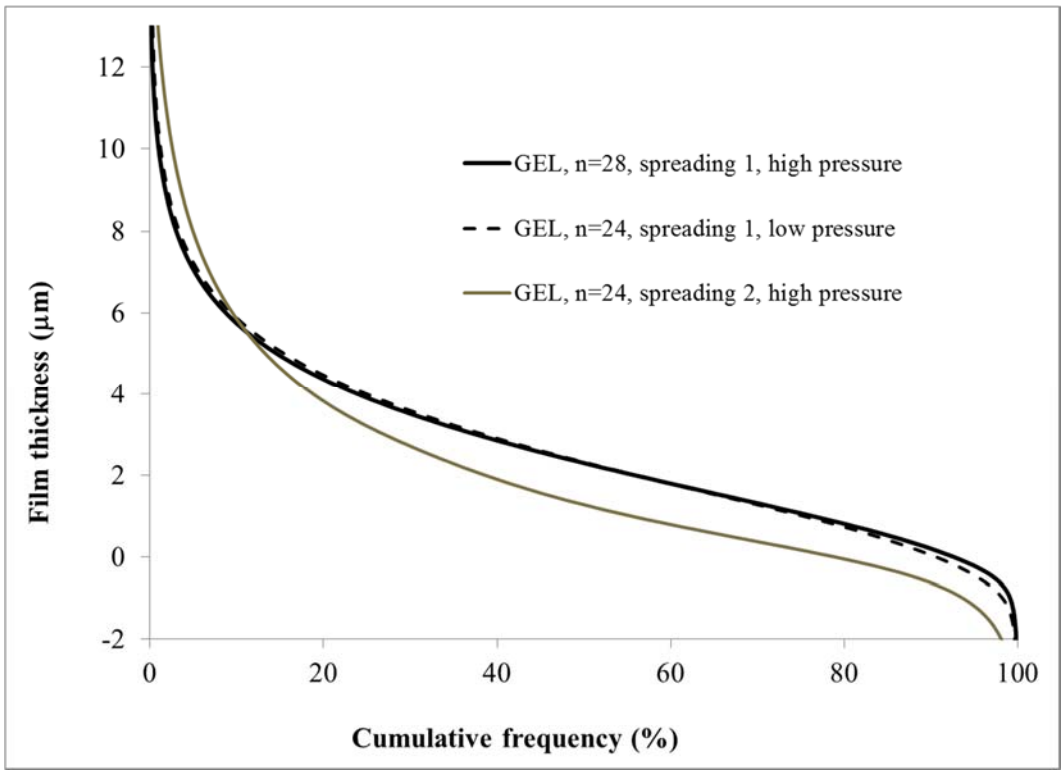

Figure 4.7. Abbott-Firestone profiles of GEL sunscreen applied with two pressure (high and low) and spreading (1 and 2) conditions

It is evident from figure 4.7. that the shape of Abbott-Firestone curve of GEL sunscreen is different between spreading 2 and spreading 1, while no difference was found between low and high pressure using spreading 1. The differences of the Abbott-Firestone curves are reflected in the Smean and Smean to median ratio.

Table 4.8. Medians of SPF *in vitro,* Smean, and Smean to median ratio of thickness distribution with interquartile range Q1 – Q3 (in brackets) for investigated conditions of application for GEL sunscreen

Application of GEL sunscreen	**SPF *in vitro***	**Smean (μm)**	**Smean to median ratio**
Spreading 1, high pressure, n=28	28 (20 – 34)	2.6 (2.4 – 3.1)	1.19 (1.16 – 1.23)
Spreading 1, low pressure, n=24	39 (30 – 54)	2.7 (2.4 – 3.1)	1.19 (1.17 – 1.21)
Spreading 2, high pressure, n=24	20 (15 – 25)	1.9 (1.5 – 2.3)	1.57 (1.50 – 1.91)

SPF *in vitro* data measured for each condition of application were compared to the SPF *in vivo* for GEL sunscreen (figure 4.8.). From this evaluation, spreading 2 with high pressure seems to give a better approximation of the SPF *in vivo*. However, as this condition could not be practically applied to all types of formulation, spreading 1 with high pressure was used as an alternative in the investigation of the different vehicles.

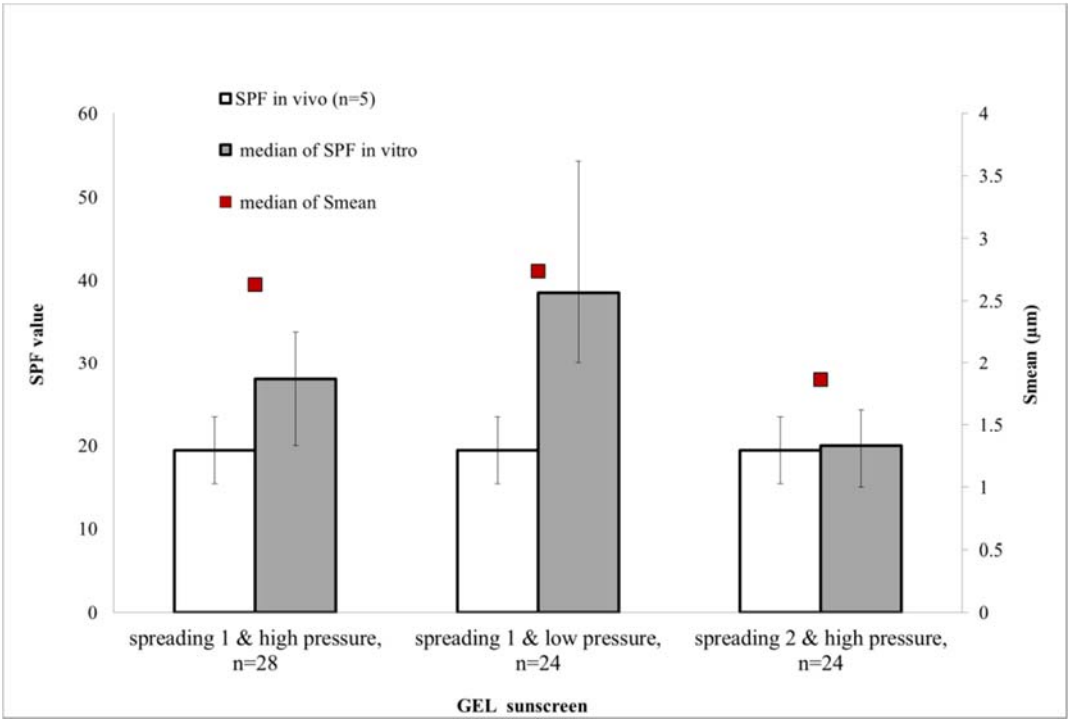

Figure 4.8. SPF *in vivo* (white columns), medians of SPF *in vitro* (gray columns) with interquartile values (bars), and medians of Smean values (square) of GEL sunscreen.

The impact of spreading (procedure 1 versus 2) and pressure (low versus high) on SPF *in vitro* and film parameters were evaluated using Mann-Whitney U test (Table 4.9.).

Table 4.9. Impact of application conditions on SPF *in vitro*, Smean and Smean to median ratio of thickness distribution of GEL sunscreen

Application condition	**Parameter**	**Statistically significant difference** [a]
Spreading	SPF *in vitro*	Yes ($p<0.05$)
(1 versus 2)	Smean	Yes ($p<0.05$)
	Smean to median ratio	Yes ($p<0.05$)
Pressure	SPF *in vitro*	Yes ($p<0.05$)
(low versus high)	Smean	No ($p>0.05$)
	Smean to median ratio	No ($p>0.05$)

[a] between tested application condition (either spreading or pressure) and SPF *in vitro*, Smean, Smean to median ratio at 5% confidence level (Mann-Whitney U test)

Spreading 2 showed a significantly smaller film thickness (Smean) and a larger Smean to median ratio compared to spreading 1 (Table 4.8. and 4.9.). Both, spreading and pressure had a significant effect on SPF *in vitro*. For spreading 2 compared to spreading 1 and high compared to low pressure a reduction of SPF *in vitro* was found. Film parameters were not influenced significantly by pressure.

4.5. Discussion

This work tests the hypothesis that film thickness distribution can be used to explain variation of SPF between sunscreen vehicles and application conditions. For this purpose, accurate measurement of film thickness was necessary.

Many techniques for assessing the film distribution of an applied sunscreen have been used providing merely qualitative or some quantitative information about its distribution.

For qualitative assessment, fluorescence resulting either from a UV filter or from an added fluorescent marker was used to visualize the homogeneity of distribution of the applied product. Sunscreen distribution was evaluated *in vivo* using an appropriate illumination source optionally combined with photography [220,276,277] or multiphoton tomography [246]; for *in vivo* and on tape strips evaluation the use of laser scanning microscopy [27] was also reported. Alternatively, for sunscreens containing titanium dioxide as UV filter, light microscopy on cross sections of skin biopsies [20] was used that gave a rough estimation of the thickness layer based on the visualization of titanium dioxide particles; optical coherent tomography [278] was also used on intact skin that detected the distribution of titanium dioxide particles within the sunscreen layer. For quantitative assessment, the use of *in vivo* fluorescence spectroscopy gave indirect information about the film thickness by converting the fluorescence intensity into an equivalent thickness of an applied product [23,269]. When sunscreens are not intrinsically fluorescent, this technique requires the addition of a fluorescent agent which, however, often produced inconclusive results because of immiscibility or interference issues [248]. An alternative approach reported the use of an *in vivo* skin swabbing technique in conjunction with sunscreen quantification by UV spectroscopy to evaluate the thickness of the film [212]. None of above mentioned methods, however, provided a full characterization of the sunscreen film in terms of thickness and homogeneity of distribution.

In our work, we started from an approach based on topographical measurements. This method was used before on skin replicates and provided a semi-quantitative assessment of film thickness [279]. In contrast to that work, we used a biological substrate for the application of sunscreen to reproduce as closely as possible the product-to-substrate adherence relevant for the *in vivo* situation. In addition, by developing a reference-corrected measurement protocol and quantitative data evaluation the complete thickness distribution could be determined. Topographical evaluation was combined with measurement of SPF *in vitro* both of which were performed in the same position and nearly the same surface area making it possible to reveal existing correlations.

The composition of the five studied vehicles principally differed in the thickener and emulsifier system, the UV filter combination remaining the same. The formulation of the vehicles had a significant effect on Smean and Smean to median ratio (Table 4.6. and Table 4.7.).

Of the two sunscreens OW-C and OW-S which differed mainly in their thickener system, OW-S showed a significantly smaller Smean and greater Smean to median ratio than OW-C. The thickeners Lanette O, Keltrol RD, and Salcare SC 91 contained in OW-C but not in OW-S corresponded to a relative weight difference of only 10% in the remaining film on the skin surface of OW-S versus OW-C, but they appear to be responsible for the significant difference of film thickness and homogeneity between the two sunscreens. This indicates that thickeners, which enable the formation of a firm film upon spreading lead also to a thicker and more homogeneous film. OW-S and CAS did not differ in their Smean and Smean to median ratio both yielding a smaller Smean and larger Smean to median ratio than the other vehicles. This also seems to be related to the absence of thickeners in both formulations. The emulsifier, that was present in the OW-S emulsion, but not in CAS which was a mono-phase, seems to play a minor role for the Smean and the Smean to median ratio. The same observation is true for OW-C and GEL sunscreens that did not differ statistically in Smean and Smean to median ratio both containing thickeners but only OW-C containing emulsifiers. WO had a statistically larger Smean than OW-C, OW-S and CAS which might be related to its continuous oil phase; yet it did not show a significant difference to GEL. With respect to Smean to median ratio, the low viscosity vehicles CAS and OW-S showed a higher positively skewed thickness distribution, hence a greater non-homogeneity of film than the high viscosity vehicles WO, OW-C and GEL. It should be pointed out that Smean differences between the vehicles were not due to differences in mass loss during application.

The formulation of the vehicles had a significant effect on SPF *in vitro* (Table 4.5.). It appears that large and small Smean values among vehicles corresponded respectively to high and low SPF *in vitro*. Therefore, the differences in SPF between vehicles may be discussed in relation to the film parameter Smean. For this we consider that smaller Smean is connected to a greater occurrence of small film thicknesses and that light transmittance, which is inversely proportional to SPF, increases exponentially with decreasing film thickness. OW-S and CAS for instance, exhibited the smallest Smean values and yielded also the lowest SPF. These two sunscreens which lacked thickeners and had the lowest viscosity compared to the rest may leave larger areas of ridges virtually uncovered while accumulating in the furrows thus leading to low SPF. Therefore, the presence of thickeners in the formulation seems to be a prevailing prerequisite for UV efficacy. Further, WO exhibited both, the largest Smean value and the highest SPF.

This is consistent with minimal surface area with very small film thickness that would be virtually unprotected. Furthermore and in contrast to the other sunscreens, the UV filters of WO are distributed in the continuous phase which does not evaporate, forming a uniform protecting film with the help of the thickeners. An increase of about 45% of SPF *in vitro* was found for the WO sunscreen compared to OW-C, which is in line with data reported previously on sunscreens with smaller SPF values [20]. CAS and OW-S as well as OW-C and GEL did not differ with respect to any of the tested criteria and can be considered as very similar in terms of film forming ability and SPF efficacy. Taken together, the SPF variation observed between sunscreens containing the same filter composition is proposed to arise from the difference in their film thickness distribution.

Within every sunscreen, Smean correlated positively with SPF *in vitro*. Further, Smean to median ratio showed a negative correlation with SPF *in vitro* for three of the five sunscreens. This demonstrates the significant connection between the film formation and sun protection efficacy and supports the observation discussed above about the differences between sunscreens. The present data addressing film formation and thickness distribution go beyond previous studies that showed that film thickness resulting from different application amount of sunscreen strongly impacts SPF efficacy [180,265].

Besides the vehicle formulation, this work demonstrated using the GEL that application conditions can significantly impact sunscreen performance. We found that a longer spreading time resulted in a larger Smean to median ratio, a smaller Smean and smaller SPF *in vitro* values (Table 4.8.) further corroborating the correlation between film characteristics and sunscreen efficacy; also, increase of pressure by 180 g resulted in a significant decrease in SPF values. Interestingly, this effect of prolonged and high pressure application was analogous to that elicited by low viscosity formulations, which might be related to a thinning of the GEL under these application conditions. The effect of application conditions on the performance of the other vehicles still needs to be investigated. Some authors reported that even a change in pressure of 50 g led to different SPF *in vitro* when using synthetic plates as substrate [188]. Former studies reported that a more rubbed application led to a smaller SPF *in vivo* [22] and a crude compared to a careful application to a smaller cream thickness [23].

Finally, more recently, the effect of careful versus crude spreading of sunscreen on the magnitude of erythema occurrence was simulated, and underlined the "importance of homogeneity of spreading on the level of delivered protection" [24].

Figure 4.9. summarizes the connection between the influencing factors, i.e., application condition and vehicle, the film distribution and the measured SPF *in vitro* of sunscreens.

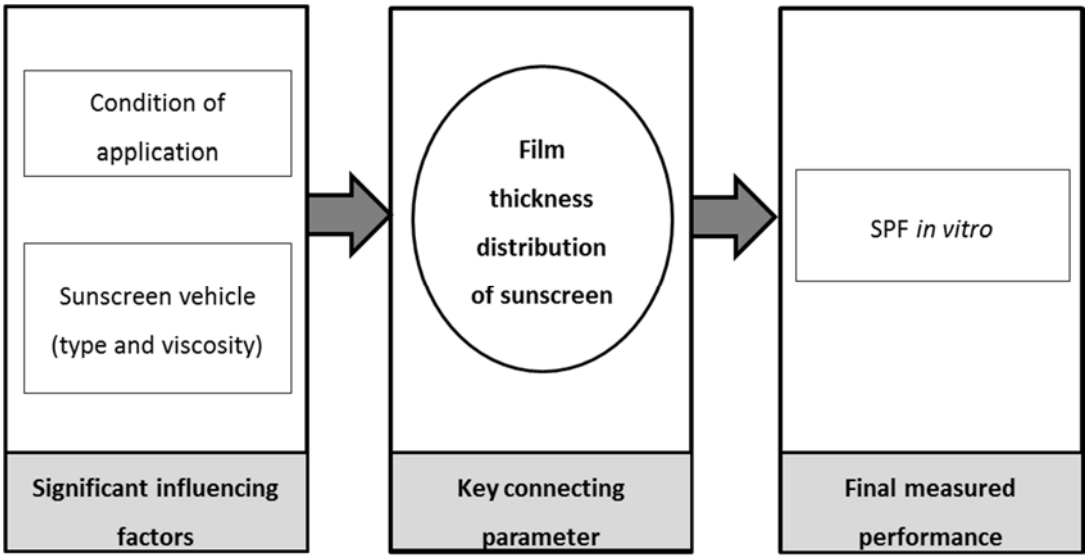

Figure 4.9. Connections between influencing factors, film distribution, and SPF efficacy

4.6. Conclusion

The type and the viscosity of sunscreen vehicles and application conditions play a role for the film thickness parameters that finally influenced the SPF efficacy. High application pressure, long spreading time, low viscosity of formulation and/or absence of thickeners were shown to impact unfavorably UV protection. As application condition can in principle be fixed, the impact of a vehicle on the formed film can now be investigated during the product development step. Sunscreen composition might be optimized accordingly to achieve a large film thickness with uniform distribution; minimization of the small thickness fraction of the film being crucial for ultimate sunscreen performance. Development of a method to quantify the film thickness distribution of sunscreen on skin was shown to be essential for understanding the mechanism influencing UV efficacy.

Chapter 5

Calculation of the SPF of sunscreens with different vehicles using measured film thickness distribution – comparison with SPF *in vitro*

5.1. Abstract

The sun protection factor (SPF) depends on UV filter composition, and amount and type of vehicle of the applied sunscreen. In chapter 4, we showed that the vehicle affected the average thickness of sunscreen film that is formed upon application to a skin substrate and that film thickness correlated significantly with SPF *in vitro*.

M. Sohn et al., "Calculation of the SPF of sunscreens with different vehicles using measured film thickness distribution – comparison with SPF in vitro" J. Photochem. Photobiol. B. 159 (2016) 74-81.

Here, we quantitatively assess the role for sunscreen efficacy of the complete film thickness frequency distribution of sunscreen measured with an oil-in-water cream, an oil-in-water spray, a gel, a water-in-oil, and an alcoholic spray formulation. A computational method is employed to determine SPF *in silico* from calculated UV transmittance based on experimental film thickness and thickness distribution, and concentration and spectral properties of the UV filters. The investigated formulations exhibited different SPF *in vitro* and different film thickness distribution especially in the small thickness range. We found a very good agreement between SPF *in silico* and SPF *in vitro* for all sunscreens. This result establishes the relationship between sun protection and the film thickness distribution actually formed by the applied sunscreen and demonstrates that variation in SPF between formulations is primarily due to their film forming properties. It also opens the possibility to integrate the influence of vehicle into tools for *in silico* prediction of the performance of sunscreen formulations. For this, use of the Gamma distribution was found to be appropriate for describing film thickness distribution.

5.2. Introduction

Topical sunscreens represent a simple, practical and efficient means [7] of protecting skin from damages inflicted by solar radiation [2-5]. The evaluation of the performance of sunscreen products is carried out by an *in vivo* methodology requiring clinical trials [9]. Although this is a laborious, time consuming, expensive and ethically questionable method, it remains to date the only validated method for determining the sun protection factor (SPF) that is approved by regulatory bodies. Therefore, alternative *in vitro* or *in silico* methods are urgently needed. A lot of effort has been put into the development of an *in vitro* method for SPF determination. Current *in vitro* methodology utilizes measurement of spectral transmittance of UV light through a layer of sunscreen applied to a suitable substrate and takes into account the erythemal effectiveness spectrum to determine SPF. Yet, no attempt has been fully successful so far in reproducing the *in vivo* results in a repeatable fashion, many issues still remaining [17-19,189,190] concerning foremostly (i) the choice of a substrate that best mimics human skin and (ii) control of the process of application [10,23]. Notably, substrates of PMMA routinely used in the industry do not provide satisfactory results [10,189,190].

Some authors introduced an *in silico* approach for an a priori calculation of the performance of sunscreens [25, 191, 192]. In analogy to SPF *in vitro*, SPF *in silico* is based on UV spectral transmittance which is combined with erythemal effectiveness.

A Spectral transmittance is calculated in this case based on the absorption properties of the UV filters, their concentration and the product layer thickness. Since thickness uniformity was found to depend on substrate roughness and the application process [195] and, moreover, to play a role for sunscreen performance [24,25,246], a reliable estimate of film thickness distribution is required. For this, a calibrated step film model at first [193,197] and later a continuous thickness distribution model [11,191,195] were used. The latter approach utilized the gamma distribution, a statistical probability distribution function containing one adjustable shape parameter, to describe the cumulative thickness distribution of the sunscreen film. By deducing the value of the shape parameter through fitting to experimental data of *in vitro* spectral absorption [191,195] or *in vivo* SPF [192,193,195] this model was shown to describe the results accurately and therefore, provide the possibility for theoretical *in silico* prediction of the performance of sunscreens. Yet the need to assume a film thickness distribution model and the choice of experimental data, i.e., formulation vehicle, application amount and process, substrate roughness, that are used as reference for defining its shape remain a limitation.

In chapter 3, we demonstrated that the use of a substrate for SPF *in vitro* measurement consisting of isolated epidermis from pig ear skin laid on quartz plates provided results that did not differ significantly from SPF determined clinically. Moreover, we developed a method based on topographical measurements to determine the accurate film thickness frequency distribution of sunscreens applied to this substrate (chapter 4). Using five different sunscreen formulations containing the same UV filter combination in different vehicle types we examined the hypothesis that divergence of efficacy between the sunscreens is related to differences in thickness of the applied product layer. The type and the viscosity of the sunscreen formulation and the procedure of application were found to affect the weighted average film thickness which exhibited a significant correlation with the measured SPF *in vitro*. This supported the validity of the tested hypothesis and explained to a large extent the differences of sun protection performance between sunscreen formulations.

The objective here is to quantitatively assess the role of film thickness frequency distribution for the performance of sunscreens and utilize this to elucidate the origin of variation of SPF observed between different sunscreen formulations.

For this purpose, a computational method was employed making use of the complete experimental thickness frequency distribution of sunscreen film for calculating the SPF value. This method is based on UV spectral transmittance taking into consideration in addition to film thickness distribution the UV filter absorption spectrum and concentration. UV transmittance is combined with the erythemal effectiveness spectrum for a standardized solar radiation spectrum yielding finally an integral SPF over a surface area of measurement roughly corresponding to that of *in vitro* and *in vivo* conditions. Compared to previous studies this work employs in the calculation measured film thickness data instead of an assumed thickness distribution making it possible to investigate differences between the used formulations.
The calculated SPF value is compared with SPF measured *in vitro* in order to establish the validity of the computational approach involving film thickness frequency distribution and, ultimately, propose a methodology for calculating SPF in order to predict the efficacy of sunscreen products. For this methodology, the possibility to express the film thickness frequency distribution by a model function for routine application is explored.

5.3. Materials and methods

5.3.1. Chemicals and equipment

The following UV filters were used: Tinosorb S abbreviated BEMT (INCI, bis-ethylhexyloxyphenol methoxyphenyl triazine), Uvinul N539T abbreviated OCR (INCI, octocrylene) from BASF SE,
Ludwigshafen, Germany; Eusolex 232 abbreviated PBSA (INCI, phenylbenzimidazol sulfonic acid) from Merck, Darmstadt, Germany; Parsol 1789 abbreviated BMDBM (INCI, butyl methoxydibenzoylmethane) from DSM, Kaiseraugst, Switzerland; Neo Heliopan OS abbreviated EHS (INCI, ethylhexyl salicylate) from Symrise, Holzminden, Germany.
Following equipment was used: Surface metrology instrument (Altisurf 500, Altimet, Thonon-lesBains, France); UV transmittance analyzer (Labsphere UV-2000S, Labsphere Inc., North Sutton, NH, USA).

Following software packages were used: Phenix and Altimap (Altimet, France) for topographical measurement and evaluation, respectively; UV-2000 (Labsphere Inc., USA) for UV transmittance measurement; Igor Pro 6.32A (WaveMetrics, Inc., Portland, OR, USA) for the data fitting and convolution operation.

5.3.2. Preparation of skin substrate

We used epidermal membrane of pig ear for sunscreen application prepared by heat separation as described in section 3.3.2., method 2 (3.3.2.2.).

5.3.3. Sunscreen vehicles

Five different sunscreen vehicles including an oil-in-water cream (OW-C), an oil-in-water spray (OWS), a water-in-oil emulsion (WO), a gel (GEL) and a clear lipo-alcoholic spray (CAS) were used. They contained the same UV filter composition and emollient. The filter system was composed of 8 w-% OCR, 5 w-% EHS, 2 w-% BMDBM, 1 w-% BEMT, and 1 w-% PBSA. The full composition of investigated sunscreen formulations is given in section 4.3.3., Table 4.1.

5.3.4. Measurement of the sun protection factor *in vitro*

SPF *in vitro* measurement was based on UV transmittance, which denotes the inverse of the UV intensity attenuation factor measured with a protecting sunscreen film [12]:

$$\text{SPF } in\ vitro = \frac{\sum_{290}^{400} s_{er}(\lambda).S_s(\lambda)}{\sum_{290}^{400} s_{er}(\lambda).S_s(\lambda).T(\lambda)} \qquad (5.1.)$$

where, the inverse transmittance (1/T) in the UV spectral range is weighted with the erythemal action spectrum, $s_{er}(\lambda)$ [9], and the spectral irradiance of the UV source, $S_s(\lambda)$ [9].
A blank transmittance spectrum recording, topographical measurement of bare skin (see section 5.3.5.), sunscreen application, new topographical measurement, and UV transmittance recording through sunscreen covered skin substrate were performed in sequence.
A sunscreen amount of 2.0 mg/cm^2 corresponding to a theoretical film thickness of approximately 0.002 cm before water evaporation was applied. This experimental procedure was described in chapter 4.

5.3.5. Assessment of the film thickness distribution of an applied sunscreen

The sunscreen film was investigated using topographical measurements with a confocal optical probe based on white light chromatic aberration principle. The film thickness was obtained as the difference of skin topography data with and without sunscreen. The result was expressed as a histogram of frequencies of film thicknesses over the measured surface area and is referred to here as film thickness distribution curve. The film was assessed in an area coinciding with that of the SPF *in vitro* determination. A detailed description of this method was given in section 4.3.6..

5.3.6. Determination of the corrected film thickness frequency distribution of an applied sunscreen using a convolution approach

The error of the method employed for measuring film thickness based on surface topography was estimated by repeated determination of the topography of the same surface and calculation of the difference between consecutive topography determinations in a point-by-point fashion with the same procedure as the one used to calculate film thickness.

The deviation of this difference from zero signified the amplitude of noise and followed a frequency distribution that was used as measurement error. This error estimation was performed with the bare substrate consisting of epidermal membrane on quartz and with sunscreen applied to the substrate. The error distribution curves also referred to as blank curves were approximated by Equation (5.2.).

$$B = \frac{B1}{(d - B2)^2 + \exp\big(-B3\ (d - B2)\big) + \exp(B4\ (d - B2)) + 1} + B5\ \exp(-B6\ (d - B2)^2) \tag{5.2.}$$

where, d is noise amplitude of film thickness measurement, and the six coefficients B1 to B6 were deduced by least square fitting to the determined error data for each tested condition. The measured film thickness distribution, M, represents the convolution of the "true" distribution, q, with the distribution of the measurement error, B (Eq. 5.3.).

$$MM = qq * BB \tag{5.3.}$$

In order, therefore, to obtain the true, i.e., corrected thickness distribution function, a deconvolution operation must be performed. Since however deconvolution of two functions is computationally difficult, the corrected film thickness frequency distribution, q, was obtained from the measured distribution, M, and the respective blank curve, B, by a convolution operation of q with B (Eq. 5.3.) and simultaneous fitting to the experimental results of M by least square analysis to determine the coefficients of function q. For this purpose, B of Eq. (5.2.) with known coefficients B1 to B6 and q described by Equation (5.4.) were used.

$$q = \frac{q1}{q2\ exp(-q3\ (d - q4))\quad + \mathrm{q5}\ (d - q4)^2 + 1} + \frac{q6}{q7\ (d - q8)^2 + 1} + q9 \tag{5.4.}$$

where, d is the film thickness, and the nine coefficients q1 to q9 were treated as adjustable parameters that were deduced from the least square optimization. The form of function q was defined making use of the assumption that this function should also provide an adequate fit of the measured film thickness distribution, M. For the convolution operation the error distribution, B, was centered on the zero point. The convolve/A option of the Igor Pro 6 software was employed.

The determined function given by Eq. (4) was then used to build the corrected film thickness distribution for each investigated sunscreen in a discrete form in 0.058 μm increment steps. A small percentage of area under the corrected thickness distribution curve was below a film thickness of 0 μm for each sunscreen. The percentage of film thickness with a value smaller than 0 μm was deleted and the thickness distribution was adjusted to 100% giving the q_{adj} distribution. Using this q_{adj} distribution made possible to calculate the SPF of every sunscreen as outlined below and to compare this to the measured SPF *in vitro* value.

5.3.7. Calculation of the sun protection factor *in silico*

The methodology for calculating the SPF *in silico* is based on the algorithm used with SPF *in vitro* measurements (Equation 5.1.). However, the measured UV transmittance in the *in vitro* method is replaced by a calculated UV transmittance according to Equation 5.5.:

$$T(\lambda) = \sum_{d=0}^{d_{max}} C_{adj}(d)10^{-\varepsilon(\lambda)cdg} \qquad (5.5.)$$

where, ε(λ) is the average molar absorption coefficient (in L/(mol.cm)), c the molar concentration of the UV filter mixture in the formulation (in mol/L), d is film thickness and g is equal to $0.0015/S_{mean}$. The factor g is used to adjust the film thickness to the value corresponding to the concentration of UV filters in the applied sunscreen and accounts, therefore, for the evaporation of volatile components of the vehicle upon application. S_{mean} is the average film thickness in cm obtained from the q_{adj} distribution. The value of 0.0015 cm is the average film thickness before evaporation. This value rather than 0.002 cm is used for the applied 2 mg/cm^2 considering that approximately 25% of sunscreen remained on the finger coat and beyond the edge of the substrate in the process of spreading as determined gravimetrically. For a sunscreen containing several UV filters, as it is generally the case, the transmittance is calculated using the average molar absorption coefficient of the UV filter mixture and molar concentration based on the average molecular weight of the used UV filters.

Consequently, to generate relevant calculated transmittance data, mixed absorbance spectra are calculated from the UV spectroscopic performances and amount of the used UV filters [193]. As Eq. (5.5.) shows, the global transmittance data of a sunscreen film is obtained as the sum of the transmittance through each thickness fraction of the film. Transmittance was calculated at wavelengths from 290 to 400 nm at 5 nm intervals. Using the transmittance values obtained from Eq. (5.5.), the SPF *in silico* was calculated with Eq. (5.1.).

A summary of the steps followed to determine the unknown coefficients of function q to obtain the corrected film thickness distribution and to calculate the SPF *in silico* of tested sunscreens is given in figure 5.1

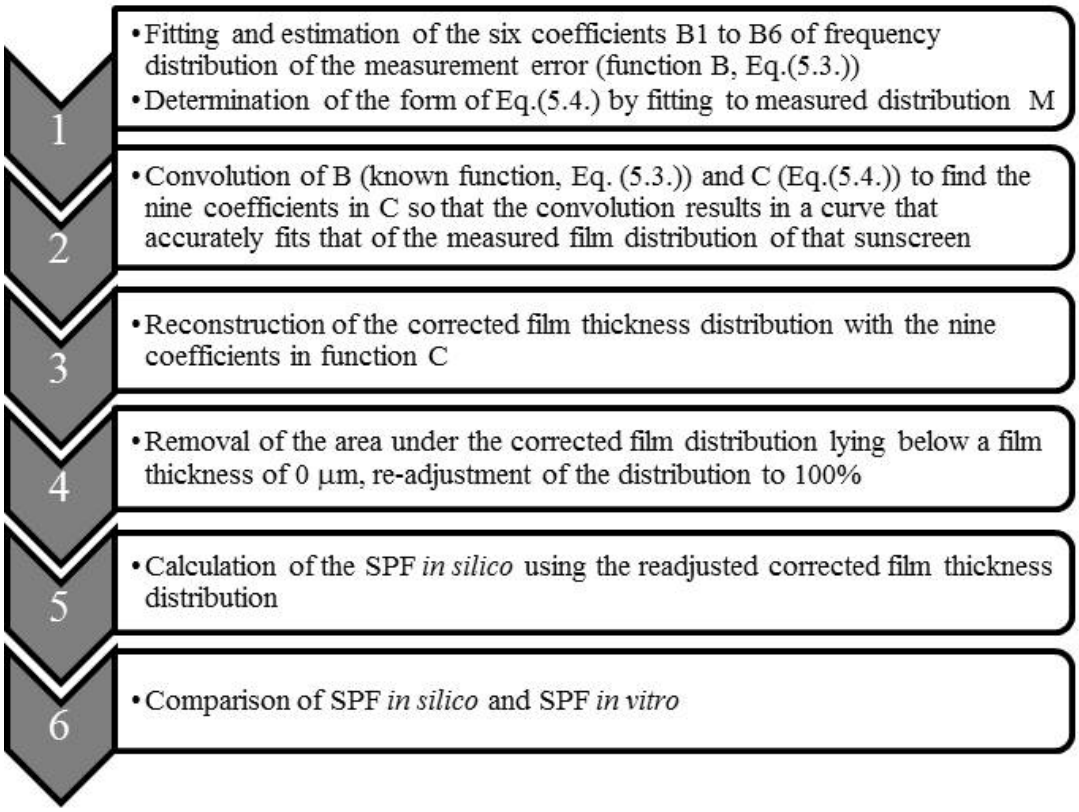

Figure 5.1. Steps for the determination of the corrected film thickness distribution and SPF *in silico* of an applied sunscreen

5.4. Results and discussion

5.4.1. Measurement error of film thickness

The experimental results of error estimation for the bare substrate and each of the five sunscreen formulations applied on the substrate are shown in Figure 5.2.

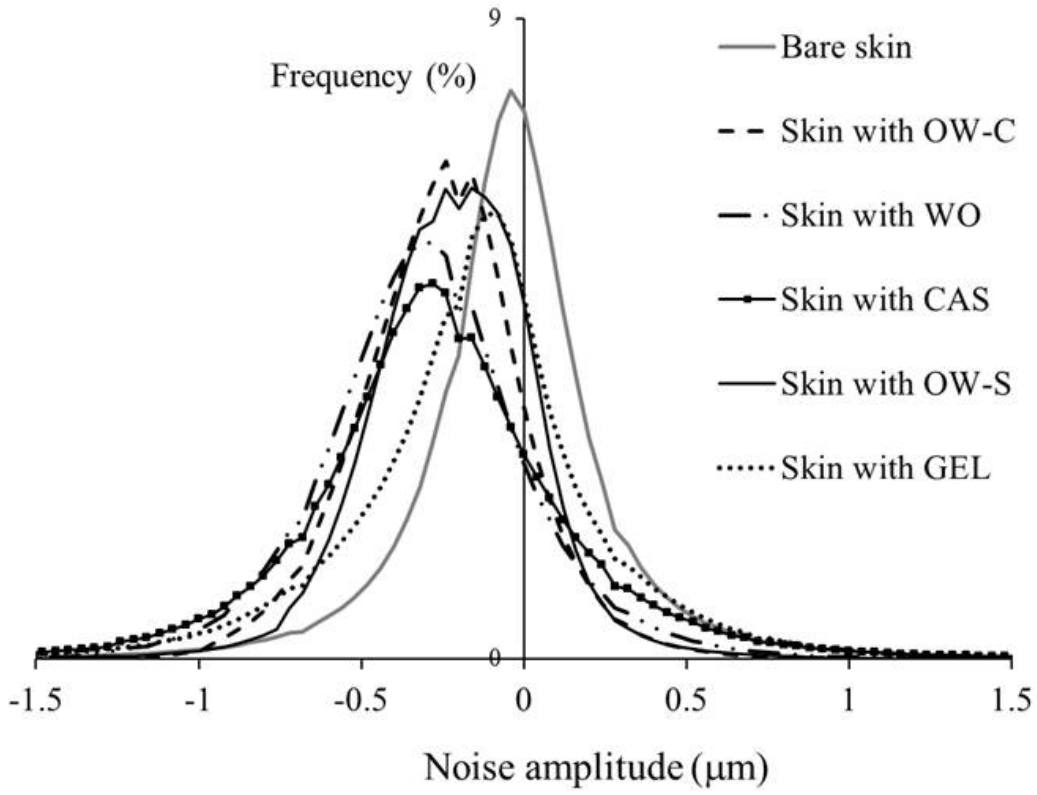

Figure 5.2. Error distribution curves for the bare substrate and each of the five sunscreen formulations applied on the substrate

The error distribution curve for the bare substrate was symmetrical around the zero point and had amplitude ranging approximately between -1 and 1 μm. The error distribution curves for the different sunscreen formulations were also symmetrical but somewhat wider than that of the bare substrate and the position of their apex was shifted into the negative value range.

The average film thickness, S_{mean}, computed as the mean of the frequency distribution was -222 nm, -215 nm, -175 nm, -169 nm, -165 nm, and -113 nm for the water-in oil (WO), clear lipo-alcoholic spray (CAS), oil-in-water cream (OW-C), oil-in-water spray (OW-S), and gel (GEL) formulation, respectively. This suggests a slight recession of the surface of the sunscreen between the two measurements probably due to evaporation of volatile components of the formulation. The magnitude of this evaporation was too small to be detected by analytical weight measurement (data not shown). By comparison, S_{mean} for the bare substrate was -12 nm.

These experimental error distributions were described by Equation (5.2.). The function given by Eq. (5.2.) was determined empirically by starting from the Lorentzian function and adding exponential terms in the denominator and a Gauss-like term to improve the approximation. The six coefficients B1 to B6 deduced by fitting for each tested condition are given in Table 5.1. The estimates were accurate as evidenced by their rather small standard error.

Table 5.1. Estimated coefficients in Equation (5.2.) for the error distribution curve B for the bare skin and each of the five investigated sunscreens

Coefficient	Bare skin	Skin covered with sunscreen				
		OW-C	OW-S	GEL	WO	CAS
B1	20.49±0.21	45.69±1.86	49.94±3.53	11.44±0.33	16.20±1.6	25.32±0.75
B2	-0.03±0.00	0.34±0.01	-0.23±0.00	-0.10±0.00	-0.31±0.00	-0.30±0.00
B3	8.68±0.14	9.75±0.07	9.36±0.17	3.75±0.07	5.13±0.17	4.86±0.07
B4	9.34±0.17	6.95±0.16	8.49±0.24	4.66±0.09	5.09±0.17	4.54±0.06
B5	1.06±0.08	-9.26±0.58	-10.19±1.15	2.45±0.11	0.42±0.53	-3.29±0.24
B6	2.42±0.15	33.37±0.72	40.75±0.91	40.03±2.78	13.38±2.97	5.49±0.31

The blank function B (Eq. (5.2.)) for each sunscreen formulation was used to correct the measured film thickness frequency distribution of the respective formulation by the convolution operation. For this purpose distribution B was centered on the zero point because a shift of the sunscreen surface is not applicable in film thickness measurement as the first topographical measurement is carried out on bare substrate.

5.4.2. Film thickness distribution of sunscreens

Figure 5.3.a. shows an example of fitting of the result of convolution of functions q with B to the measured thickness distribution M for the GEL sunscreen. The corresponding error distribution, B, is also shown on a different scale for comparison. An excellent agreement between the fitted and the measured film thickness frequency distribution curve was obtained. The corrected film thickness distribution, q, was slightly narrower especially in the left flank of the curve compared to the measured curve (Fig. 5.3.b.).

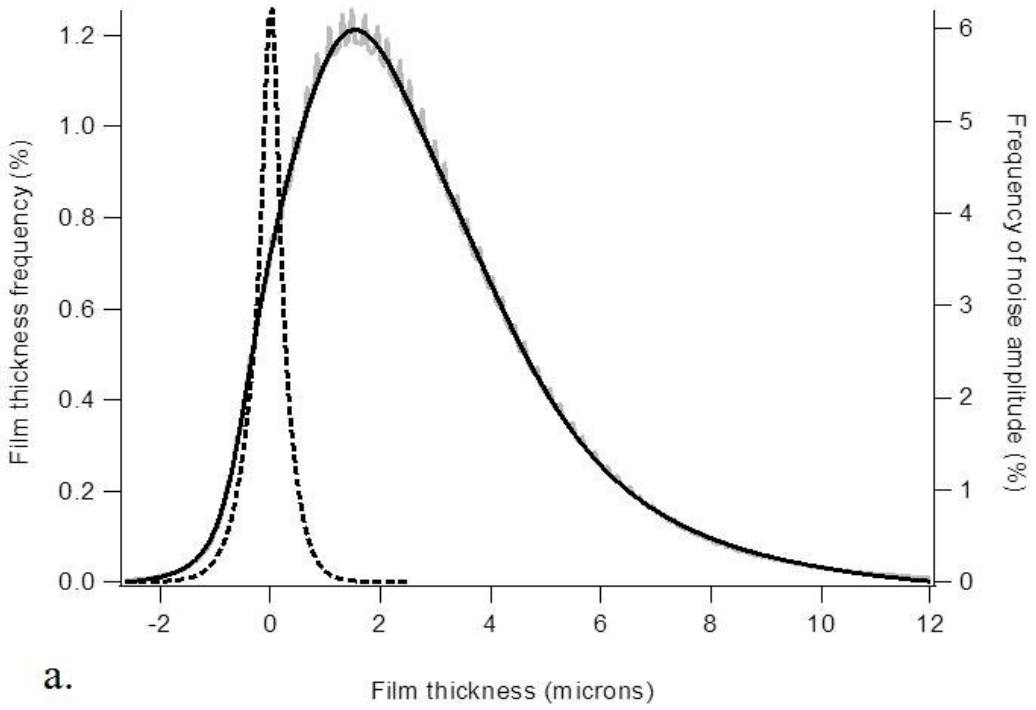

a.

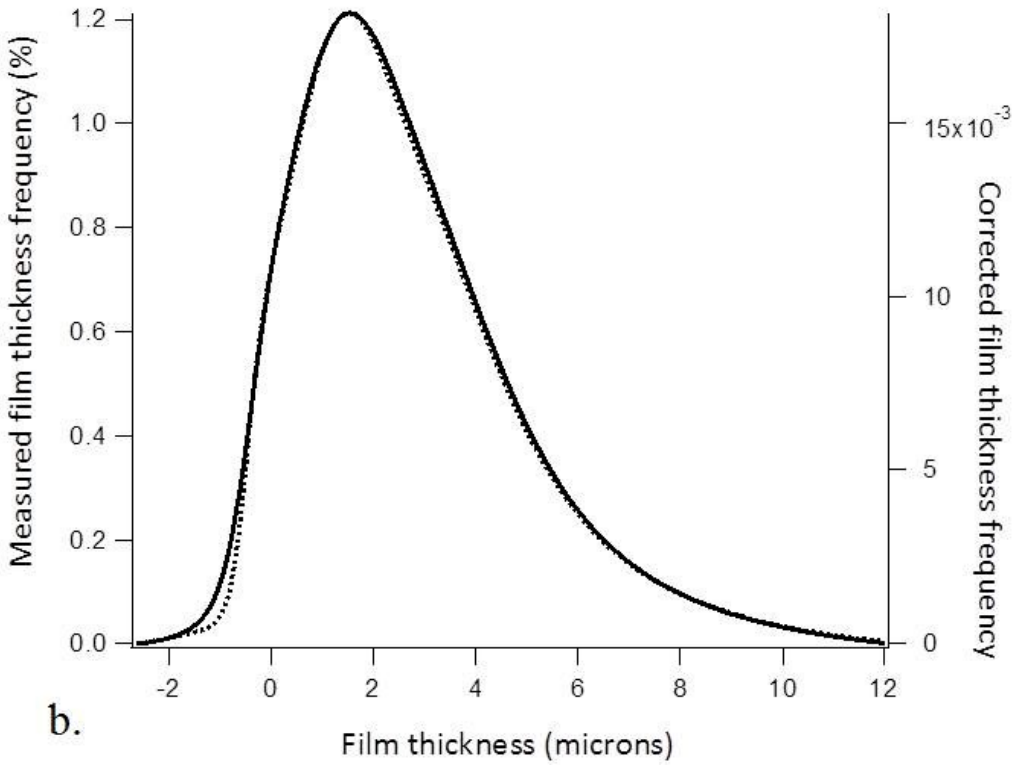

Figure 5.3. Example of fitting the result of the convolution q∗B for the GEL sunscreen; (a) Fitted (black line) and measured (gray line) film thickness frequency distributions (left axis); dashed line is error distribution (right axis). (b) Corrected film thickness distribution (dotted line, right axis) compared to the distribution fitted to the measured data (solid line, left axis).

The values of the nine coefficients q1 to q9 of function q deduced from the fitting are given for all tested sunscreen formulations in Table 5.2.. The standard errors of the estimated coefficients were rather small evidencing the goodness of the approximation.

Table 5.2. Estimated coefficients ± standard error of distribution q (Eq. 5.4.) for each investigated sunscreen

Coefficient	OW-C	OW-S	GEL	WO	CAS
q1	0.0233±0.0005	0.0191±0.0003	0.0155±0.0002	0.0201±0.0003	0.0255±0.0003
q2	0.130±0.050	0.044±0.014	3.1e-6±4.9e-6	0.021±0.009	0.034±0.012
q3	3.957±0.152	3.412±0.141	7.124±0.836	3.735±0.214	7.965±0.473
q4	0.493±0.060	0.063±0.036	1.340±0.016	1.464±0.031	-0.037±0.042
q5	0.355±0.017	0.388±0.018	0.303±0.014	0.501±0.026	0.362±0.014
q6	0.0043±0.0002	0.0051±0.0002	0.0060±0.0003	0.0060±0.0002	0.0025±0.0001
q7	0.225±0.012	0.187±0.007	0.2±0.012	0.303±0.012	0.117±0.009
q8	2.620±0.068	2.246±0.041	3.311±0.052	3.250±0.034	3.126±0.077
q9	-4e-4±2.8e-5	-3e-4±2e-5	-8e-4±5.7e-5	-4e-4±2.4e-5	-3e-4±2.4e-5

The form of function q given by Eq. (5.4.) was defined empirically based on the assumption that this function should also fit the measured film thickness distribution, M (fit not shown). Eq. (5.4.) consists of two overlapping Lorentzian functions one of which contains an exponential function in the denominator to account for the asymmetry of the distribution. Frequency values corresponding to film thickness smaller than 0 µm were deleted as they probably originated from application and measurement artifacts. For example, sharp ridges on the skin surface may be crushed during spreading of the sunscreen due to the applied pressure. These ridges are present and measured in the first topographical measurement on bare skin but not in the second measurement on sunscreen covered skin resulting in a lower recorded surface height and hence, negative thickness values. Also sharp ridges may lead to erroneous focus with the used optical technique [280]. The final film thickness distribution was adjusted to a total frequency (area under the curve) of 100% for further consideration.

Figure 5.4. displays the corrected and adjusted film thickness frequency distribution of all investigated sunscreens. It is evident that the distribution curve differed considerably between the sunscreens. All sunscreens exhibited a certain percentage of film with thickness equal to 0 µm reflecting an unprotected skin surface area in terms of UV light exposure; this percentage differed between the sunscreens.

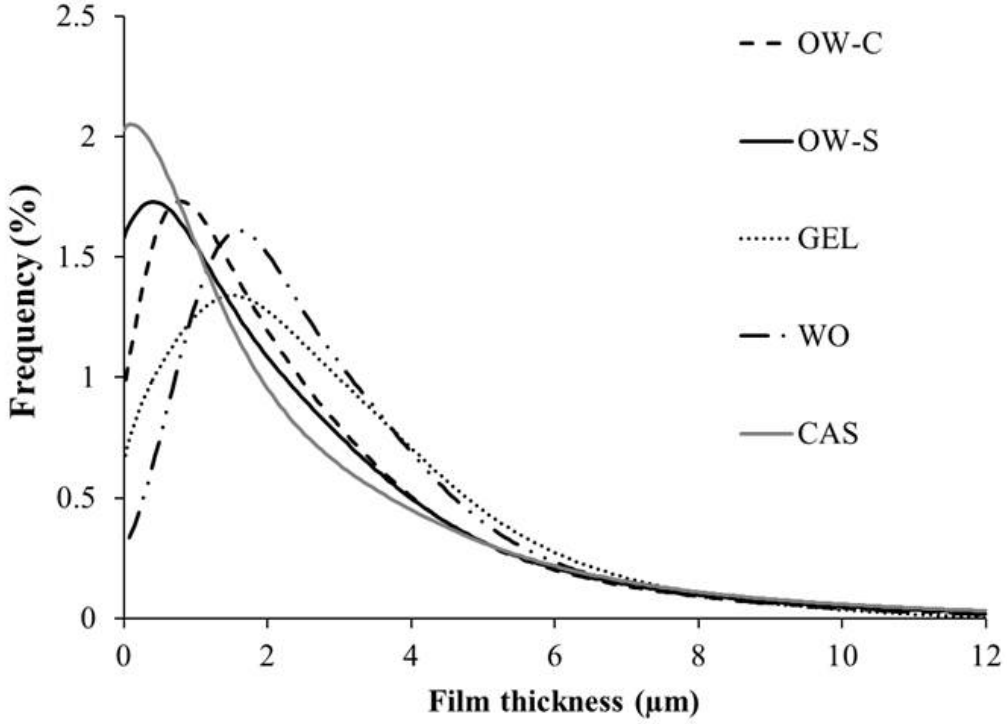

Figure 5.4. Corrected and adjusted film thickness frequency distribution of all investigated sunscreens

For example, CAS and OW-S exhibited more than 2% and 1.6%, respectively, of film with thickness = 0 µm and the largest percentage of small film thicknesses compared to the other formulations. WO, by comparison, showed less than 0.3% of film with thickness = 0 µm and the smallest percentage of small film thicknesses. Furthermore, WO exhibited the thickest film, the maximum film thickness frequency occurring at approximately 2 µm, closely followed by GEL. The studied formulations exhibited the maximum (peak) of their thickness frequency distribution at decreasing thickness in the order WO>GEL>OW-C>OW-S>CAS. No differentiation between the formulations was found above 8 µm. Notably, CAS and OW-S had the lowest viscosity of all formulations. WO, on the other hand, was the only formulation consisting of a non-evaporating continuous phase. These characteristics may be responsible for the different film forming properties of the vehicles and were discussed in detail chapter 4. Film thickness frequency distribution reflects film irregularity over the surface area of application which is found to depend strongly on the used formulation. It should be pointed out that the substrate used in the present study consisted of heat separated epidermis.

The roughness of this substrate is much smaller that the roughness of full thickness skin and also smaller than the roughness of the PMMA plates routinely used in industry for SPF *in vitro* determination. Yet the heat separated epidermis substrate was found in an earlier study to provide SPF *in vitro* results much better matching the SPF determined *in vivo* (chapter 3). This was attributed to the better product-to-substrate affinity afforded by the heat separated epidermis compared to the artificial plates. Therefore, this substrate was used in subsequent studies. It is worth mentioning that SPF *in vitro* cannot be measured with full thickness skin because of the optical non-transparency of the tissue. Further, film thickness frequency distribution on full thickness skin or on PMMA plates has not been determined. Therefore, the effect of substrate roughness and nature on film irregularity cannot be ascertained although literature reports have suggested that increased substrate roughness may promote film irregularity . Finally, the influence of the total amount of applied sunscreen on film thickness distribution was not investigated.

5.4.3. Sun protection factor *in silico* and *in vitro*

For calculating SPF *in silico* of a sunscreen with Eq. (5.1.), UV spectral transmittance is required. This was calculated with Eq. (5.5.) using the corrected film thickness frequency distribution data shown in Fig. 5.4. Further, the spectral average molar absorption coefficient and the molar concentration of the employed UV filter mixture, as well as the average film thickness were used. The concentration of the UV filters in the sunscreens was determined prior to application by HPLC (data not shown). As explained under methods (5.3.7), an average film thickness of the sunscreen before evaporation of 15 µm was used for the application amount of 2 mg/cm^2.

The obtained calculation results are shown in Fig. 5.5. together with SPF *in vitro* values measured on the same preparations as those used for film thickness measurement. As the calculation of SPF *in silico* was carried out with the average film thickness distribution of all measurements, the reported variation of SPF *in silico* values was based on the variation of thickness frequencies between individual measurements for each sunscreen. Also, percentage values of sunscreen film exhibiting a thickness of 0 µm are reported.

SPF values differed considerably between the different sunscreen formulations. Figure 5.5. reveals a very good agreement between SPF *in silico* and SPF *in vitro* for every sunscreen; the agreement was perfect for WO while the difference between the two SPF values was between 6 and 7% for the three sunscreens OW-C, OW-S and CAS, the greatest difference of 21% being found for the GEL sunscreen.

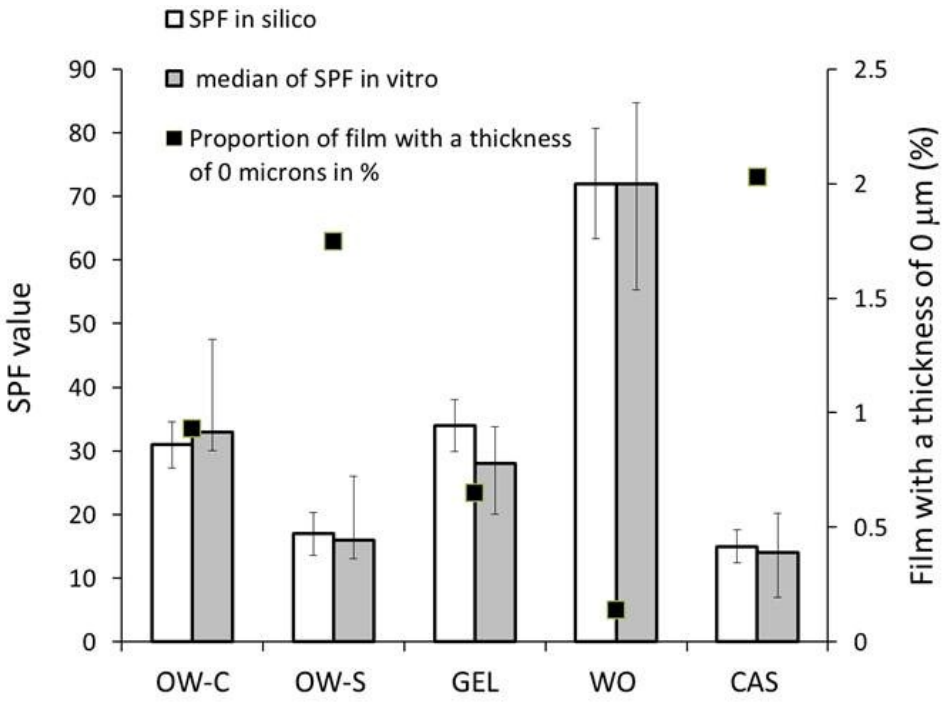

Figure 5.5. Calculated SPF *in silico* (white columns) with variation range (bars), medians of measured SPF *in vitro* (gray columns) with interquartile values (bars), and percentage values of sunscreen film exhibiting a thickness of 0 µm for the investigated sunscreens; n=27 for OW-C, n=20 for OW-S, n=28 for GEL, n=24 for WO, n=20 for CAS.

Thus, using the measured film thickness frequency distribution for calculating SPF resulted for all sunscreens in very good agreement with SPF *in vitro* data obtained from UV transmittance measurements performed on the same preparations. This agreement supports the validity of the calculation procedure involving film thickness measurement for prediction of SPF. The procedure offers the possibility to take quantitatively into account film irregularity for the performance of sunscreens.

Therefore, it is proposed as a valid first line option for the *in silico* prediction of UV light protection efficacy of sunscreens. For the used formulation examples, the determined SPF *in vitro* was in rather good agreement with clinical SPF values (Fig. 4.6. in section 4.4.2.). Before, however, the claim of the present procedure for *in silico* prediction of SPF is definitely established, additional validation with clinical SPF data will have to take place using further formulations of the same type, different types of formulation, e.g. oils, lotions, silicon based, and different UV filter compositions.

The agreement of the calculated SPF for all sunscreens based on the procedure using film thickness distribution with the SPF *in vitro* further strongly indicates that the difference in SPF between sunscreen formulations with the same UV filter composition is foremostly because of the difference in film forming properties between the formulations. Hence, the empirical correlation between average film thickness of sunscreen and SPF established in chapter 4 is confirmed by the present exact evaluation. The inverse correlation of the percentage of film with a thickness = 0 µm with SPF implied by Fig. 5.5. points out the relevance of unprotected substrate areas for the resulting SPF given that light transmittance increases exponentially with decreasing film thickness. These results demonstrate the advantage of vehicles forming continuous regular layers on the skin for optimized UV light protection.

The formulation may additionally affect sunscreen performance by modifying UV filter repartition upon vehicle transformation due to evaporation of volatile components on the skin surface. Ongoing work of this group on this question is to be reported in the near future.

Finally, photolability was not of concern in the SPF *in vitro* measurement with the Labsphere equipment because of the very short exposure time used and was not taken into account in the SPF *in silico* calculation. Hence, the comparability of the two values was assured. However, taking into account photolability is possible in the model calculation as shown [11,275].

5.4.4. Modeling film thickness frequency distribution

The measurement of film thickness distribution elucidated the marked differences between formulations with the same UV filter composition with respect to SPF. Film thickness distribution of each sunscreen reflects the film irregularity over the surface area of application. Existing methodologies for SPF prediction taking into account film irregularity rely on the use of a model function to describe film thickness distribution of the applied product [11,25,191,197] . The Gamma distribution has been used as a model to describe the highly asymmetric film thickness distribution using one adjustable shape parameter [191,195]. A model function generally is more convenient for routine use because it circumvents laborious film thickness measurement. However, the use of a model entails the assumption that the model adequately describes the film thickness distribution and, moreover, it needs to be calibrated with experimental data. No such calibration taking into account the effect of formulation or application procedure of the product exists so far.

In order to test whether the Gamma distribution can be adopted to describe the experimental film thickness results, the probability density function of the Gamma distribution given in Eq. (5.6.) was fitted to the film thickness frequency distribution data of the used sunscreens.

$$f = \frac{\left(\frac{d-d0}{b}\right)^{c-1} exp\left(\frac{d-d0}{b}\right)}{b\ \Gamma(c)} \qquad (5.6.)$$

where, d is thickness, b and c are scale and shape parameters, respectively, Γ(c) is Gamma function with argument c and d0 is the shift of the thickness axis to account for a finite frequency of zero thickness. All three, c, b and d0 were treated as adjustable parameters in the fitting.

The results are shown in Fig. 5.6. An excellent approximation of the experimental results by the function of the Gamma distribution was found. These results provide evidence that the Gamma distribution can indeed describe film irregularity of applied sunscreen in an adequate manner.

Furthermore, by adjusting the value of its parameters this distribution can be adapted to reflect experimental differences between formulations. Hence, this work provides for the first time indication that the Gamma distribution can be universally used to describe film irregularity.

For different formulations and application procedures the model will have to be recalibrated and validated based on additional *in vitro* and clinical experimental data.

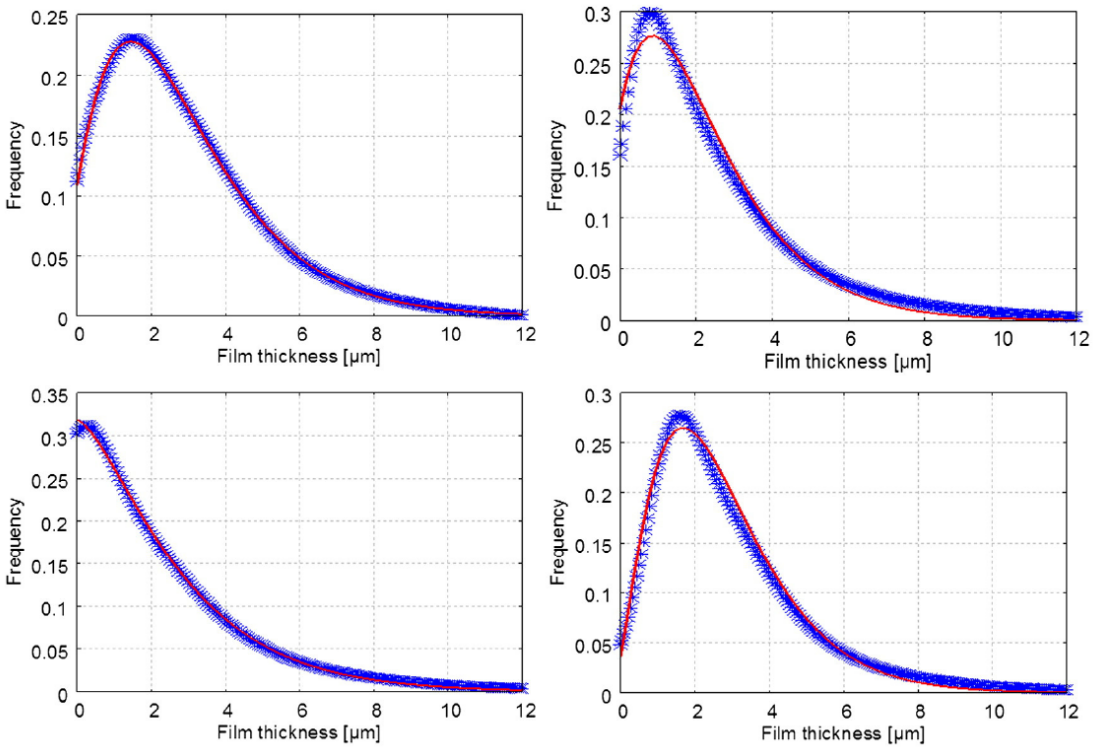

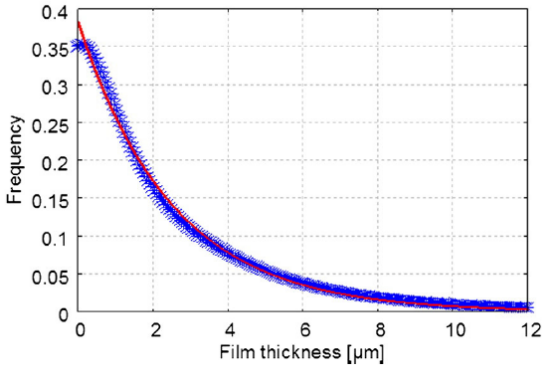

Figure 5.6. Experimental corrected and adjusted film thickness frequency distribution of sunscreens (stars) and fitted probability density function of the Gamma distribution given by Eq. 6.6. (continuous (red) curve). Sunscreen formulations and deduced parameter values of Eq. (6.6.): Top left: GEL, c=2.515, b=1.377, d0=0.64. Top right: OW-C, c=2.26, b=1.25, d0=0.733. Middle left: OW-S, c=1.49, b=1.92, d0=1.07. Middle right: WO, c=2.8, b=1.08, d0=0.275. Bottom left: CAS, c=1.0, b=2.51, d0=1.45.

5.5. Conclusion

The difference between sun protection efficacies of different sunscreen formulations with the same UV filter composition is shown to be because of differences in film thickness and thickness frequency distribution yielded by these sunscreens. The presence of very small film thicknesses is particularly crucial in this respect. Emulsion type and viscosity appear to be the dominant characteristics for film forming properties of the formulation. Hence, the vehicle is shown to substantially impact sunscreen performance. This study demonstrates that use of the film thickness frequency distribution with the proposed computational method provides accurate results and is, therefore, of high relevance for the prediction of sun protection efficacy. Given the inadequacy of current *in vitro* methods for accurate SPF determination, *in silico* tools represent a valid alternative. The present results may serve to further improve the power of currently available tools for the *in silico* prediction of sunscreen performance [273] by developing methodology to integrate vehicle related parameters. This could be achieved based on the Gamma distribution by defining parameter values that reflect vehicle related effects. This is of high interest for the development of sunscreen products.

Chapter 6

Repartition of oil miscible and water soluble UV filters in an applied sunscreen film determined by confocal Raman microspectroscopy

6.1. Abstract

Photoprotection provided by topical sunscreens is expressed by the sun protection factor (SPF) which depends primarily on the UV filters contained in the product and the applied sunscreen amount. Recently, the vehicle was shown to significantly impact film thickness distribution of an applied sunscreen and sunscreen efficacy.

M. Sohn et al., "Repartition of oil miscible and water soluble UV filters in an applied sunscreen film determined by confocal Raman microspectroscopy" Photochem. Photobiol. Sci. 15 (2016) 861-71.

In the present work, repartition of the UV filters within the sunscreen film upon application is investigated for its role to affect sun protection efficacy. The spatial repartition of an oil-miscible and a water-soluble UV filter within the sunscreen film was studied using confocal Raman microspectroscopy. Epidermis of pig ear skin was used as substrate for application of three different sunscreen formulations, an oil-in-water emulsion, a water-in-oil emulsion, and a clear lipo-alcoholic spray (CAS) and SPF *in vitro* was measured. Considerable differences in the repartition of the UV filters upon application and evaporation of volatile ingredients were found between the tested formulations. A nearly continuous phase of lipid-miscible UV filter was formed only for the WO formulation with dispersed aggregates of water-soluble UV filter. OW emulsion and CAS exhibited interspersed patches of the two UV filters, whereas the segregated UV filter domains of the latter formulation were by comparison of a much larger scale and spanned the entire thickness of the sunscreen film. CAS therefore differed markedly from the other two formulations with respect to filter repartition. This difference should be reflected in SPF when the absorption spectra of the employed UV filters are not the same. Confocal Raman microspectroscopy was shown to be a powerful technique for studying this mechanism of sun protection performance of sunscreens.

6.2. Introduction

The performance of a sunscreen depends mainly on the absorption properties of the UV filters contained in the product [281].This performance is principally characterized by the sun protection factor (SPF) whose determination is based on the sensitivity of human skin to erythema caused primarily by UVB radiation while protection from health damage induced by UVA radiation is addressed by UVA-PF [2,3,67,201]. *In vivo*[9], *in vitro*[10], or *in silico*[11,282] methodologies are available for determining SPF, but only the *in vivo* method is currently approved by regulatory bodies. Initial data have indicated that SPF values of sunscreens with the same UV filter composition may differ when different vehicles are used to formulate the sunscreen [20,21]. Furthermore, uniformity of distribution of the sunscreen on the skin was found to play a role for SPF *in vivo* [27] . Hence, knowledge of the factors besides UV filter composition that affect performance is essential for understanding the mechanism of action of sunscreens.

In chapter 4, we developed a method to determine the precise thickness distribution of the applied sunscreen film based on topographical measurements in order to examine the relationship between sunscreen film thickness and efficacy.

Using five different sunscreen formulations containing the same UV filter combination we showed that the vehicle significantly impacted the average film thickness and the SPF *in vitro* value and that a positive correlation existed between average film thickness and SPF. We validated this finding with a newly developed computational methodology making use of the complete thickness frequency distribution of a sunscreen film for calculating SPF. The divergence of efficacy between different sunscreen vehicles was demonstrated with this method to be strongly related to differences in the average thickness and thickness distribution of the applied sunscreen film (chapter 5). However, beyond the behavior of the complete sunscreen formulation with respect to film formation upon application, repartition of UV filters within the applied film needs to be considered. Commonly, mixtures of UV filters are used in order to cover the UVA and the UVB range of the spectrum and to attain photo-stability [157,161]. For these reasons the different UV filters must be homogeneously distributed in the sunscreen. As UV filters can be lipid- or water-soluble or miscible, the employed formulation type may influence filter repartition within the applied film and therefore sunscreen performance. Only isolated reports on the distribution of a particulate UV filter can be found in the literature [283].

The aim of the present work was to investigate the spatial repartition of an oil-miscible and a water-soluble UV filter within the sunscreen film upon application of three different types of vehicle. For this purpose, we developed a method using confocal Raman microspectroscopy. Raman spectroscopy provides the possibility to identify molecules based on their characteristic vibrational spectrum and in combination with confocal microscopy allows a spatial analysis in x, y, and z direction of the studied sample. This is a powerful technique which requires no tissue preparation, is non-invasive, works in real-time, and is label free. It has been previously employed to study molecular composition and conformational nature of human skin, nail, and hair [284], to measure stratum corneum thickness in humans *in vivo* [254] or on porcine ear skin *ex vivo* (chapter 3) and to determine skin constituents and their distribution throughout the skin [285,286].

Further uses included detection of molecular abnormalities in benign and malignant skin lesions for cancer diagnosis [287], following of drug permeation through the skin barrier [286,288-290] , monitoring of changes in protein structure and lipid composition of human skin for the development of anti-ageing formulations [291], determination of water concentration [254] and hydration status of the skin [285], and assessment of the distribution of natural skin antioxidants [292,293] .

In this study we used epidermal membrane of pig ear skin as a biological substrate for sunscreen application which in a previous study provided better in vitro predictive results of SPF than other substrates (chapter 3) and therefore continued to be used (chapter 4 & 5). First, a line scan as a function of depth analysis was carried out for assessing the thickness and the repartition of the two UV filters along the depth of the sunscreen layer and secondly, a surface scan as a function of depth analysis was performed for assessing the lateral repartition of the UV filters within the applied sunscreen. Spatial complementarity or co-localization of the employed UV filters was assessed and the effect of transformation of the three different vehicles upon application on repartition was evaluated. Finally, the SPF *in vitro* of the three sunscreens was measured in order to relate UV filter repartition with sun protection efficacy.

6.3. Materials and methods

6.3.1. Chemicals and equipment

Following chemicals were used: Potassium carbonate from Sigma-Aldrich, St Gallen, Switzerland; Uvinul MC80 abbreviated EHMC (INCI, ethylhexyl methoxycinnamate), Neutrol TE (INCI, tetrahydroxypropyl ethylenediamine), Eumulgin VL75 (INCI, lauryl glucoside (and) polyglyceryl-2 dipolyhydroxystearate (and) glycerin), Dehymuls LE (INCI, PEG-30 dipolyhydroxystearate), isopropyl palmitate, Lanette O (INCI, cetearyl alcohol) from BASF SE, Ludwigshafen, Germany; Eusolex 232 abbreviated PBSA (INCI, phenylbenzimidazol sulfonic acid) from Merck, Darmstadt, Germany; Arlacel 165 (INCI, glyceryl stearate (and) PEG-100 stearate) from Croda East Yorkshire, England; Keltrol RD

(INCI, xanthan gum) from CP Kelco, Atlanta, Georgia; Sepigel 305 (INCI, polyacrylamide (and) C13-14 isoparaffin (and) laureth-7) from Seppic, Puteaux, France.

Quartz plates with a size of 2 cm × 2 cm were obtained from Hellma Analytics (Zumikon, Switzerland).

Following equipment was used: Balance (XS104, Mettler-Toledo, Columbus, OH, USA); UV transmittance analyzer (Labsphere UV-2000S, Labsphere Inc., North Sutton, NH, USA); confocal Raman microspectrometer (Alpha 500R, WITec, Ulm, Germany).

Following software packages were used: WITec Control and WITec Project Four (WITec, Germany) for the acquisition and evaluation of Raman measurements, respectively; Stream Motion (Olympus, Tokyo, Japan) for image processing; UV-2000 (Labsphere Inc., USA) for UV transmittance measurement; Igor Pro 6.32A (WaveMetrics, Inc., Portland, OR, USA) for data fitting.

6.3.2. Preparation of skin substrate

We used epidermal membrane of pig ears for cream application as described earlier in section 3.3.2., method 2 (3.3.2.2.). The epidermal membrane was isolated using a heat separation procedure, cut to a dimension of 2 cm × 2 cm, laid flat on carrier quartz plates, and stored at 4°C in a desiccator over saturated potassium carbonate solution until use.

6.3.3. Sunscreen vehicles

We selected EHMC as oil miscible and PBSA as water soluble UV filter. EHMC was used at a concentration of 10 wt% and PBSA at a concentration of 6 wt%. Both UV filters were incorporated in three different vehicles, i.e., an oil-in-water emulsion (OW), a water-in-oil emulsion (WO), and a clear lipo-alcoholic spray (CAS). PBSA was neutralized with Neutrol TE in water for the OW and WO vehicles and in ethanol for the CAS vehicle. The full composition of the sunscreen formulations is given in Table 6.1.

Placebo formulations (without UV filters) of the OW and WO sunscreens were prepared for Raman measurements. In the placebo formulations, the amount of EHMC was replaced by isopropyl palmitate and the amount of PBSA and Neutrol TE by water.

Table 6.1. Composition (w-%) of investigated formulations

Sunscreen designation		**OW**	**WO**	**CAS**
Ingredient type	**Trade name**	**Composition (w-%)**		
Emulsifier system	Arlacel 165	2.0	-	-
	Eumulgin VL75	5.0	-	-
	Dehymuls LE	-	1.0	-
	Tegin OV	-	2.0	-
Emollient	Isopropyl palmitate	11.0	11.0	13.0
Thickening	Lanette O	1.5	1.5	-
	Keltrol RD	0.3	-	-
	Sepigel 305	3.0	-	-
Filter system	EHMC	10.0		
	PBSA	6.0		
Neutralizing agent	Neutrol TE	Qs to pH 7		
Additional ingredients	Glycerin	3.0	3.0	-
	Water	Qsp 100%	Qsp 100%	-
	Ethanol	2.5	2.5	Qsp 100%
	Magnesium sulfate	-	0.8	-

6.3.4. Measurement of the sun protection factor *in vitro*

Measurement of SPF *in vitro* was based on diffuse UV transmission spectroscopy as proposed by Sayre [12]:

$$\text{SPF } in\ vitro = \frac{\sum_{290}^{400} s_{er}(\lambda).S_s(\lambda)}{\sum_{290}^{400} s_{er}(\lambda).S_s(\lambda).T(\lambda)} \quad (6.1.)$$

where, the inverse transmittance (1/T) in the UV spectral range is weighted with the erythema action spectrum, $s_{er}(\lambda)$ [9], and the spectral irradiance of the UV source, $S_s(\lambda)$ [9]. As data for $s_{er}(\lambda)$ and $S_s(\lambda)$ are available from literature, the SPF *in vitro* can be determined only from UV transmittance measurements registered from 290 to 400 nm in 1 nm increment steps through skin substrate preparations after sunscreen application. The UV transmittance of four positions per 2 cm × 2 cm skin substrate plate was measured to cover virtually the complete surface area of the skin preparation. In total, four skin substrate plates per sunscreen were used. A blank transmittance spectrum was recorded at first for each single position. Subsequently, 2.0 mg/cm^2 of sunscreen was applied with the fingertip using a pre-saturated finger coat in form of 20 to 30 small drops. The sunscreen was spread using light circular movements followed by left-to-right linear strokes from top to bottom starting at each side of the skin preparation. Transmittance measurement was carried out 15 minutes after sunscreen application to allow for equilibration with environmental conditions.

6.3.5. Confocal Raman microspectroscopy measurements

Confocal Raman laser scanning microspectroscopy was performed on sunscreens applied to skin substrate preparations as described for SPF *in vitro* measurements. Data were collected with a WITec Alpha 500R instrument equipped with a EMCCD high intensity low noise camera and a high precision piezoelectric scanning stage.

Raman spectra were recorded from 0 to 4000 cm^{-1} (spectral grating of 600 g/mm, spectral resolution of 3 cm^{-1} per pixel) using a 532 nm excitation green laser source. As pinhole a glass fiber with a diameter of 50 μm was used. The power of the laser was adjusted to an intensity of 6 mW for all measurements. All measured spectra were treated with the CRR (Cosmic Ray Removal) option in the WITec Project Four software and were background corrected by baseline subtraction using a polynomial function of 5th order.

The Raman spectra of neat EHMC and of PBSA at a concentration of 37.5% in water neutralized with Neutrol TE were recorded. A peak that was unique for each UV filter was selected to detect and differentiate the UV filters in the samples. The filter manager option available in the WITec Project Four data treatment software was used to identify and visualize the UV filters based on their spectral peak characteristic.

The combination of Raman spectroscopy with confocal microscopy allowed a depth-resolved analysis. Two different kinds of measurement were performed, a line depth scan analysis for assessment of the sunscreen layer thickness and a surface depth scan analysis for assessing the lateral repartition of the UV filters at different depths in the sunscreen layer.

6.3.5.1. Line depth scan

The sunscreen was scanned over a line of 100 μm in x direction at 225 points per line and over a depth of 30 μm in z direction with 50 lines per image resulting to a total of 11250 recorded individual spectra. The measurements were performed using a 50× objective (Nikon EPI plan) with a numeric aperture NA of 0.80 permitting an x-y (lateral) resolution of 405 nm according to the Rayleigh criterion and a diffraction limited z (axial) resolution of around 1.2 μm assuming a refractive index of the sample =1. An integration time of 0.05s was used. Six individual depth line scan measurements were performed per sunscreen at different locations of the sample. This measurement provided two-dimensional (2D) images in the x-z plane showing the UV filter location in the sunscreen film.

6.3.5.2. Surface depth scan

Scans of a surface area of the sunscreen with dimension 100 µm × 100 µm were performed in the x-y plane with 180 points per line and 180 lines per image, thus, acquiring a total of 32400 individual spectra per surface. A 50× objective (Nikon EPI plan) was used with a numeric aperture NA of 0.55 permitting an x-y resolution of 590 nm and a z resolution of approximately 2.5 µm, with an integration time of 0.05s.

Surface scans were repeated at 1 µm steps in the z direction along the depth of the sunscreen film starting with the first surface measurement clearly in the air above the sunscreen film as illustrated by surface S1 in Fig. 6.1. and ending well below the sunscreen film into the skin as illustrated by surface Sx in Fig. 6.1. These measurements provided 2D images in the x-y plane showing the lateral location of the UV filters at different z positions in a color-coded fashion using the combined picture option of the software. Percentage of surface of the images corresponding to each color was calculated with the stream motion software. These images were further superimposed for all z positions to produce a single 2D image illustrating the abundance of the UV filters throughout the complete sunscreen layer.

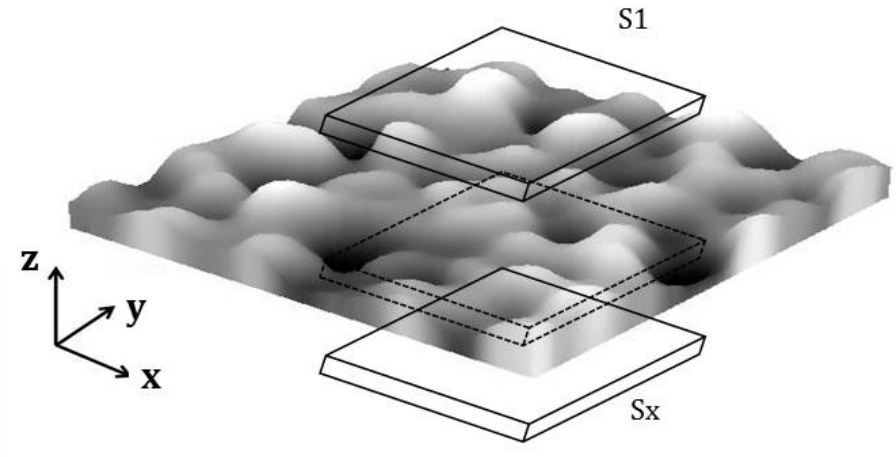

Figure 6.1. Three-dimensional visualization of skin with a schematization of the surface scan measurements performed throughout the sunscreen film, S1 corresponding to the first surface measurement on the top outside the sunscreen film into the air and Sx to the last measurement ending on the bottom into the skin, each surface scan measurement being spaced by 1 µm in the z axis

Since intensity of the Raman signal decreased with increasing depth of measurement in the sample, a correction of each individual surface scan for Raman signal attenuation had to be performed as explained below. The surface scan data were corrected for signal attenuation, CRR treated and background subtracted before use for further evaluation.

6.3.5.3. Control experiment for correction of Raman signal attenuation

The decrease of intensity of the measured Raman signal at increasing depth due to light scattering was determined for each sunscreen formulation. For this purpose, two cover slips were positioned on a glass slide and the gap between them was filled first with an excess of sunscreen using a pipette; then a third cover slip was glided over the sunscreen to attain a film thickness equal to the thickness of the cover slips. The amount of sunscreen applied on the glass slide thus produced an estimated film thickness of roughly 60 µm or more after evaporation of volatile components of the formulation and was much larger than the thickness obtained by the usual application of 2 mg/cm^2 of sunscreen. Raman measurements along a line of 4 µm in the x direction with 8 points per line and in a depth of 60 µm in z direction with 120 lines per image were performed. Measurements started in the air above the sunscreen. Raman spectra were acquired with the 50× objective, NA 0.55 and an integration time of 1s. The intensity of the spectral band at a Raman shift of 1613 cm^{-1} was measured and averaged over the 8 points per line. The data of signal intensity as a function of depth were treated mathematically as described earlier [294] and were used to correct for the Raman signal attenuation occurring at increasing depth in the surface-depth scanning experiments.

6.4. Results and discussion

6.4.1. Raman spectra of EHMC and PBSA

Figure 6.2. gives the Raman spectra of the pure UV filters used in this study. EHMC is an oily liquid that was measured neat while PBSA was measured in a 37% w/v water solution that was titrated to pH 7 with Neutrol TE. EHMC and PBSA show peaks at 1170 cm^{-1} and 1545 cm^{-1}, respectively, which are unique to these compounds. The peak at 1170 cm^{-1} of the Raman spectrum of EHMC was also previously reported [295] and attributed to the C-H bend in the molecule while no previous study was found for PBSA. These peaks also appear in the Raman spectrum of the sunscreen formulations containing both UV filters (Fig. 6.3.). Therefore, they were used to detect the UV filters and assess their location in the preparations of sunscreen applied to skin substrate. The placebo formulations were shown not to interfere with this detection (Fig. 6.3.). The peak at 1613 cm^{-1}, on the other hand, was present in the Raman spectrum of both UV filters and was used for the correction of the Raman intensity attenuation.

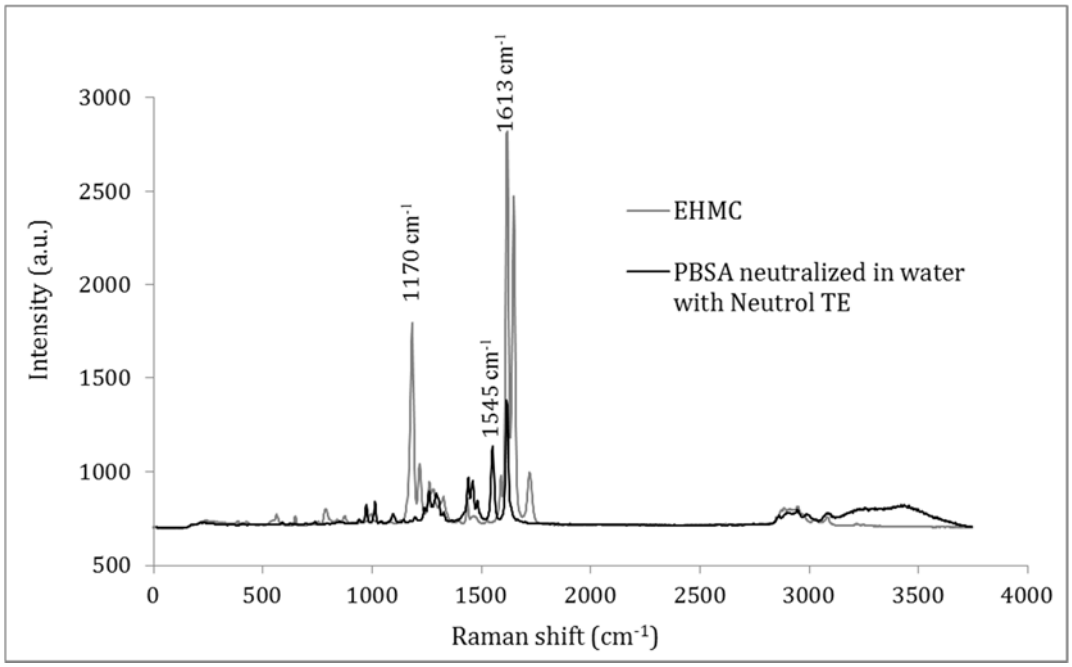

Figure 6.2. Raman spectra of UV filter EHMC (gray line) and UV filter PBSA (black line)

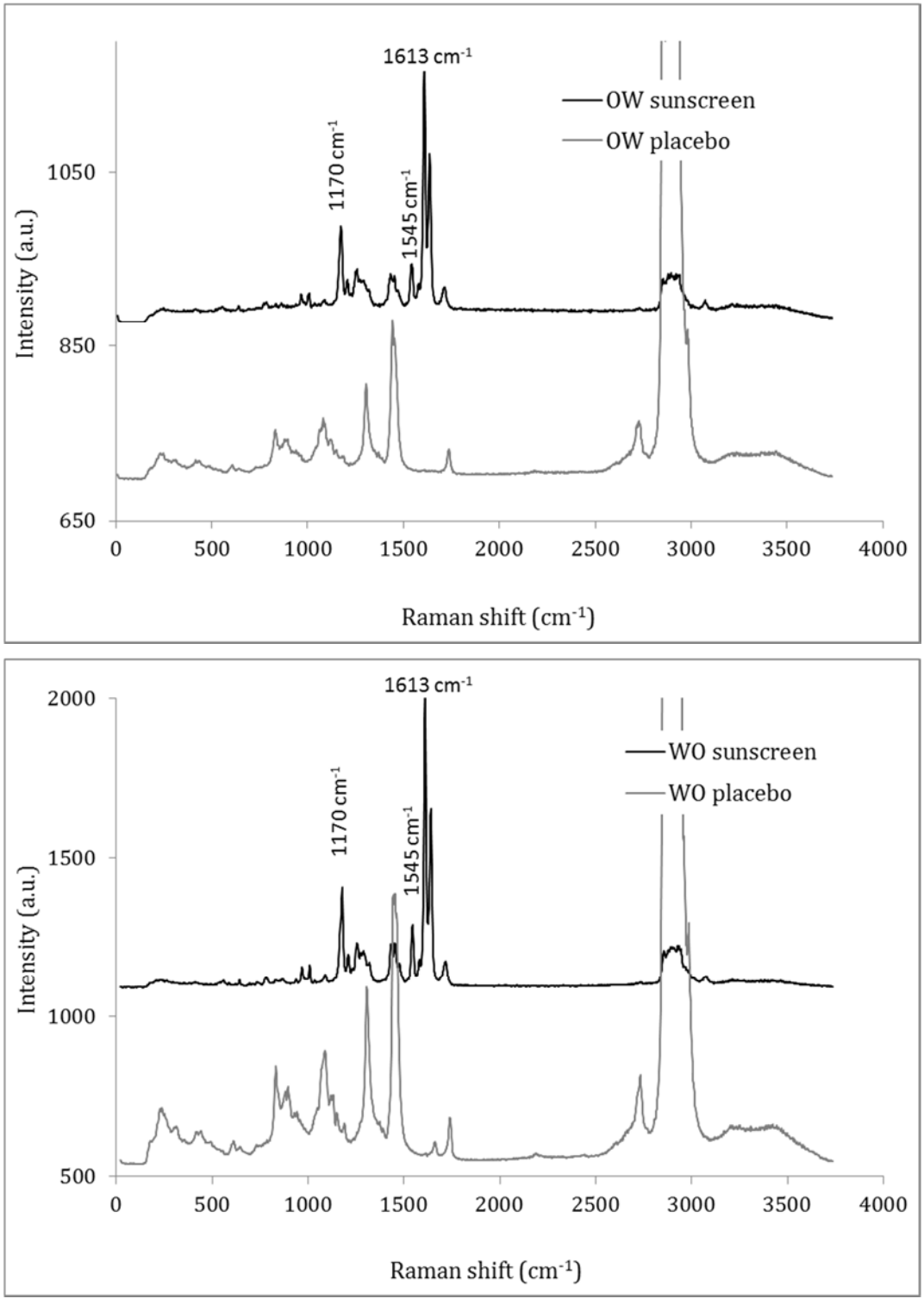

Figure 6.3. Raman spectra of sunscreen formulations containing UV filters (black line) and placebo formulations without UV filters (gray line). Top, for OW; bottom, WO sunscreen

6.4.2. Correction for Raman signal attenuation

To assure that signal intensity in the depth scan experiments provided an accurate representation of the abundance of UV filter in the produced images, a correction for Raman signal attenuation due to light scattering as a function of depth was performed. For this purpose, signal intensity as a function of depth was calibrated with control experiments. Figure 6.4. displays the change of measured intensity of the peak at 1613 cm^{-1} for each sunscreen with increasing depth. For the CAS formulation, the intensity of the Raman signal remained unchanged up to a depth of approximately 10 µm. This depth is larger than the film thickness of the applied sunscreen in which Raman measurement was carried out, taking into account thickness reduction due to evaporation of volatile components. Therefore, no correction of signal intensity was performed for this formulation.

For the OW and WO sunscreens, the intensity of Raman signal decreased markedly within a depth of 10 µm. The signal attenuation of these sunscreens was described with Eq. (6.2.) and Eq. (6.3.), respectively.[32]

$$I_{OW}(z) = a \cdot exp\left(-\frac{z}{b}\right) + (1 - a) \qquad (6.2.)$$

$$I_{WO}(z) = a \cdot z + 1 \qquad (6.3.)$$

where, I is intensity of Raman signal, z is depth with z≥0 and z=0 corresponding to the surface of the sunscreen.

The coefficients a and b were deduced by fitting Eq. (6.2.) and Eq. (6.3.) to the intensity data of Fig. 6.4. whereas for WO only data from 0 to 12.5 µm depth were used. The intensity was normalized to a maximum value of I(z=0) = 1. For the OW sunscreen a= 0.9924 and b=10.78 and for the WO sunscreen a=−0.064 was obtained.

The measured intensity of the Raman signal in the surface-depth scanning experiments was corrected for the attenuation of the signal as a function of depth by

$$corrected(z) = \frac{measured(z)}{I(z)} \qquad (6.4.)$$

where, I(z) was obtained for the corresponding depth from Eq. (6.2.) and Eq. (6.3.) for the OW and the WO formulation, respectively using the deduced coefficient values.

This correction was applied to each acquired surface scan measurement for producing the corresponding image.

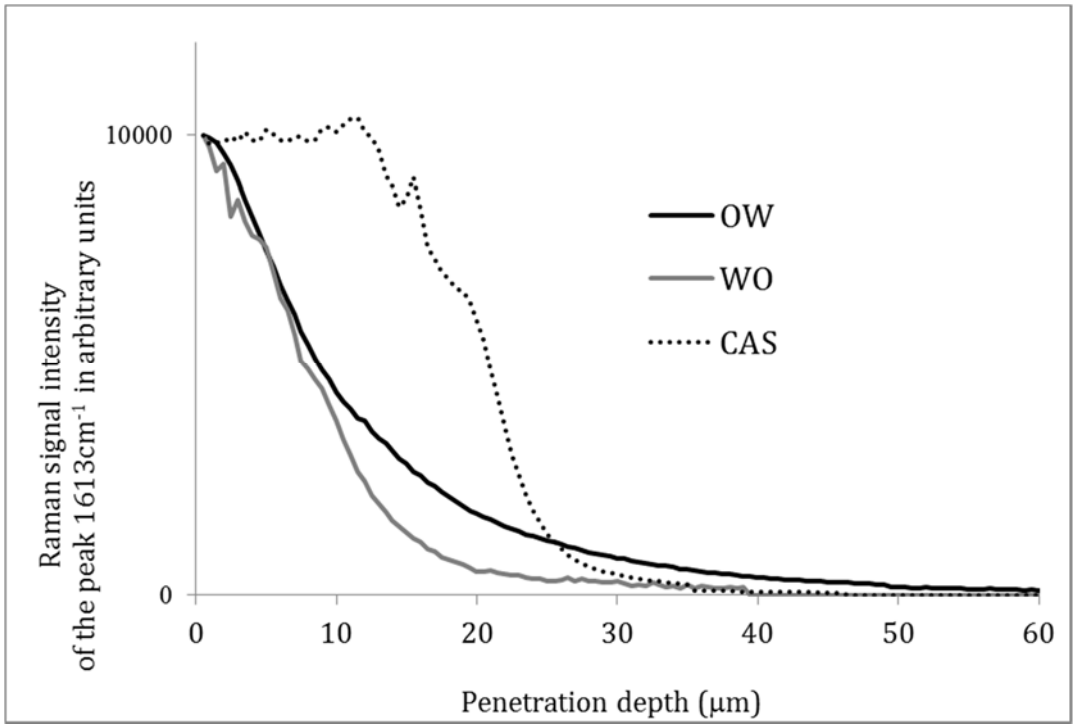

Figure 6.4. Raman signal intensity of the peak at 1613 cm^{-1} as a function of depth into the formulation for the OW, WO and CAS sunscreens. Each curve represents the average of three measurements

6.4.3. Line depth scan

Figure 6.5. gives an example of 2D images (x-z plane) of the line-depth scan measurements. UV filters EHMC and PBSA were identified based on spectral bands at Raman shift 1170 cm^{-1} and 1545 cm^{-1}, depicted in green and red color, respectively. Yellow color resulted from superposition of green and red.

A continuous layer of UV filters of the sunscreens is evident with an apparent thickness of 2 to 5 µm. Black-depicted regions located above and below the sunscreen layer provided no signal at the specific Raman shifts and are attributed to air and skin, respectively.

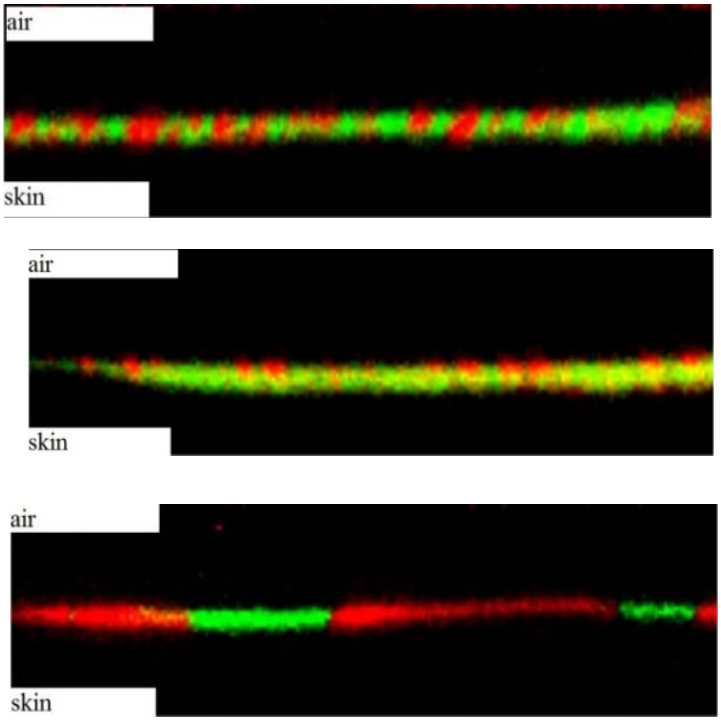

Figure 6.5. Two-dimensional images in the x-z plane resulting from line-depth confocal Raman scan. Full scale length = 100 µm; full scale height of each image = 30 µm. Green color represents EHMC, red color represents PBSA. Black regions above and below the UV filters correspond to air and skin, respectively. Top, OW sunscreen; middle, WO sunscreen; bottom, CAS sunscreen.

The images demonstrate that confocal Raman scanning microscopy allows the localization and detection of repartition of individual UV filters in the applied sunscreen film. For the OW and the WO formulations, a tight interspersion along the x-axis of small areas of the oil miscible EHMC and the water soluble PBSA was observed. Some co-localization (yellow spots) of the UV filters was seen in the WO formulation. However, distribution of the UV filters along the z axis could not be accurately ascertained in this visual representation.

Notably, rather large domains of EHMC and PBSA were observed along the x axis in the CAS formulation, which appear to span the entire thickness of the sunscreen film. Hence, a large difference of lateral repartition of the UV filters after sunscreen application is evident between the used formulations. This is discussed in more detail in the surface-depth scan results.

6.4.4. Surface depth scan

All surface scan measurements were first corrected for signal attenuation, CRR treated and background subtracted. The detection of the UV filters was performed as above. Raman signal of EHMC and of PBSA from surface scans were combined within one 2D image (x-y plane) for each measured position along the z (depth) axis. In Figures 6.6.a., 6.6.b., and 6.6.c. Raman spectral maps corresponding to individual surface scans that were recorded in depth intervals of 1 μm are pasted together for the three investigated sunscreens. The top left and the bottom right image in each of the Figs. 6.6.a., 6.6.b., and 6.6.c. correspond to air and skin above and below the sunscreen, respectively, and appear black reflecting the absence of the specific Raman spectral bands. As surface scanning progresses along the z axis, the sunscreen layer is traversed which is evidenced by the detection of Raman signal of the UV filters. The sunscreens appear to span a thickness of approximately 8 μm along the depth axis which, given the worse z resolution of the surface-depth scan measurements compared to the line-depth scan, is consistent with the results of Fig. 6.5. The positional pattern of signal detection in the succession of optical sections implies that the sunscreen layer was not perfectly horizontal and/or had not a uniform thickness.

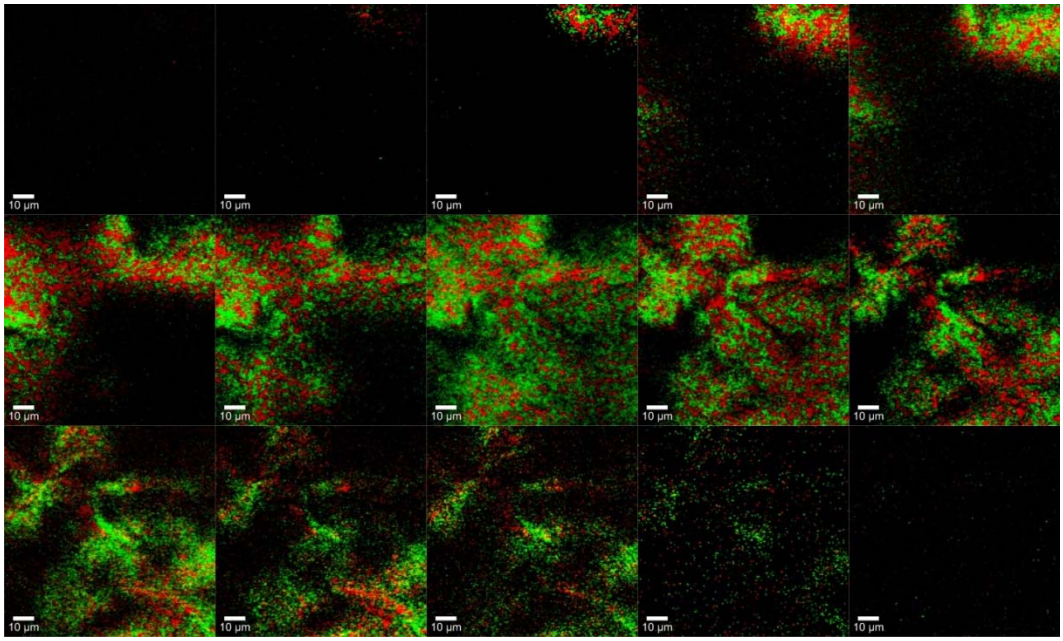

Fig. 6.6.a.

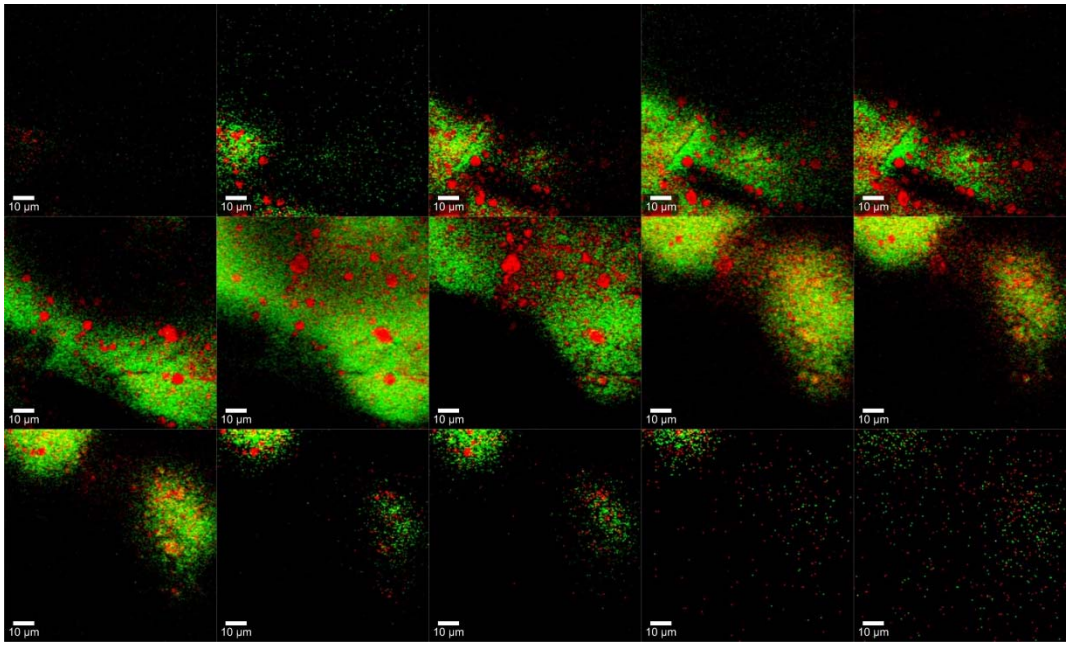

Fig. 6.6.b

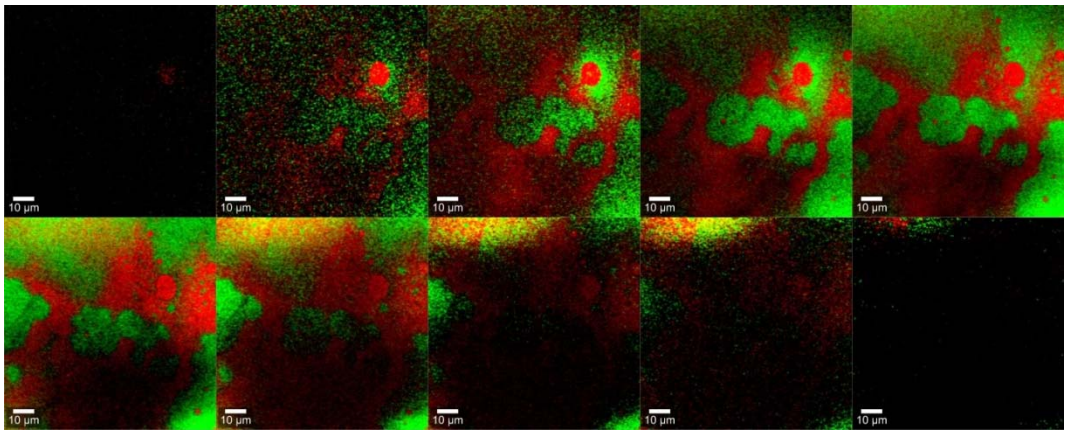

Fig. 6.6.c.

Figure 6.6. Pasting of all images from individual confocal Raman surface scans (x-y plane) recorded in intervals of 1 µm along the z coordinate. Sequence starts at top left and ends at bottom right in the order from left to right and top to bottom. White bar in every image = 10 µm. Green color represents EHMC, red color represents PBSA. a, OW sunscreen; b, WO sunscreen; c, CAS sunscreen.

Green color corresponds to EHMC, which is a lipid-miscible UV filter. In the OW sunscreen this represented together with the emollient the dispersed phase of the formulation. Fig. 6.6.a. (detail in Fig. 6.7.) shows that although discrete green spots of < 5 μm were discernible, aggregation and possibly some coalescence of the dispersed phase have taken place upon application and evaporation of volatile components of the continuous phase of the formulation. The average droplet size of the freshly made OW emulsion was around 2 μm. Red color corresponds to PBSA which is a water-soluble UV filter. Independent experiments have verified that upon water evaporation PBSA does not crystallize when it is neutralized with tetrahydroxypropyl ethylenediamine (Neutrol TE) instead forming a viscous mass. This is detected as red spots interspersed among EHMC of the oil phase. However, no continuous phase was evident. Also, no co-localization (yellow color) was detected at the used resolution.

In the WO sunscreen (Fig. 6.6.b. and detail in Fig.6.7.), EHMC is detected as continuous green color reflecting the external phase of the formulation. Rather large spots of red color were found indicating clustering of PBSA contained in the dispersed phase.

The CAS formulation (Fig. 6.6.c. and detail in Fig. 6.7.) produced segregated domains of EHMC and PBSA that were much larger than the spots observed in the other two formulations. Hence, repartition of UV filters on the surface of skin upon sunscreen application is demonstrated to strongly depend on the type of formulation in use.

The proportion of green and red color corresponding to EHMC and PBSA was quantified in the images of Fig. 6.7.

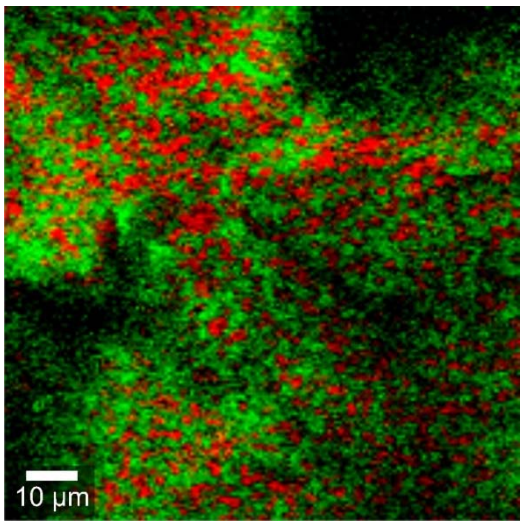

Fig. 6.7.a.

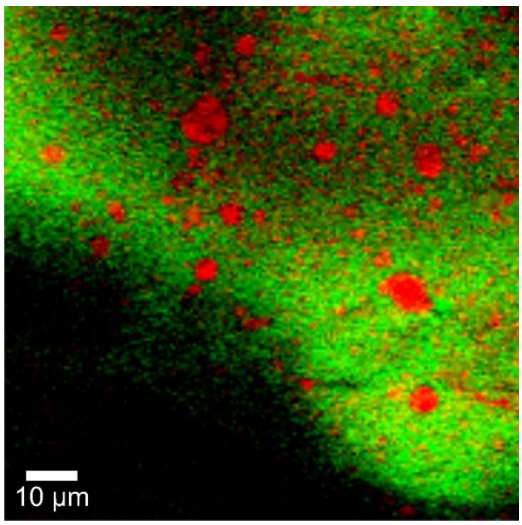

Fig. 6.7.b.

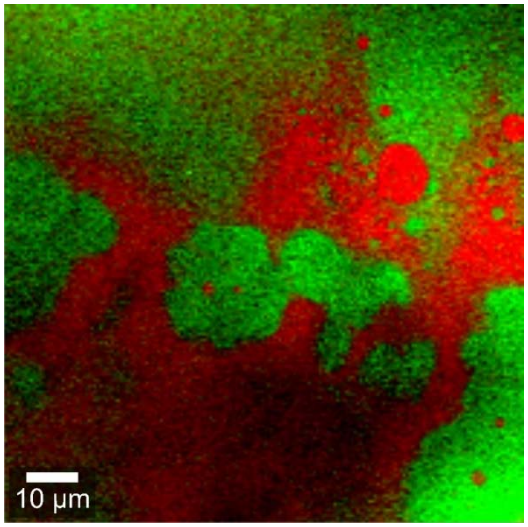

Fig. 6.7.c.

Figures 6.7. Combined 2D picture (x-y plane) for investigated sunscreens in a surface scan measured at one z coordinate illustrating the location at which Raman signal was detected for EHMC (green zones) and PBSA (red zones), a. OW; b. WO; c. CAS sunscreen

EHMC occupied 33%, 36%, and 48% and PBSA occupied 16%, 15%, and 52% of the surface area of the image of the OW sunscreen, the WO sunscreen, and the CAS sunscreen, respectively. The difference of the sum of these numbers to 100% reflects the black area (no signal) of the images.

The ratio of EHMC to PBSA abundance in the sections of the OW and the WO sunscreen is in perfect agreement with the amount of these UV filters in the formulations. The abundance of PBSA in the CAS image was probably overestimated because a clear distinction of the red color from black was not possible in this image.

Hence, the present work allows the identification and localization of the UV filters in the applied sunscreen film. The two UV filters were found to be mutually interspersed occupying adjacent areas within the optical sections taken at 1 μm intervals with little or no co-localization being detected at the applicable resolution. The scale pattern of their repartition is influenced by the phases preexisting in the applied formulations. Thus, the oil and the water phases of the OW and the WO sunscreens containing EHMC and PBSA, respectively, could be distinguished although aggregation and probably some coalescence took place upon evaporation of the water phase. The CAS sunscreen consisted of a single phase in which both UV filters were dissolved. Upon evaporation of the ethanol, the UV filters repartitioned forming rather large domains. This might be related to the absence of emulsifier in this formulation.

To get a complete view of the sunscreen film, superposition of all individual surface scans was performed (Fig. 6.8.). Since the intensity of the surface scan measurements was corrected for signal attenuation as a function of depth, the signal (color) intensity in the final image is proportional to the total abundance of the UV filters and consequently to film thickness.

Large yellow areas were found for the OW and the WO sunscreens (Fig. 6.8.) indicating overlap of the EHMC and the PBSA specific signals at the respective x-y coordinates. This suggests an overlap of the UV filters along the z (depth) axis. However, also areas covered solely by EHMC or PBSA are observed. For the CAS sunscreen, on the other hand, very little overlap was detected, most of the image area being covered by rather large domains of either EHMC or PBSA. This shows that the domains of the UV filters detected in the Raman spectral maps of the surface scans (Fig. 6.6.c.) extended through the entire film thickness of this sunscreen. These findings from the superimposed images of the CAS sunscreen are congruent with those of the line-depth scanning experiment (Fig. 6.5.). EHMC and PBSA, hence, are shown to form comparatively large segregated pools after application of this formulation. These results underscore the relevance of formulation for UV filter repartition. The bright and dark areas of the images on Fig. 6.8. reflect fluctuations of sunscreen film thickness.

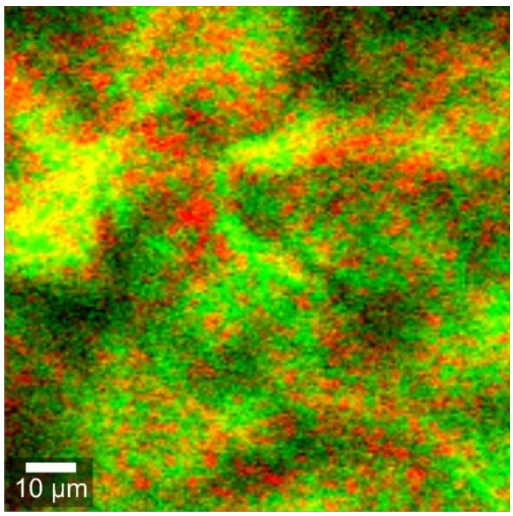

Fig. 6.8.a.

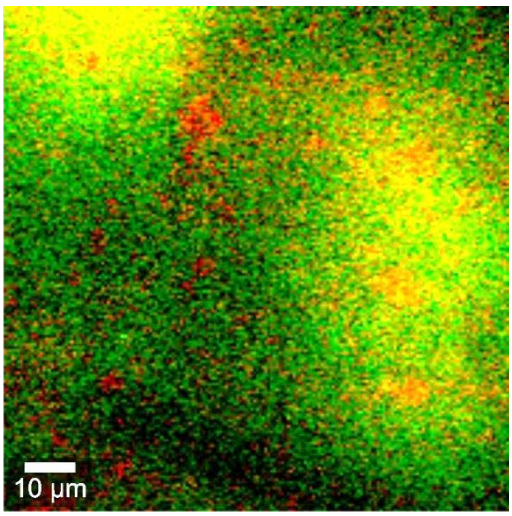

Fig. 6.8.b.

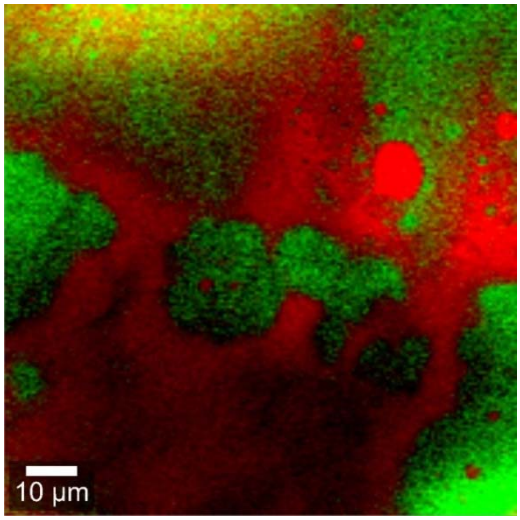

Fig. 6.8.c.

Figure 6.8. Combined 2D picture (x-y plane) from the superimposition of all individual surface scan measurements for investigated sunscreens to visualize the presence and location of the two UV filters in the complete sunscreen film; detected Raman signal for EHMC in green, for PBSA in red, overlapping of EHMC and PBSA in yellow; a. for OW, b. for WO, c. for CAS sunscreen

This work underscores the advantages of confocal Raman microspectroscopy for obtaining 3D location-specific molecular and structural information on the investigated sample as demonstrated in the biological [284-286], the pharmaceutical [286-290] and the cosmetic [254,285,292,293] field before.

6.4.5. Consequences for sun protection

For effective sun protection, a complete coverage of the skin by sunscreen is essential. However, manual application defies standardization so that a uniform film thickness of sunscreen cannot be possibly attained. Under the conditions employed in this work the skin was mostly covered by UV filters although some locations may have remained exposed, i.e., poorly protected as shown in Fig. 6.8.. A detailed quantitative study on the relationship between film thickness frequency distribution and sun protection factor illustrating the dramatic effect of a relatively small uncovered skin surface area on sun protection were given in chapter 4 and 5.

In addition, the absorption spectrum of the UV protection system should ideally be the same throughout the covered skin area. Since UV filter combinations are normally used in order to guarantee absorption throughout the entire spectrum of terrestrial sunlight, this entails that the UV filters should be homogeneously distributed in the sunscreen layer. For sunscreen vehicles consisting of an oil and a water phase it is considered essential that both phases contain UV filter in order to assure an uninterrupted coverage of the skin [192,196].

The optical sections of the present study (Figs. 6.6. and 6.7.) demonstrate a complementarity of EHMC and PBSA in the x-y plane. These UV filters are mutually immiscible and were found to form distinct phases at the lateral resolution of 590 nm. In the z dimension, however, an overlap of these UV filters was observed for the OW and the WO formulations (Fig. 6.8.) assuring a combined UV absorption spectrum in fairly large areas of the applied sunscreen. Yet, it should be pointed out that there were still areas in which either one of the UV filters dominated. This might be due to a small thickness of the sunscreen film in those areas. Film thickness frequency distributions reported in chapter 4 and 5 support this view. For the CAS formulation, pools of EHMC and PBSA were fully segregated throughout the thickness of the sunscreen film. This would result in a non-uniform UV absorption across the covered area and, hence, a compromised sun protection efficacy. With the used UV filters, therefore, the CAS formulation appears to be inferior to the other two formulations in terms of UV filter repartition and consequently sun protection when the UV filters have different absorption spectra.

Thus, this work reveals a mechanism by which the type of the used vehicle may influence sun protection efficacy of a sunscreen in addition to the role of the vehicle for the film forming properties of the product that were shown to also influence performance.

6.4.6. In vitro sun protection factor

To evaluate the effect of UV filter repartition on sun protection afforded by the different formulations, the SPF *in vitro* was determined. The OW sunscreen, the WO sunscreen and the CAS sunscreen yielded an SPF *in vitro* value of 20, 21 and 18, respectively, showing that there was no considerable difference in the UV protection efficacy between the three sunscreen formulations. This is probably because the absorption spectrum and the maximum absorbance of EHMC and PBSA are very similar [142,158]. Therefore, the observed difference of repartition of the two UV filters between the sunscreens did not elicit a difference in light absorption between the different skin areas. However, the situation may change for market products containing a combination of several UV filters exhibiting different absorption properties. In future work, combinations of UV filters with different absorption properties applied over large surface area will be used to more closely study the relationship between filter repartition and sunlight protection efficacy.

6.5. Conclusion

The type of vehicle strongly influences repartition of a water-soluble and a lipid-miscible UV filter in the sunscreen film upon application to skin. Following evaporation of volatile components of the formulation, a nearly continuous phase of lipid-miscible UV filter is formed only for the WO emulsion vehicle with dispersed aggregates of water-soluble UV filter. OW emulsion and clear lipo-alcoholic formulation (CAS) on the other hand, exhibit interspersed patches of the two UV filters, whereas the segregated UV filter domains of the latter formulation are by comparison of a much larger scale and span the entire thickness of the sunscreen film.

Since UV filter combinations are always used in sunscreen products in order to cover the wavelength range of terrestrial sunlight and achieve filter photo-stability, repartition behavior of UV filters and potential segregation may influence photoprotection efficacy. This mechanism of contribution to the performance of sunscreens has not been investigated before. Confocal Raman microspectroscopy is shown to deliver precise data at micrometer resolution about the location of the investigated compounds on skin surface.

Chapter 7

Conclusion and outlook

The *in vivo* prediction of sunscreen efficacy is of great interest for a fast and effective development of new sunscreen formulations. However, predictions of sunscreen efficacy lack accuracy. The present thesis aimed at improving the understanding of the working mechanism of sunscreens with the identification of factors that may influence efficacy using *in vitro* and *in silico* methodologies, advanced analytical means, and mathematical modeling to ultimately improve *in vivo* predictions of the performance of sunscreens.

The *in vitro* assessment of sunscreen performance with the measurement of the sun protection factor requires an adequate substrate for sunscreen application to give reproducible results. We selected skin of pig ear as biological substrate to better reproduce the product-to-substrate affinity relevant for the *in vivo* situation. We identified film thickness distribution of an applied sunscreen as a significant factor for sunscreen efficacy. We found a strong influence of vehicle on sunscreen efficacy arising from differences in the film thickness assumed to originate from the difference in some of the formulation excipients. Further, we investigated the repartition of two UV filters in an applied sunscreen film and found considerable differences between sunscreen vehicles as well.

However, a direct relationship between UV filter repartition and SPF could not be drawn due to the similarity of the absorbance properties of the two studied UV compounds. In a future work, one may confirm this observation in a larger surface area using UV filters that show different absorbance characteristics to investigate the relationship between UV filter repartition and UV efficacy more extensively.

An outlook is the full understanding of the modification of a sunscreen formulation upon application with the core questions being how the sunscreen layer looks like after application of the formulation on skin that is related to the film thickness distribution and how the UV filters re-distribute on skin after application. We developed methodologies to assess these two aspects and showed an effect of vehicle from different formulation types. However, a future work may focus more in detail of the impact of different functional excipients in a sunscreen formulation on the UV efficacy by examining the connection between film formation and UV filter repartition with SPF. The achievement of an homogeneous film and an homogeneous UV filter repartition upon application for an improved performance through an optimized ingredient composition is the goal of next generation of sunscreens.

The advancements in the knowledge of the factors influencing sunscreen efficacy put forward in this work may markedly improve the prediction of sunscreen performance. The present thesis allowed a great step forward toward an accurate prediction of sun protection provided by a topical sunscreen.

Bibliography

1. Reichrath J 2007. Vitamin D and the skin: an ancient friend, revisited. *Experimental Dermatology* 16(7):618-625.
2. Moyal DD, Fourtanier AM 2008. Broad-spectrum sunscreens provide better protection from solar ultraviolet-simulated radiation and natural sunlight-induced immunosuppression in human beings. *Journal of the American Academy of Dermatology* 58(5):149-154.
3. Seite S, Fourtanier A, Moyal D, Young AR 2010. Photodamage to human skin by suberythemal exposure to solar ultraviolet radiation can be attenuated by sunscreens: a review. *British Journal of Dermatology* 163(5):903-914.
4. Green AC, Williams GM, Logan V, Strutton GM 2011. Reduced melanoma after regular sunscreen use: randomized trial follow-up. *Journal of Clinical Oncology* 29(3):257-263.
5. Green A et. al. 1999. Daily sunscreen application and betacarotene supplementation in prevention of basal-cell and squamous-cell carcinomas of the skin: a randomised controlled trial. *Lancet* 354(9180):723-729.
6. Robinson JK, Rademaker AW 1998. Sun protection by families at the beach. *Archives of Pediatrics & Adolescent Medicine* 152(5):466-470.
7. Diffey BL, Norridge Z 2009. Reported sun exposure, attitudes to sun protection and perceptions of skin cancer risk: a survey of visitors to Cancer Research UK's SunSmart campaign website. *British Journal of Dermatology* 160(6):1292-1298.
8. Shaath NA 2010. Ultraviolet filters. *Photochemical & Photobiological Sciences* 9(4):464-469.

9. ISO 24444:2010 - Cosmetics - Sun protection test methods - In vivo determination of the sun protection factor (SPF).
10. Fageon L, Moyal D, Coutet J, Candau D 2009. Importance of sunscreen products spreading protocol and substrate roughness for in vitro sun protection factor assessment. *International journal of cosmetic science* 31(6):405-418.
11. Herzog. 2010. Models for the calculation of sun protection factors and parameters characterizing the UVA protection ability of cosmetic sunscreens. In Wiley-VCH Verlag GmbH & Co. KGaA Weinheim G, editor Colloid Stability, ed. 275-308.
12. Sayre RM, Agin PP, Levee GJ, Marlowe E 1979. Comparison of in vivo and in vitro testing of sunscreening formulas. *Photochemistry and Photobiology* 29(3):559-566.
13. Springsteen A, Yurek R, Frazier M, Carr KF 1999. In vitro measurement of sun protection factor of sunscreens by diffuse transmittance. *Analytica Chimica Acta* 380(2-3):155-164.
14. Pearse AD, Edwards C 1993. Human stratum corneum as a substrate for in vitro sunscreen testing. *International Journal of Cosmetic Science* 15(6):234-244.
15. Diffey BL, Robson J 1989. A new substrate to measure sunscreen protection factors throughout the ultraviolet-spectrum. *Journal of the Society of Cosmetic Chemists* 40(3):127-133.
16. Ferrero L et. al. 2006. Importance of substrate roughness for in vitro sun protection assessment. *IFSCC magazine* 9(2).
17. Pissanini M, S, Dehais A, Ferrero L, Zastrow L 2009. Characterizing roughness: a new substrate to measure SPF. *Cosmetics & Toiletries magazine* 124(9):56-64.
18. Miura Y, Hirao T, Hatao M 2012. Influence of application amount on sunscreen photodegradation in in vitro sun protection factor evaluation: proposal of a skin-mimicking substrate. *Photochemistry and Photobiology* 88(2):475-482.
19. Rohr M et. al. 2010. In vitro Sun Protection Factor: Still a Challenge with No Final Answer. *Skin Pharmacology and Physiology* 23(4):201-212.
20. Schulz J et. al. 2002. Distribution of sunscreens on skin. *Advanced Drug Delivery Reviews* 54:157-163.
21. Chatelain E, Gabard B, Surber C 2003. Skin penetration and sun protection factor of five UV filters: Effect of the vehicle. *Skin Pharmacology and Applied Skin Physiology* 16(1):28-35.

22. Sayre RM, Powell J, Rheins LA 1991. Product application technique alters the sun protection factor. *Photodermatology Photoimmunology & Photomedicine* 8(5):222-224.
23. Rhodes LE, Diffey BL 1997. Fluorescence spectroscopy: A rapid, noninvasive method for measurement of skin surface thickness of topical agents. *British Journal of Dermatology* 136(1):12-17.
24. Pissavini M, Diffey B 2013. The likelihood of sunburn in sunscreen users is disproportionate to the SPF. *Photodermatology Photoimmunology & Photomedicine* 29(3):111-115.
25. Oneill JJ 1984. Effect of film irregularities on sunscreen efficacy. *Journal of Pharmaceutical Sciences* 73(7):888-891.
26. Farr PM, Diffey BL 1985. How reliable are sunscreen protection factors. *British Journal of Dermatology* 112(1):113-118.
27. Lademann J et. al. 2004. Influence of nonhomogeneous distribution of topically applied UV filters on sun protection factors. *Journal of Biomedical Optics* 9(6):1358-1362.
28. Rowland FS 1996. Stratospheric ozone depletion by chlorofluorocarbons (Nobel lecture). Angewandte Chemie-International Edition in English 35(16):1786-1798.
29. Slaper H, Velders GJM, Daniel JS, deGruijl FR, vanderLeun JC 1996. Estimates of ozone depletion and skin cancer incidence to examine the Vienna Convention achievements. *Nature* 384(6606):256-258.
30. Battie C, Verschoore M 2012. Cutaneous solar ultraviolet exposure and clinical aspects of photodamage. *Indian Journal of Dermatology Venereology & Leprology* 78:9-14.
31. Kochevar I, Taylor C, Krutmann J. 2008. Fundamentals of cutaneous photobiology and photoimmunology. In Wolff K, LA. G, Katz K, editors. Fitzpatrick´s Dermatology in General Medicine, ed., New York:Mc Graw-Hill. 797-815.
32. Diffey BL 2002. What is light? *Photodermatology Photoimmunology & Photomedicine* 18(2):68-74.
33. Sabziparvar AA, Shine KP, Forster PMD 1999. A model-derived global climatology of UV irradiation at the earth's surface. *Photochemistry and Photobiology* 69(2):193-202.
34. Schroeder P, Krutmann J 2010. What is needed for a sunscreen to provide complete protection. *Skin therapy letter* 15(4):4-5.

35. Zastrow L et. al. 2009. The Missing Link - Light-Induced (280-1,600 nm) Free radical formation in human skin. *Skin Pharmacology and Physiology* 22(1):31-44.
36. Calles C et. al. 2010. Infrared A radiation influences the skin fibroblast transcriptome: mechanisms and consequences. *Journal of Investigative Dermatology* 130(6):1524-1536.
37. Schroeder P, Lademann J, Darvin ME, Stege H, Marks C, Bruhnke S, Krutmann J 2008. Infrared radiation-induced matrix metalloproteinase in human skin: Implications for protection. *Journal of Investigative Dermatology* 128(10):2491-2497.
38. Jantschitsch C, Majewski S, Maeda A, Schwarz T, Schwarz A 2009. Infrared radiation confers resistance to UV-induced apoptosis via reduction of DNA damage and upregulation of antiapoptotic Proteins. *Journal of Investigative Dermatology* 129(5):1271-1279.
39. Osmola-Mankowska A et. al. 2012. The sun - our friend or foe? *Annals of Agricultural and Environmental Medicine* 19(4):805-809.
40. Cripps DJ 1981. Natural and artificial photoprotection. *Journal of Investigative Dermatology* 77(1):154-157.
41. Downs N, Parisi A 2012. Mean exposure fractions of human body solar UV exposure patterns for application in different ambient climates. *Photochemistry and Photobiol*ogy 88(1):223-226.
42. Frederick JE, Qu Z, Booth CR 1998. Ultraviolet radiation at sites on the Antarctic coast. *Photochemistry and Photobiology* 68(2):183-190.
43. Kolanko M, Brzezinska-Wcislo L 2011. Vitamin D and its receptor - role and activity in the human body. Anomalies of metabolism and structure associated with psoriasis. *Postepy Dermatologii I Alergologii* 28(3):212-216.
44. Diker-Cohen T, Koren R, Liberman UA, Ravid A 2003. Vitamin D protects keratinocytes from apoptosis induced by osmotic shock, oxidative stress, and tumor necrosis factor. Apoptosis: from Signaling Pathways to Therapeutic Tools 1010:350-353.
45. Reichrath J, Reichrath S 2012. Hope and challenge: The importance of ultraviolet (UV) radiation for cutaneous Vitamin D synthesis and skin cancer. *Scandinavian Journal of Clinical & Laboratory Investigation* 72:112-119.
46. Giovannucci E 2005. The epidemiology of vitamin D and cancer incidence and mortality: A review (United States). *Cancer Causes & Control* 16(2):83-95.

47. Forman JP, et. al. 2007. Plasma 25-hydroxyvitamin D levels and risk of incident hypertension. *Hypertension* 49(5):1063-1069.
48. Weatherhead SC, Farr PM, Reynolds NJ 2013. Spectral effects of UV on psoriasis. *Photochemical & Photobiological Sciences* 12(1):47-53.
49. Urbach F, Berger D, Davies R 1968. Action spectrum of UV induced erythema. *Journal of Investigative Dermatology* 50(4):355.
50. Gilchrest BA, Soter NA, Stoff JS, Mihm MC 1981. The human sunburn reaction - histologic and biochemical studies. *Journal of the American Academy of Dermatology* 5(4):411-422.
51. de Gruijl FR 2002. Photocarcinogenesis: UVA vs. UVB radiation. *Skin Pharmacology and Applied Skin Physiology* 15(5):316-320.
52. Freeman SE et. al. 1989. Wavelength dependence of pyrimidine dimer formation in DNA of human skin irradiated in situ with ultraviolet light. Proceedings of the National Academy of Sciences of the United States of America 86(14):5605-5609.
53. Cadet J, Mouret S, Ravanat J-L, Douki T 2012. Photoinduced damage to cellular DNA: direct and photosensitized reactions. *Photochemistry and Photobiology* 88(5):1048-1065.
54. Cadet J, Sage E, Douki T 2005. Ultraviolet radiation-mediated damage to cellular DNA. *Mutation Research-Fundamental and Molecular Mechanisms of Mutagenesis* 571(1-2):3-17.
55. Ziegler A et. al. 1994. Sunburn and P53 in the onset of skin cancer. *Nature* 372(6508):773-776.
56. Ziegler A et. al. 1993. Mutation hotspots due to sunlight in the P53 gene of non melanoma skin cancers. Proceedings of the National Academy of Sciences of the United States of America 90(9):4216-4220.
57. Brash DE et. al. 1991. A role for sunlight in skin cancer - UV-induced P53 mutations in squamous-cell carcinoma. Proceedings of the National Academy of Sciences of the United States of America 88(22):10124-10128.
58. You YH et. al. 2001. Cyclobutane pyrimidine dimers are responsible for the vast majority of mutations induced by UVB irradiation in mammalian cells. *Journal of Biological Chemistry* 276(48):44688-44694.

59. Ananthaswamy HN, Loughlin SM, Ullrich SE, Kripke ML 1998. Inhibition of UV-induced p53 mutations by sunscreens: implications for skin cancer prevention. The journal of investigative dermatology Symposium proceedings / the Society for Investigative Dermatology, Inc [and] European Society for Dermatological Research 3(1):52-56.
60. Rosen CF, Jacques SL, Stuart ME, Gange RW 1990. Immediate pigment darkening - visual and reflectance spectrophotometric analysis of action spectrum. *Photochemistry and Photobiology* 51(5):583-588.
61. Pathak MA, Riley FC, Fitzpatrick TB 1962. Melanogenesis in human skin following exposure to long-wave ultraviolet and visible light. *The Journal of investigative dermatology* 39:435-443.
62. Chardon A, Moyal D, Hourseau C. 1996. Persistent pigment darkening response as a method for evaluation UVA protection assays. In Lowe N, Shaath N, Pathak M, editors. Sunscreens: development, evaluation, and regulatory aspects, 2nd ed.: Marcel Dekker, 559-582
63. Young AR 2002. How much photoprotection does a tan afford? *Biologic Effects of Light* 2001:103-112.
64. Kaidbey KH, Barnes A 1991. Determination of the UVA protection factors by means of immediate pigment darkening in normal skin. *Journal of the American Academy of Dermatology* 25(2):262-266.
65. Ou-Yang H, Stamatas G, Saliou C, Kollias N 2004. A chemiluminescence study of UVA-induced oxidative stress in human skin in vivo. *The Journal of investigative dermatology* 122(4):1020-1029.
66. Krutmann J 2000. Ultraviolet A radiation-induced biological effects in human skin: relevance for photoaging and photodermatosis. *Journal of Dermatological Science* 23:22-26.
67. Krutmann J 2001. The role of UVA rays in skin aging. *European Journal of Dermatology* 11(2):170-171.
68. Vielhaber G et. al. 2006. Sunscreens with an absorption maximum of >= 360 nm provide optimal protection against UVA1-induced expression of matrix metalloproteinase-1, interleukin-1, and interleukin-6 in human dermal fibroblasts. *Photochemical & Photobiological Sciences* 5(3):275-282.
69. Seite S et. al. 2006. Elastin changes during chronological and photo-ageing: the important role of lysozyme. *Journal of the European Academy of Dermatology and Venereology* 20(8):980-987.

70. Warren R et. al. 1991. Age, sunlight, and facial skin - a histological and quantitative study. *Journal of the American Academy of Dermatology* 25(5):751-760.
71. Lavker RM, Veres DA, Irwin CJ, Kaidbey KH 1995. Quantitative assessment of cumulative damage from repetitive exposures to suberythemogenic doses of UVA in human skin. *Photochemistry and Photobiology* 62(2):348-352.
72. Chung JH 2003. Photoaging in Asians. *Photodermatology Photoimmunology & Photomedicine* 19(3):109-121.
73. Moyal DD, Fourtanier AM 2002. Effects of UVA radiation on an established immune response in humans and sunscreen efficacy. *Experimental Dermatology* 11:28-32.
74. Yaar M, Gilchrest BA 2007. Photoageing: mechanism, prevention and therapy. *British Journal of Dermatology* 157(5):874-887.
75. Baumann L 2007. Skin ageing and its treatment. *Journal of Pathology* 211(2):241-251.
76. Fisher GJ et. al. 1997. Pathophysiology of premature skin aging induced by ultraviolet light. *New England Journal of Medicine* 337(20):1419-1428.
77. Roza L, Baan RA, Vanderleun JC, Kligman L, Young AR 1989. UVA Hazards in skin associated with the use of tanning equipment. *Journal of Photochemistry and Photobiology B-Biology* 3(2):281-287.
78. Rabe JH et. al. 2006. Photoaging: Mechanisms and repair. *Journal of the American Academy of Dermatology* 55(1):1-19.
79. Young AR et. al. 1998. The similarity of action spectra for thymine dimers in human epidermis and erythema suggests that DNA is the chromophore for erythema. *Journal of Investigative Dermatology* 111(6):982-988.
80. Tewari A, Sarkany RP, Young AR 2012. UVA1 induces cyclobutane pyrimidine dimers but not 6-4 photoproducts in human skin in vivo. *Journal of Investigative Dermatology* 132(2):394-400.
81. Mouret S et. al. T 2006. Cyclobutane pyrimidine dimers are predominant DNA lesions in whole human skin exposed to UVA radiation. Proceedings of the National Academy of Sciences of the United States of America 103(37):13765-13770.
82. Young AR et. al. 1998. Human melanocytes and keratinocytes exposed to UVB or UVA in vivo show comparable levels of thymine dimers. *Journal of Investigative Dermatology* 111(6):936-940.
83. Peak MJ, Peak JG, Carnes BA 1987. Induction of direct and indirect single-strand breaks in human cell DNA by far-ultraviolet and near-ultraviolet radiations - action spectrum and mechanisms. *Photochemistry and Photobiology* 45(3):381-387.

84. Halliday GM, Byrne SN, Damian DL 2011. Ultraviolet A radiation: its role in immunosuppression and carcinogenesis. Seminars in Cutaneous Medicine and Surgery 30(4):214-221.
85. Kelfkens G, Degruijl FR, Vanderleun JC 1991. Tumorigenesis by short-wave ultraviolet-A - papillomas versus squamous cell carcinomas. C*arcinogenesis* 12(8):1377-1382.
86. Marrot L, Meunier J-R 2008. Skin DNA photodamage and its biological consequences. *Journal of the American Academy of Dermatology* 58(5):139-148.
87. Wang SQ et. al. 2001. Ultraviolet A and melanoma: A review. *Journal of the American Academy of Dermatology* 44(5):837-846.
88. El Ghissassi F et. al. 2009. A review of human carcinogens - Part D: radiation. *Lancet Oncology* 10(8):751-752.
89. Rigel DS 2010. Epidemiology of Melanoma. Seminars in Cutaneous Medicine and Surgery 29(4):204-209.
90. de Gruijl FR, van Kranen HJ, Mullenders LHF 2001. UV-induced DNA damage, repair, mutations and oncogenic pathways in skin cancer. *Journal of Photochemistry and Photobiology B-Biology* 63(1-3):19-27.
91. National Institute for Cancer Epidemiology and Registration S 2011. *Statistics of Cancer Incidence* 1984-2008,3 (2011) (www.nicer.org).
92. Parkin DM, Bray F, Ferlay J, Pisani P 2005. Global cancer statistics, 2002. *Cancer Journal for Clinicians* 55(2):74-108.
93. Osterwalder U, He Q, Sohn M, Herzog B. 7-2012. Sustainable Sun Protection with Sunscreens Requires the Right Technology and Good Compliance. *SÖFW-Journal* 138:2-18
94. Dennis LK, Freeman LEB, VanBeek MJ 2003. Sunscreen use and the risk for melanoma: A quantitative review. *Annals of Internal Medicine* 139(12):966-978.
95. Diffey BL 2009. Sunscreens as a preventative measure in melanoma: an evidence-based approach or the precautionary principle? *British Journal of Dermatology* 161, Suppl 3:25-27
96. van der Pols JC, Williams GM, Pandeya N, Logan V, Green AC 2006. Prolonged prevention of squamous cell carcinoma of the skin by regular sunscreen use*. Cancer Epidemiology Biomarkers & Prevention* 15(12):2546-2548.
97. FDA. 2011. Federal Register, Vol. 76, No. 117, June 17, 2011, Rules and regulations, dpt. of health and human service, FDA, 21 CFR Part 201 and 310, Docket No. FDA–1978–N–0018. In FDA, editor, ed.

98. Weinstock MA et. al. 1989. Non familial cutaneous melanoma incidence in women associated with sun exposure before 20 years of age. *Pediatrics* 84(2):199-204.
99. Whiteman DC, Whiteman CA, Green AC 2001. Childhood sun exposure as a risk factor for melanoma: a systematic review of epidemiologic studies. *Cancer Causes & Control* 12(1):69-82.
100. Geller AC et. al. 2007. Study of health outcomes in school children: Key challenges and lessons learned from the Framingham schools' natural history of nevi study. *Journal of School Health* 77(6):312-318.
101. Godar DE, Wengraitis SP, Shreffler J, Sliney DH 2001. UV doses of Americans. *Photochemistry and Photobiology* 73(6):621-629.
102. Fears TR, Scotto J, Schneiderman MA 1976. Skin cancer, melanoma, and sunlight. *American Journal of Public Health* 66(5):461-464.
103. Halder RM, Bridgemanshah S 1995. Skin cancer in African Americans. *Cancer* 75(2):667-673.
104. Lookingbill DP, Lookingbill GL, Leppard B 1995. Actinic damage and skin-cancer in albinos in Northern Tanzania - findings in 164 patients enrolled in an outreach skin care program. *Journal of the American Academy of Dermatology* 32(4):653-658.
105. Barker D et. al. 1995. Comparison of the responses of human melanocytes with different melanin contents to ultraviolet-B irradiation. *Cancer Research* 55(18):4041-4046.
106. Pathak MA, Stratton K 1968. Free radicals in human skin before and after exposure to light. *Archives of Biochemistry and Biophysics* 123(3):468-476.
107. Lister T, Wright PA, Chappell PH 2012. Optical properties of human skin. *Journal of Biomedical Optics* 17(9):090901.
108. Tearney GJ et. al. 1995. Determination of the refractive index of highly scattering human tissue by optical coherence tomography. *Optics Letters* 20(21):2258-2260.
109. Xie S, Li H, Li B 2003. Measurement of optical penetration depth and refractive index of human tissue. *Chinese Optics Letters* *1*(1):44-46.
110. Scheuplein RJ 1964. A survey of some fundamental aspects of the absorption and reflection of light by tissue. *Journal of the Society of Cosmetic Chemists* 15:111-122.
111. Anderson RR, Parrish JA 1981. The optics of human skin. *Journal of Investigative Dermatology* 77(1):13-19.
112. Young AR et. al. 1991. Photoprotection and 5-MOP photochemoprotection from UVR-induced DNA damage in humans - the role of skin type. *Journal of Investigative Dermatology* 97(5):942-948.

113. Gniadecka M, Wulf HC, Mortensen NN, Poulsen T 1996. Photoprotection in vitiligo and normal skin - A quantitative assessment of the role of stratum corneum, viable epidermis and pigmentation. *Acta Dermato-Venereologica* 76(6):429-432.
114. Quevedo WC, Fitzpatrick TB, Pathak MA, Jimbow K 1975. Role of light in human skin color variation. *American Journal of Physical Anthropology* 43(3):393-408.
115. Ou-Yang H, Stamatas G, Kollias N 2004. Spectral responses of melanin to ultraviolet A irradiation. *Journal of Investigative Dermatology* 122(2):492-496.
116. Thody AJ, Higgins EM, Wakamatsu K, Ito S, Burchill SA, Marks JM 1991. Pheomelanin as well as Eumelanin is present in human epidermis. *Journal of Investigative Dermatology* 97(2):340-344.
117. Thody AJ 1995. Epidermal melanocytes - their regulation and role in skin pigmentation. *European Journal of Dermatology* 5(7):558-565.
118. Fitzpatrick TB 1988. The validity and practicality of sun-reactive skin type-I through type_IV. *Archives of Dermatology* 124(6):869-871.
119. Alaluf S et. al. 2002. Ethnic variation in melanin content and composition in photoexposed and photoprotected human skin. *Pigment Cell Research* 15(2):112-118.
120. Kollias N et. al. 1996. Erythema and melanogenesis action spectra in heavily pigmented individuals as compared to fair-skinned Caucasians. *Photodermatology Photoimmunology & Photomedicine* 12(5):183-188.
121. Jablonski NG, Chaplin G 2000. The evolution of human skin coloration. *Journal of Human Evolution* 39(1):57-106.
122. Jablonski NG 2004. The evolution of human skin and skin color. *Annual Review of Anthropology* 33:585-623.
123. Jablonski NG, Chaplin G 2002. Skin deep. *Scientific American* 287(4):74-81.
124. Kollias N, Sayre RM, Zeise L, Chedekel MR 1991. Photoprotection by melanin. *Journal of Photochemistry and Photobiology B-Biology* 9(2):135-160.
125. Young AR, Sheehan JM. 2001. UV-induced pigmentation in human skin. In Sun protection in Man by Giacomoni PU, editor.
126. Kollias N, Baqer A 1985. Spectroscopic characteristics of human melanin in vivo. *Journal of Investigative Dermatology* 85(1):38-42.
127. Montagna W, Prota G, Kenney JA. 1993. Black Skin : Structure and Function. San Diego: Academic Press:1-12.

128. Kaidbey KH, Agin PP, Sayre RM, Kligman AM 1979. Photo-protection by melanin - comparison of black and Caucasian skin. *Journal of the American Academy of Dermatology* 1(3):249-260.
129. Strickland PT, Bruze M, Creasey J 1988. Cyclobuta-dithymidine induction by solar-simulating UV-radiation in human skin.1. protection by constitutive pigmentation. *Photodermatology* 5(4):166-169.
130. Parrish JA, Jaenicke KF, Anderson RR 1982. Erythema and melanogenesis action spectra of normal human skin. *Photochemistry and Photobiology* 36(2):187-191.
131. Sheehan JM, Potten CS, Young AR 1998. Tanning in human skin types II and III offers modest photoprotection against erythema. *Photochemistry and Photobiology* 68(4):588-592.
132. Bock C et. al. 2013. Sunbed use in Germany: trends, user histories and factors associated with cessation and readiness to change. *British Journal of Dermatology* 169(2):441-449
133. Green A et. al. 2007. The International Agency for Research on Cancer Working Group on artificial ultraviolet (UV) light and skin cancer. The association of use of sunbeds with cutaneous malignant melanoma and other skin cancers: A systematic review (vol 120, pg 1116, 2007). *International Journal of Cancer* 120(11):2526-2526.
134. Boniol M, Autier P, Boyle P, Gandini S 2012. Cutaneous melanoma attributable to sunbed use: systematic review and meta-analysis. *British Medical Journal* 345.
135. Wehner MR et. al. 2012. Indoor tanning and non-melanoma skin cancer: systematic review and meta-analysis. *British Medical Journal* 345.
136. Gandini S, Autier P, Boniol M 2011. Reviews on sun exposure and artificial light and melanoma. *Progress in Biophysics & Molecular Biology* 107(3):362-366.
137. Karagas MR et. al. 2002. Use of tanning devices and risk of basal cell and squamous cell skin cancers. *Journal of the National Cancer Institute* 94(3):224-226.
138. Veierod MB et. al. 2003. A prospective study of pigmentation, sun exposure, and risk of cutaneous malignant melanoma in women. *Journal of the National Cancer Institute* 95(20):1530-1538.
139. Sinclair C, Makin JK 2013. Implications of lessons learned from tobacco control for tanning bed reform. *Preventing chronic disease* 10:28-28.
140. Schulze R 1956. Einige Versuche und Bemerkungen zum Problem der handelüblichen Lichtschutzmittel. *Parfümerie und Kosmetik.*

141. Osterwalder U, Herzog B, Wang SQ 2011. Advance in sunscreens to prevent skin cancer. *Expert Review of Dermatology* 6(5):479-491.
142. Osterwalder U, Herzog B 2010. The long way towards the ideal sunscreen-where we stand and what still needs to be done. *Photochemical & Photobiological Sciences* 9(4):470-481.
143. Manaia EB, Kiatkoski Kaminski RC, Correa MA, Chiavacci LA 2013. Inorganic UV filters. *Brazilian Journal of Pharmaceutical Sciences* 49(2):201-209.
144. Egerton TA, Tooley IR 2012. UV absorption and scattering properties of inorganic-based sunscreens. *International Journal of Cosmetic Science* 34(2):117-122.
145. Lademann J et. al. 2005. Synergy effects between organic and inorganic UV filters in sunscreens. *Journal of Biomedical Optics* 10(1):14008.
146. Herzog B. 2011. Influence of Particles on the Performance of Sunscreens. 11th International Sun Protection Conference, London.
147. Shaath NA 1987. On the theory of ultraviolet absorption by sunscreen chemicals. *Journal of the Society of Cosmetic Chemists* 38(3):193-207.
148. Herzog B, Katzenstein A, Quass K, Stehlin A, Luther H 2004. Physical properties of organic particulate UV-absorbers used in sunscreens I. Determination of particle size with fiber-optic quasi-elastic light scattering (FOQELS), disc centrifugation, and laser diffractometry. *Journal of Colloid and Interface Science* 271(1):136-144.
149. Müller S, Herzog B, Giesinger J, Quass K, Osterwalder U. 2005. Micronization as a tool in the developement of innovative UV filters. *SÖFW-Journal* 131(7):32-38.
150. Herzog B, Quass K, Schmidt E, Muller S, Luther H 2004. Physical properties of organic particulate UV absorbers used in sunscreens - II. UV-attenuating efficiency as function of particle size. *Journal of Colloid and Interface Science* 276(2):354-363.
151. Schlossmann D, Shao Y. 2005. Inorganic ultraviolet filters. In N.A. Shaath Ed. Sunscreens - regulations and commercial development. 3RD edition, Boca Raton (FL). Taylor & Francis, 239.
152. Kollias N 1999. The absorption properties of "physical" sunscreens. *Archives of Dermatology* 135(2):209-210.
153. Fonseca de Lima J, Serra OA 2013. Cerium phosphate nanoparticles with low photocatalytic activity for UV light absorption application in photoprotection. *Dyes and Pigments* 97(2):291-296.
154. Seixas VC, Serra OA 2014. Stability of sunscreens containing CePO4: proposal for a new inorganic UV filter. *Molecules* 19(7):9907-9925.

155. Serpone N, Dondi D, Albini A 2007. Inorganic and organic UV filters: Their role and efficacy in sunscreens and suncare product. *Inorganica Chimica Acta* 360(3):794-802.
156. Osterwalder U, Champ S, Flösser-Müller H, Herzog B. 2010. Evolution of UVA protection. In T4 International B, Hertfordshire, editor Cosmetics Science Technology, ed.
157. Osterwalder U, Luther H, Herzog B. 2001. Sun protection beyond the sun protection factor - new efficient and photostable UV-A filters. *SÖFW-Journal* 127 (7):45-54.
158. Kockler J, Oelgemoeller M, Robertson S, Glass BD 2012. Photostability of sunscreens. *Journal of Photochemistry and Photobiology C-Photochemistry Reviews* 13(1):91-110.
159. Schwack W, Rudolph T 1995. Photochemistry of Dibenzoyl Methane UVA filters.1. *Journal of Photochemistry and Photobiology B-Biology* 28(3):229-234.
160. Chatelain E, Gabard B 2001. Photostabilization of butyl methoxydibenzoylmethane (Avobenzone) and ethylhexyl methoxycinnamate by bis-ethylhexyloxyphenol methoxyphenyl triazine (Tinosorb S), a new UV broadband filter. *Photochemistry and Photobiology* 74(3):401-406.
161. Herzog B, Wehrle M, Quass K 2009. Photostability of UV absorber systems in sunscreens. *Photochemistry and Photobiology* 85(4):869-878.
162. Dondi D, Albini A, Serpone N 2006. Interactions between different solar UVB/UVA filters contained in commercial suncreams and consequent loss of UV protection. *Photochemical & Photobiological Sciences* 5(9):835-843.
163. Mturi GJ, Martincigh BS 2008. Photostability of the sunscreening agent 4-tert-butyl-4 '-methoxydibenzoylmethane (avobenzone) in solvents of different polarity and proticity. *Journal of Photochemistry and Photobiology a-Chemistry* 200(2-3):410-420.
164. Sayre RM et. al. 2005. Unexpected photolysis of the sunscreen octinoxate in the presence of the sunscreen avobenzone. *Photochemistry and Photobiology* 81(2):452-456.
165. Gaspar LR, Campos P 2006. Evaluation of the photostability of different UV filter combinations in a sunscreen. *International Journal of Pharmaceutics* 307(2):123-128.
166. Kikuchi A, Yagi M 2011. Direct observation of the intermolecular triplet-triplet energy transfer from UV-A absorber 4-tert-butyl-4 '-methoxydibenzoylmethane to UV-B absorber octyl methoxycinnamate. *Chemical Physics Letters* 513(1-3):63-66.

167. Bonda C. 2008. Research pathways to photostable sunscreens. *Cosmetics & Toiletries magazine* 123(2):49-59.
168. Bonda C. 2009. Sunscreen photostability 101. *Happi* 46(10):72-75.
169. Shaath NA. 2007. SPF Boosters & Photostability of Ultraviolet Filters. *Happi*.77-83.
170. Cole CA, Vollhardt J, Mendrok C. 2008. Formulation and Stability of Sunscreen Products. Clinical Guide to Sunscreens and Photoprotection, First ed. 39-52.
171. Chaudhuri RK et. al. 2006. Design of a photostabilizer having built-in antioxidant functionality and its utility in obtaining broad-spectrum sunscreen formulations. *Photochemistry and Photobiology* 82(3):823-828.
172. Gonzenbach H, Hill TJ, Truscott TG 1992. The triplet energy levels of UVA sunscreens and UVB sunscreens. *Journal of Photochemistry and Photobiology B*-Biology 16(3-4):377-379.
173. Herzog B, Huglin D, Borsos E, Stehlin A, Luther H 2004. New UV absorbers for cosmetic sunscreens - A breakthrough for the photoprotection of human skin. *Chimia* 58(7-8):554-559.
174. Shaath N, A. 2007. Chapter 3. Worldwide Regulations. in The Encyclopedia of Ultraviolet Filters, ed.: Allured Publishing Corporation.
175. Wang SQ, Dusza SW 2009. Assessment of sunscreen knowledge: a pilot survey. *British Journal of Dermatology* 161:28-32.
176. McKinlay AF, Diffey BL. 1987. A reference action spectrum for ultraviolet induced erythema in human skin. ed.: CIE research note.
177. Anders A, Altheide HJ, Knalmann M, Tronnier H 1995. Action spectrum for erythema in humans investigated with dye lasers. *Photochemistry and Photobiology* 61(2):200-205.
178. Kaidbey KH, Kligman AM 1979. Acute effects of long-wave ultraviolet-radiation on human skin. *Journal of Investigative Dermatology* 72(5):253-256.
179. Farr PM, Diffey BL 1985. The erythemal response of human skin to ultraviolet-radiation. *British Journal of Dermatology* 113(1):65-76.
180. Brown S, Diffey BL 1986. The effect of applied thickness on sunscreen protection - in vivo and in vitro studies. *Photochemistry and Photobiology* 44(4):509-513.
181. Weigmann H-J et. al. 2009. Comparison of human and porcine skin for characterization of sunscreens. *Journal of Biomedical Optics* 14(2):024027.
182. Pescia AC et. al. 2012. On the assessment of photostability of sunscreens exposed to UVA irradiation: From glass plates to pig/human skin, which is best? *International Journal of Pharmaceutics* 427(2):217-223.

183. Sayre RM, Agin PP, Desrochers DL, Marlowe E 1980. Sunscreen testing methods - in vitro predictions of effectiveness. *Journal of the Society of Cosmetic Chemists* 31(3):133-143.
184. Kelley KA et. Al. 1993. In vitro sun protection factor evaluation of sunscreen products. *Journal of the Society of Cosmetic Chemists* 44(3):139-151.
185. Lott DL, Stanfield J, Sayre RM, Dowdy JC 2003. Uniformity of sunscreen product application: a problem in testing, a problem for consumers. *Photodermatology Photoimmunology & Photomedicine* 19(1):17-20.
186. Miksa S, Lutz D, Guy C. 2013. In vitro/vivo SPF correlation and repeatability according to substrate. *Cosmetics & Toiletries magazine* 28(9):648-657.
187. Miksa S, Lutz D, Guy C. 2013. UV transmission assessment: influence of temperature on substrate surface. *Cosmetics & Toiletries magazine* 128(7):484-494.
188. Miksa S, Lutz D, Guy C. 2013. Influence of pressure during spreading on UV transmission results. Cosmetics & Toiletries magazine 128(11):822.
189. Miksa S, Lutz D, Ongenaed J, Candau D 2013. Adjusting Substrate/Product Interfacial Properties to Improve In vivo/In vitro SPF correlation. *Cosmetics & Toiletries magazine* 128(3):170-181.
190. Marguerie S, Pissavini M, Baud A, Carayol T, Doucet O 2012. A new chemical approach to optimize the in vitro SPF method on the HD6 PMMA plate. *Journal of cosmetic science* 63(4):243-254.
191. Ferrero L, Pissavini M, Marguerie S, Zastrow L 2003. Efficiency of a continuous height distribution model of sunscreen film geometry to predict a realistic sun protection factor. *Journal of cosmetic science* 54(5):463-481.
192. Herzog B (2009) Models for Simulation of Sun Protection Factors and Indices Characterizing the UVA Protection of Sunscreens: Principles and Applications, 56th SEPAWA Congress and European Detergents Conference.
193. Herzog B 2002. Prediction of sun protection factors by calculation of transmissions with a calibrated step film model. *Journal of Cosmetic Science* 53(1):11-26.
194. Tunstall DF 2000. A mathematical approach for the analysis of in vitro sun protection factor measurements. *Journal of Cosmetic Science* 51(5):303-315.
195. Ferrero L, Pissavini M, Doucet O 2010. How a calculated model of sunscreen film geometry can explain in vitro and in vivo SPF variation. *Photochemical & Photobiological Sciences* 9(4):540-551.

196. Herzog B et. al. (2006). Improved simulation of sun protection factors and UVA-parameters - a useful tool for the development of sunscreen formulations, 24th IFSCC International Congress, Osaka.
197. Herzog B, Mongiat S, Quass K, Deshayes C 2004. Prediction of sun protection factors and UVA parameters of sunscreens by using a calibrated step film model. *Journal of pharmaceutical sciences* 93(7):1780-1795.
198. Osterwalder U, Herzog B 2009. Sun protection factors: world wide confusion. *British Journal of Dermatology* 161:13-24.
199. Boots company 2011. Measurement of the UVA :UVB ratios according to the Boots star rating system.
200. ISO 24442:2011 - In vivo determination of sunscreen UVA protection.
201. ISO 24443:2012 - Determination of sunscreen UVA photoprotection in vitro.
202. FDA. 2011. Final monograph for Sunscreen Drug Products for Over-the-Counter Human Use.
203. Diffey B 2012. The FDA final rule on labelling and effectiveness testing of sunscreens: Too little, too late? *Journal of the American Academy of Dermatology* 66(1):162-163.
204. Herzog B et. al. 2002. In vivo and in vitro assessment of UVA protection by sunscreen formulations containing either butyl methoxy dibenzoyl methane, methylene bis-benzotriazolyl tetramethylbutylphenol, or microfine ZnO. *International journal of cosmetic science* 24(3):170-185.
205. Bimczok R et. al. 2007. Influence of applied quantity of sunscreen products on the sun protection factor - A multicenter study organized by the DGK task force sun protection. *Skin Pharmacology and Physiology* 20(1):57-64.
206. Sayre RM, Dowdy JC, Lott DL, Marlowe E 2008. Commentary on 'UVB-SPF': the SPF labels of sunscreen products convey more than just UVB protection. *Photodermatology Photoimmunology & Photomedicine* 24(4):218-220.
207. Bech-Thomsen N, Wulf HC 1992. Sunbathers' application of sunscreen is probably inadequate to obtain the sun protection factor assigned to the preparation. *Photodermatology, photoimmunology & photomedicine* 9(6):242-244.
208. Stenberg C, Larko O 1985. Sunscreen application and its importance for the sun protection factor. *Archives of Dermatology* 121(11):1400-1402.

209. Autier P, Boniol M, Severi G, Dore JF, European Org Res Treatment C 2001. Quantity of sunscreen used by European students. *British Journal of Dermatology* 144(2):288-291.
210. Pissavini M, Doucet O, Diffey B 2013. A novel proposal for labelling sunscreens based on compliance and performance. *International Journal of Cosmetic Science* 35(5):510-514.
211. Azurdia RM, Pagliaro JA, Diffey BL, Rhodes LE 1999. Sunscreen application by photosensitive patients is inadequate for protection. *British Journal of Dermatology* 140(2):255-258.
212. Bauer U, O'Brien DS, Kimlin MG 2010. A New Method to Quantify the Application Thickness of Sunscreen on Skin. *Photochemistry and Photobiology* 86(6):1397-1403.
213. Sayre RM, Dowdy JC 2010. The FDA proposed solar simulator versus sunlight. *Photochemical & Photobiological Sciences* 9(4):535-539.
214. Sayre RM, Stanfield J, Bush AJ, Lott DL 2001. Sunscreen standards tested with differently filtered solar simulators. *Photodermatology Photoimmunology & Photomedicine* 17(6):278-283.
215. Solan JL, Laden K 1977. Factors affecting penetration of light through stratum corneum. *Journal of the Society of Cosmetic Chemists* 28(3):125-137.
216. Lademann J et.al. 2004. In vivo determination of UV-photons entering into human skin. *Laser Physics* 14(2):234-237.
217. Kahn G 1971. Photosensitivity from occlusion. *Archives of Dermatology* 103(3):340-340
218. Owens DW, Knox JM, Hudson HT, Troll D 1975. Influence of humidity on ultraviolet injury. *Journal of Investigative Dermatology* 64(4):250-252.
219. European commission 2006. Commission recommendation of 22 September 2006 on the efficacy of sunscreen products and the claims made relating thereto 2006/647/EC
220. Lademann J et.al. 2004. Sunscreen application at the beach. *Journal of cosmetic dermatology* 3(2):62-68.
221. Solky BA et. al. 2007. Patient preferences for facial sunscreens: A split-face, randomized, blinded trial. *Journal of the American Academy of Dermatology* 57(1):67-72.
222. Diffey BL, Grice J 1997. The influence of sunscreen type on photoprotection. *British Journal of Dermatology* 137(1):103-105.

223. Pissavini M, Diffey B, Marguerie S, Carayol T, Doucet O 2012. Predicting the efficacy of sunscreens in vivo veritas. *International Journal of Cosmetic Science* 34(1):44-48.
224. Wang SQ, Halpern AC. 2008. Public education in photoprotection. In Lim HW, Draelos ZD, editors. Clinical guide to sunscreens and photoprotection, ed., New York London: Informa Healthcare.
225. Mahler HIM, Fitzpatrick B, Parker P, Lapin A 1997. The relative effects of a health-based versus an appearance-based intervention designed to increase sunscreen use. *American Journal of Health Promotion* 11(6):426-429.
226. Mahler HIM, Kulik JA, Gibbons FX, Gerrard M, Harrell J 2003. Effects of appearance-based interventions on sun protection intentions and self-reported behaviors. *Health Psychology* 22(2):199-209.
227. Jones JL, Leary MR 1994. Effects of appearance based admonitions against sun exposure on tanning intentions in young adults. *Health Psychology* 13(1):86-90.
228. Welsh C, Diffey B 1981. The protection against solar actinic radiation afforded by common clothing fabrics. *Clinical and Experimental Dermatology* 6(6):577-581.
229. Berne B, Fischer T 1980. Protective effects of various types of clothes against UV radiation. *Acta Dermato-Venereologica* 60(5):459-460.
230. Hatch KL, Osterwalder U 2006. Garments as solar ultraviolet radiation screening materials. *Dermatologic Clinics* 24(1):85-100.
231. Schmalwieser AW et. al. 2010. UV Exposition during typical lifestyle behavior in an urban environment. *Photochemistry and Photobiology* 86(3):711-715.
232. Phillips TJ et. al. 2000. Effect of daily versus intermittent sunscreen application on solar simulated UV radiation-induced skin response in humans. *Journal of the American Academy of Dermatology* 43(4):610-618.
233. Seite S, Fourtanier AMA 2008. The benefit of daily photoprotection. *Journal of the American Academy of Dermatology* 58(5):160-166.
234. Hughes MCB, Williams GM, Baker P, Green AC 2013. Sunscreen and prevention of skin aging a randomized trial. *Annals of Internal Medicine* 158(11):781-790.
235. Lejeune F, Christiaens F, Bernerd F 2008. Evaluation of sunscreen products using a reconstructed skin model exposed to simulated daily ultraviolet radiation: relevance of filtration profile and SPF value for daily photoprotection. *Photodermatology Photoimmunology & Photomedicine* 24(5):249-255.
236 Thompson SC, Jolley D, Marks R 1993. Reduction of solar keratoses by regular sunscreen use. *New England Journal of Medicine* 329(16):1147-1151.

237. Damian DL, Halliday GM, Barnetson RS 1997. Broad-spectrum sunscreens provide greater protection against ultraviolet-radiation-induced suppression of contact hypersensitivity to a recall antigen in humans. *Journal of Investigative Dermatology* 109(2):146-151.
238. Matsumura Y, Ananthaswamy HN 2004. Toxic effects of ultraviolet radiation on the skin. *Toxicology and Applied Pharmacology* 195(3):298-308.
239. Sekkat N, Kalia YN, Guy RH 2002. Biophysical study of porcine ear skin in vitro and its comparison to human skin in vivo. *Journal of Pharmaceutical Sciences* 91(11).
240. Jacobi U et. al. 2007. Porcine ear skin: an in vitro model for human skin. *Skin Research and Technology* 13(1):19-24.
241. Simon GA, Maibach HI 2000. The pig as an experimental animal model of percutaneous permeation in man: Qualitative and quantitative observations - An overview. *Skin Pharmacology and Applied Skin Physiology* 13(5):229-234.
242. Carrer DC, Vermehren C, Bagatolli LA 2008. Pig skin structure and transdermal delivery of liposomes: A two photon microscopy study. *Journal of Controlled Release* 132(1):12-20.
243. Lademann J et. al. 2008. Determination of the thickness and structure of the skin barrier by in vivo laser scanning microscopy. *Laser Physics Letters* 5(4):311-315.
244. Popov AP, Lademann J, Priezzhev AV, Myllyla R. Conference on Diagnostic Optical Spectroscopy in Biomedicine IV, Munich, GERMANY, Jun 19-21 2007.
245. Mihara M 1988. Scanning electron microscopy of skin surface and the internal structure of corneocyte in normal human skin – an application of the osmium dimethyl sulfoxide osmium method. *Archives of Dermatological Research* 280(5):292-299.
246. Vergou T et. al. 2013. Methods for the evaluation of the protective efficacy of sunscreen products. *Skin pharmacology and physiology* 26(1):30-35.
247. Kligman AM, Christophel E 1963. Preparation of isolated sheets of human stratum corneum. *Archives of Dermatology* 88(6):702-705.
248. Stokes RP, Diffey BL 1999. The feasibility of using fluorescence spectroscopy as a rapid, noninvasive method for evaluating sunscreen performance. *Journal of Photochemistry and Photobiology B-Biology* 50(2-3):137-143.
249. ISO 25178-2 : 2012 Geometrical product specifications (GPS) - Surface texture: Areal - Terms, definitions and surface texture parameters.

250. Piche E, Hafner HM, Hoffmann J, Junger M 2000. FOITS (Fast Optical In-vivo Topometry of human Skin): New approaches to the 3D analysis of surface structures of human skin. *Biomedizinische Technik* 45(11):317-322.
251. ISO 4287 : 2009. Geometrical Product Specifications (GPS) - Surface texture: profile method - Terms, definitions and surface texture parameters.
252. Pia T et. al. 1998. Epidermal thickness measured by light microscopy: a methodological study. *Skin Research and Technology* 4(4):174-179.
253. Franzen L, Windbergs M, Hansen S 2012. Assessment of near-infrared densitometry for in situ determination of the total stratum corneum thickness on pig skin: influence of storage time. *Skin Pharmacology and Physiology* 25(5):249-256.
254. Egawa M, Hirao T, Takahashi M 2007. In vivo estimation of stratum corneum thickness from water concentration profiles obtained with Raman spectroscopy. *Acta Dermato-Venereologica* 87(1):4-8.
255. Schaefer H 1996. Skin Barrier Principles of Percutaneous Absorption. ed.: Karger. Redelmeier TE (Paris)
256. Caspers PJ et. al. 1998. In vitro and in vivo Raman spectroscopy of human skin. *Biospectroscopy* 4(5):S31-S39.
257. Rajadhyaksha M, Gonzalez S, Zavislan JM, Anderson RR, Webb RH 1999. In vivo confocal scanning laser microscopy of human skin II: Advances in instrumentation and comparison with histology. *Journal of Investigative Dermatology* 113(3):293-303.
258. Tan G 2010. Hydration effects on skin microstructure as probed by high-resolution cryo-scanning electron microscopy and mechanistic implications to enhanced transcutaneous delivery of biomacromolecules. *Journal of Pharmaceutical Sciences* 99(2):730-740.
259. Edwards C, Heggie R, Marks R 2003. A study of differences in surface roughness between sun-exposed and unexposed skin with age. *Photodermatology Photoimmunology & Photomedicine* 19(4):169-174.
260. Jaspers S 1999. Rapid in vivo measurement of the topography of human skin by active image triangulation using a digital micromirror device. *Skin Research and Technology* 5(3):195-207.
261. Rhouzlane A, Makki S, Millet J, Humbert P 2002. La microscopie confocale: interet pour l'analyse du relief cutane. Un outil d'evaluation dermo-cosmetique. *International journal of cosmetic science* 24(6):349-356.

262. Corcuff P, Pierard GE 1998. Skin imaging: State of the art at the dawn of the year 2000. *Skin Bioengineering* 26:1-11.
263. Miksa S, Lutz D, Ongenaed J, Candau D 2013. Adjusting Substrate/Product Interfacial Properties to Improve In vivo/In vitro SPF correlation. *Cosmetics & Toiletries magazine* 128(3):170-181.
264. Herzog B, Sommer K. (2000) Investigations on photostability of UV-Absorbers for cosmetic sunscreens, 21Ith IFSCC International Congress, Berlin.
265. Stokes R, Diffey B 1997. How well are sunscreen users protected? *Photodermatology Photoimmunology & Photomedicine* 13(5-6):186-188.
266. Liu W et. al. 2012. Sunburn protection as a function of sunscreen application thickness differs between high and low SPFs. *Photodermatology Photoimmunology & Photomedicine* 28(3):120-126.
267. Faurschou A, Wulf HC 2007. The relation between sun protection factor and amount of suncreen applied in vivo. *British Journal of Dermatology* 156(4):716-719.
268. Schalka S, Silva dos Reis VM, Cuce LC 2009. The influence of the amount of sunscreen applied and its sun protection factor (SPF): evaluation of two sunscreens including the same ingredients at different concentrations. *Photodermatology Photoimmunology & Photomedicine* 25(4):175-180.
269. Rhodes LE, Diffey BL 1996. Quantitative assessment of sunscreen application technique by in vivo fluorescence spectroscopy. *Journal of the Society of Cosmetic Chemists* 47(2):109-115.
270. Gebauer V et. al. 2012. Influence of skin aging effects on the skin surface profile and the correlated distribution of topically applied sunscreens. *Journal of Biophotonics* 5(3):274-282.
271. Brozyna A, Chwirot BW 2006. Porcine skin as a model system for studies of ultraviolet A effects in human skin. *Journal of Toxicology and Environmental Health-Part a-Current Issues* 69(12):1155-1165.
272. Gupta VK, Zatz JL, Rerek M 1999. Percutaneous absorption of sunscreens through micro-Yucatan pig skin in vitro. *Pharmaceutical Research* 16(10):1602-1607.
273. Anonymous 2010. BASF sunscreen simulator. https://www.sunscreensimulator.basf.com/. Accessed March 12th 2015
274. Abbott E, Firestone F. 1933. Specifying surface quality. *Mechanical Engineering*, 55:569-572.
275. Herzog B, Osterwalder U. 2011. In silico Determination of Topical Sun Protection in Cosmetic Science Technology, T4 International, Boxmoor, Hertfordshire .

276. Grencis PW, Stokes R 1999. An evaluation of photographic methods to demonstrate the uniformity of sunscreen applied to the skin. *The Journal of audiovisual media in medicine* 22(4):171-177.
277. Loesch H, Kaplan DL 1994. Pitfalls in sunscreen application. *Archives of Dermatology* 130(5):665-666.
278. Lademann J et.al. 2005. Application of optical coherent tomography for skin diagnostics. *Laser Physics* 15(2):288-294.
279. Teichmann A et.al. 2006. Investigation of the homogeneity of the distribution of sunscreen formulations on the human skin: characterization and comparison of two different methods. *Journal of Biomedical Optics* 11(6):064005.
280. ISO 25178-602:2010 - Geometrical product specifications (GPS) - Surface texture: Areal - Part 602: Nominal characteristics of non-contact (confocal chromatic probe) instruments.
281. Osterwalder U, Sohn M, Herzog B 2014. Global state of sunscreens. *Photodermatology, Photoimmunology, Photomedicine* 30:62-80
282. Herzog B, Osterwalder U 2015. Simulation of sunscreen performance. *Pure Appl. Chem.* 87:937-951
283. Adlhart C, Baschong W 2011. Surface distribution and depths profiling of particulate organic UV absorbers by Raman imaging and tape stripping. *International Journal of Cosmetic Science* 33(6):527-534.
284. Williams AC, Edwards HGM, Barry BW 1994. Raman spectra of human keratotic biopolymers – skin, callus, hair and nail. *Journal of Raman Spectroscopy* 25(1):95-98.
285. Caspers PJ et. al. 2001. In vivo confocal Raman microspectroscopy of the skin: Noninvasive determination of molecular concentration profiles. *Journal of Investigative Dermatology* 116(3):434-442.
286. Ashtikar M et.al. 2013. Non-invasive depth profile imaging of the stratum corneum using confocal Raman microscopy: First insights into the method. *European Journal of Pharmaceutical Sciences* 50(5):601-608.
287. Gniadecka M et.al. 1997. Distinctive molecular abnormalities in benign and malignant skin lesions: Studies by Raman spectroscopy. *Photochemistry and Photobiology* 66(4):418-423.
288. Tfayli A, Piot O, Pitre F, Manfait M 2007. Follow-up of drug permeation through excised human skin with confocal Raman microspectroscopy. *European Biophysics Journal with Biophysics Letter*s 36(8):1049-1058.

289. Pudney PDA, Melot M, Caspers PJ, van der Pol A, Puppels GJ 2007. An in vivo confocal Raman study of the delivery of trans-retinol to the skin. *Applied Spectroscopy* 61(8):804-811.
290. Alber C, et. al. 2013. Effects of water gradients and use of urea on skin ultrastructure evaluated by confocal Raman microspectroscopy. *Biochimica Et Biophysica Acta-Biomembranes* 1828(11):2470-2478.
291. Tosato MG et.al. 2012. Raman Spectroscopic Investigation of the Effects of Cosmetic Formulations on the Constituents and Properties of Human Skin. *Photomedicine and Laser Surgery* 30(2):85-91.
292. Darvin ME et.al. 2009. In vivo distribution of carotenoids in different anatomical locations of human skin: comparative assessment with two different Raman spectroscopy methods. *Experimental Dermatology* 18(12):1060-1063.
293. Darvin M et.al. 2008. Cutaneous concentration of lycopene correlates significantly with the roughness of the skin. *European Journal of Pharmaceutics and Biopharmaceutics* 69(3):943-947.
294. Franzen L, Selzer D, Fluhr JW, Schaefer UF, Windbergs M 2013. Towards drug quantification in human skin with confocal Raman microscopy. *European Journal of Pharmaceutics and Biopharmaceutics* 84(2):437-444.
295. Beyere L, Yarasi S, Loppnow GR 2003. Solvent effects on sunscreen active ingredients using Raman spectroscopy. *Journal of Raman Spectroscopy* 34(10):743-750.

List of Abbreviations

2D	Two-dimensional
BCC	Basal cell carcinoma
BMDBM	Butyl methoxydibenzoylmethane
BEMT	Bis-ethylhexyloxyphenol methoxyphenyl triazine
CAS	Clear alcoholic spray
CPD	Cyclobutane pyridimine dimers
CRM	Confocal Raman microspectroscopy
CRR	Cosmic ray removal
EHMC	Ethylhexyl methoxycinnamate
EHT	Ethylhexyl triazone
EMCCD	Electron multiplying charge-coupled device
DTS	Drometrizole trisiloxane
FDA	Food and drug administration
IMC	Isoamyl p-methoxycinnamate
INCI	Ingredient nomenclature of cosmetic ingredients
IPD	Immediate pigment darkening
IR	Infrared
JCIA	Japanese cosmetic industry association
MBBT	Methylene bis-benzotriazolyl tetramethylbutylphenol

MED	Minimal erythemal dose
MMP	Matrixmetalloproteinase
MPPDD	Minimal persistent pigment darkening dose
NA	Numerical aperture
OCR	Octocrylene
OW	Oil-in Water
PBSA	Phenylbenzimidazol sulfonic acid
PMMA	Polymethylmethacrylate
PPD	Persistent pigment darkening
RI	Refractive index
ROS	Reactive oxygen species
SC	Stratum corneum
SCC	Squamous cell carcinoma
SCCS	Scientific commitee on consumer safety
SPF	Sun protection factor
TBPT	Tris biphenyl triazine
TDSA	Terephthalylidene dicamphor sulfonic acid
TEA	Time and extent application
TiO2	Titanium dioxide
UV	Ultraviolet
UVA-PF	UVA protection factor
VIS	Visible
WO	Water-in-Oil
ZnO	Zinc oxide

List of Symbols

E1,1	Absorption at a concentration of 1% (w/v) solution at an optical thickness of 1cm
λ c	Critical wavelength
λ max	Wavelength with the maximum absorbance
Sa	Arithmetical mean height
$\mathbf{S_{er}}(\lambda)$	Erythema action spectrum at wavelength λ
$\mathbf{S_{mean}}$	Average of film thickness over a measured area
$\mathbf{S_{PPD}}(\lambda)$	Persistence pigment darkening action spectrum at wavelength λ
$\mathbf{S_s}(\lambda)$	Spectral irradiance of the UV source at wavelength λ
$\mathbf{S_{UVA}}(\lambda)$	Spectral irradiance of the UVA source at wavelength λ
T(λ)	Transmittance at wavelength λ

List of Figures

Chapter 2

Chapter 3

Chapter 4

Chapter 5

Chapter 6

List of Tables

Chapter 2

Chapter 3

Chapter 4

Chapter 5

Chapter 6

Curriculum Vitae

Myriam Sohn

9D rue Savigneux

68128 Rosenau, France

Tel : 0033 6 63 61 46 97

Born in Strasbourg, France

October 26th, 1977

Education

2011 – 2015 **Ph.D. studies in Pharmaceutical Sciences**
University of Basel and University of Applied Sciences and Arts Northwestern, Switzerland

2001 – 2002 **Master's Degree M2 in Cosmetology,** Minor in **Management and Marketing** field
University of Lyon 1, faculty of Pharmacy, France

1997 – 1999 **Master's Degree M1 in Health Engineering, Formulation and Control of Cosmetic Products**, passed with honors
University of Montpellier 1, faculty of Pharmacy, France

Work experience

2009 – today **BASF Grenzach, GmbH** , Grenzach-Whylen, Germany
(after acquisition of Ciba Specialty Chemicals by BASF)

2012 - today Technical manager of key account customers in Sun Care application

2009 - 2012 Senior Laboratory Head of the Technical Service for BASF UV filters

2002 – 2009 **Ciba Specialty Chemicals**, Grenzach-Whylen, Germany
Laboratory Head Technical Service for Ciba cosmetic raw materials

2000 – 2001 **STRAND Cosmetics EUROPE**, France
(subcontracting company for custom made cosmetic formulations)
Formulation scientist of decorative cosmetic products

List of publications

- Sohn M, Buehler T, Imanidis G. (2016) "Repartition of oil miscible and water soluble UV filters in an applied sunscreen film determined by confocal Raman microspectroscopy". *Photochem. Photobiol. Sci.* 15:861-871.

- Sohn M, Herzog B, Osterwalder U, Imanidis G. (2016) "Calculation of sun protection factor of sunscreens with different vehicles using measured film thickness distribution – comparison with SPF *in vitro". J. Photochem. Photobiol. B* 159:74-81.

- Sohn M. (2016) UV booster and photoprotection in Principles and Practice of Photoprotection, Ed. Steven Q. Wang and Henry W. Lim, Springer Publisher Chapter 13:227-245

- Sohn M, Korn V, Herzog B, Imanidis G. (2015) "Porcine ear skin as a biological substrate for in vitro testing of sunscreen performance". *Skin Pharmacol. Physiol.* 28:31-41.

- Sohn M, Heche A, Herzog B, Imanidis G. (2014) "Film thickness frequency distribution of different vehicles determines sunscreen efficacy". *J. Biomed. Opt.* 19:115005.

- Osterwalder U, Sohn M, Herzog B. (2014) "Global state of sunscreens", review article. *Photodermatol. Photoimmunol. Photomed.* 30:62-80.

List of posters and oral presentations

- Sohn M, Herzog B, Imanidis G. (2015) "Film thickness frequency distribution of different vehicles determines sunscreen efficacy" (oral presentation)
  Sun Care Conference, London, UK, June 2015.

- Sohn M, Herzog B, Imanidis G. (2015) "Film thickness frequency distribution of different vehicles determines sunscreen efficacy" (oral presentation)
  DGK (Deutsche Gesellschaft für Wissenschafltiche und Angewandte Kosmetik) Symposium Mensch und Sonne, Darmstadt, Germany, May 2015.

- Sohn M, Herzog B, Imanidis G. (2015) "Film thickness frequency distribution of different vehicles determines sunscreen efficacy" (oral presentation)
  Annual Research Meeting, Department of Pharmaceutical Sciences, University of Basel, Switzerland, February 2015.

- Sohn M, Herzog B, Imanidis G. (2014) "Film thickness frequency distribution of different vehicles determines sunscreen efficacy" (oral presentation)
  GPEN (The Globalization of Pharmaceutics Education Network) meeting, Helsinki, Finland, August 2014.

- Sohn M, Herzog B, Imanidis G. (2014) "Impact of vehicle on film thickness and performance of sunscreens" (poster presentation)
  IFSCC (International Federation of Societies of Cosmetic Chemists) congress, Paris, France, October 2014.

- Sohn M, Imanidis G. (2013) "Film layer thickness and homogeneity of distribution of applied sunscreens" (poster presentation)
  Journées Jean-Paul Marty, Paris, France, December 2013.